Diss. ETH No. 16995

# Radiation Grafted Fuel Cell Membranes with Improved Oxidative Stability

A dissertation submitted to the
SWISS FEDERAL INSTITUTE OF TECHNOLOGY
For the degree of
DOCTOR OF SCIENCES

presented by
Michał Wiesław Ślaski
Master of Science (Warsaw University of Technology, Poland)
born 29.09.1973
citizen of Poland

Accepted on the recommendation of
Prof. Dr. Alexander Wokaun, examiner
Prof. Dr. A. Dieter Schlüter, co-examiner
Dr. Günther G. Scherer, co-examiner
Dr. Selmiye Alkan Gürsel, co-examiner

Zürich, 2007

# Acknowledgement

**This work I would like to dedicate to my parents Wiesław & Joanna.**

# Table of Contents

# Abstract

This thesis contains results from the research work toward radiation grafted membranes for polymer electrolyte fuel cell with improved oxidative stability. Fuel cell membranes are now one of the most expensive parts of a fuel cell, the prices of 800 USD/m$^2$ of commercially available Nafion® trigger researchers to undertake research for cheaper materials.

New materials for the synthesis of radiation grafted membranes were proposed in literature. The monomers AMS (α-methylstyrene) and MAN (methacrylonitrile) were grafted with preirradiation technique from FEP. The obtained material, FEP grafted with poly(AMS-co-MAN) side chains, branching from a main chain of the backbone, was sulfonated in order to provide proton conductivity. The fuel cell test confirmed the expected better oxidative stability for a membrane synthesized by grafting of AMS and MAN from FEP than uncrosslinked styrene based membranes. The membrane performed 500 hrs, most of this time at 80 °C, the performance time is 10 times longer than for uncrosslinked styrene based membranes, which perform only 50 hrs and the working temperature can not be elevated to 80 °C because it results in sudden failure.

Studies of grafting AMS and MAN from FEP were carried out in order to find the optimum grafting parameters. A mixture of isopropanol and water was found to be the best solvent for the grafting reaction, yielding the highest graft levels.

As a step, to improve oxidative stability, a study addressing the topic of crosslinked radiation grafted membranes, was carried out. Two crosslinkers were investigated, well known commercially available DVB (divinylbenzene) and DIPB (1,3-diisopropenylbenzene), both showed typical effects for membranes, e.g. reduced IEC, reduced swelling, brittleness when applied in high extend. The fuel cell test of DVB-crosslinked membranes showed improved oxidative stability by crosslinking. The first AMS/MAN/DVB crosslinked membrane performed 1000 hrs until the failure. The second test was terminated by the operator after 1000 hrs in order to estimate the lost of IEC during the operation time. Post mortem analysis results showed a difference between the two crosslinked membranes, yielding 43% and 16%, for the first membrane and the second membrane, respectively. Until now crosslinked AMS/MAN membranes did not yet reach performance of the optimized styrene based

crosslinked membranes. Therefore, the future work should focus on a crosslinker optimization.

# Kurzfassung

Diese Dissertation enthält Resultate aus der Forschungsarbeit, die das Ziel hatte die Herstellung von strahlengepfropften Membranen für Polymer Elektrolyt Brennstoffzellen mit verbesserter Oxidationsstabilität zur ermöglichen. Membranen in Brennstoffzellen zählen mit einem Preis von ca. 800 USD/m$^2$ für kommerziell erhältliche Produkte wie, DuPonts Nafion, gegenwärtig zu den teuersten Komponenten in der Brennstoffzelle. Dieser Umstand veranlasst Forscher, nach billigeren Materialien mit vergleichbaren oder besseren chemischen Eigenschaften zu forschen.

Aufbauend auf Literaturstudien wurden neue Materialien für die Synthese von strahlengepfropften Membranen vorgeschlagen. Die Monomere AMS (α-Methylstyrol) und MAN (Methacrylnitril) wurden als viel versprechende Komponenten für die Pfropfung fluorierter Polymere befunden, um Zwischenprodukte zur Herstellung von Membranen zu erhalten. Das Konzept, AMS und MAN gleichzeitig auf das perfluorierte Polymergrundgerüst FEP (poly(Hexafluoropropylen-co-tetrafluoro-ethylen)) zu pfropfen, erwies sich dabei am erfolgreichsten. Das so dargestellte Material, ein FEP Basisfilm mit poly(AMS-co-MAN) Seitenketten, wurde anschliessend sulfoniert, um Protonenleitfähigkeit zu erzielen. Tests dieser FEP basierten Membranen in der Brennstoffzelle zeigten bessere Oxidationsstabilitäten als die nicht vernetzten styrolbasierten Membranen. Die Membrane überdauerte 500 Stunden Betrieb bei 80 °C, was einer 10fachen Verbesserung gegenüber der nicht vernetzten styrolbasierten Membranen entspricht. Diese überdauerten lediglich 50 Stunden bei einer Zelltemperatur unter 80 °C; der Betrieb der Brennstoffzelle bei höherer Temperatur hätte zu einem noch schnelleren Ausfall geführt. Die optimalen Parameter bei der Pfropfung von AMS und MAN auf FEP wurden ermittelt. Es zeigte sich, dass eine Mischung aus Isopropanol in Wasser das beste Lösungsmittel für die Pfropfreaktion darstellte und den höchsten Pfropfgrad ergab. Um die Oxidationsstabilität weiter zu erhöhen, wurde in einem nächsten Schritt das Potential vernetzter Membranen untersucht. Dabei wurden zwei Vernetzer untersucht; das schon bekannte DVB (Divinylbenzol) und DIPB (1,3-Diisopropyl-benzol). Die hiermit hergestellten, vernetzten Membranen zeigten typisches Verhalten, wie etwa verminderte Ionenaustauschkapazität (IEC), verminderte Wasseraufnahme und Quellung und Brüchigkeit im Falle hochvernetzer Filme. Die erste mit DVB vernetzte

AMS/MAN Membran hielt im Brennstoffzellentest 1000 Stunden. Der zweite Test wurde vom Experimentator nach 1000 Stunden unterbrochen, um den Verlust an IEC zu ermitteln. Diese *post mortem* Analysen ergaben einen Verlust an IEC der beiden vernetzten Membranen von 43% bzw. 16%. Bis jetzt erreichten die AMS/MAN Membranen nicht die Haltbarkeit von optimierten, vernetzten und auf Styrol basierenden Membranen. Die weitere Forschung sollte sich daher auf die Optimierung des Vernetzers konzentrieren.

# List of Abbreviations

$\Delta G$ – Gibbs Free Energy

$\Delta g$ – Gibbs Free Energy in Molar Quantities

$\Delta H$ – Enthalpy

$\Delta h$ – Enthalpy in Molar Quantities

$\lambda$ – stoichiometry

AMS – α-methylstyrene

DC – Direct Current

DIPB – 1,3- diisopropenylbenzene

DVB – divinylbenzene

ETFE – poly(etylene-co-tetrafluoroethylene)

FEP – poly(hexafluoropropylene-co-tetrafluoroethylene)

FEP – poly(tetrafluoroethylene-co-hexafluoropropylene)

GDL – Gas Diffusion Layer

Gl – Graft Level

HOR – Hydrogen Oxidation Reaction

IEC – Ion Exchange Capacity

MAN – methacrylonitrile

MEA – Membrane Electrode Assembly

OCV – Open Circuit Voltage

ORR – Oxygen Reduction Reaction

PEFC – Polymer Electrolyte Fuel Cell

PTFE – polytetrafluoroethlene

PVDF – poly(vinylidenefluoride)

$R_m$ – monomer ratio ([AMS]/[MAN])

Z – impedance (Re – real component, Im – imaginary component)

$X_m$ – monomer fraction ([AMS]/([AMS]+[MAN]))

# Theoretical Introduction

## 1. Fuel Cell Principle

A fuel cell is an electrochemical device converting directly the chemical energy of a fuel to electrical energy, with a continuous replenishment of the consumed fuel. Unlike the batteries, fuel cells do not need to be charged and the electrodes do not undergo consumption in the process of energy production. The electrodes play the role of a catalyst for a reaction in which energy is obtained.

Up to now, several types of fuel cells are known. The difference between the types of fuel cells is expressed mainly in the reactions taking place on electrodes and in consequence, the type of fuel used. A polymer electrolyte fuel cell (PEFC) is a kind of fuel cell where fuel and oxidant are separated by an ion-conductive polymer membrane. For example, a fuel, hydrogen is electro-oxidized at the anode giving off electrons, which are transported through a polymer membrane. On the other electrode, cathode, oxygen is reduced and water is produced. Both electrodes are made out of the catalyst and gas diffusion layer (GDL). The catalyst is platinum supported on carbon black with loadings of about 0.9-0.1 mgPt/cm$^2$ and an ionomer improving the three boundary phase. The GDL, being an electron conductive material, provides electric contact as well as fuel distribution from a flow field to the catalyst. The two electrodes are separated by a polymer membrane, which provides proton conductivity. The same membrane plays also two other very important roles of a gas separator and an electronic insulator. Membrane and electrodes together are called membrane electrode assembly (MEA). On both sides, directly to the MEA, the flow fields are attached, providing gas distribution by a network of channels. In order to reduce the internal resistance and space occupation, fuel cells are designed as stacks where a bipolar plate provides a gas distribution for two cells, hydrogen on one and oxygen on the other side. The standard potential of hydrogen/oxygen fuel cell is 1.229 V, when both the fuel and the oxidant are gases and the product is liquid water. The potential decreases linearly (only when $\Delta S$=const) with increasing temperature. The variation of voltage with temperature originated from the differential expression for the Gibbs free energy:

$$dG = -SdT + Vdp$$

Because Vdp =0 at constant pressure, the expression is given as follows:

$$\left(\frac{dG}{dT}\right)_p = -S$$ For molar quantities is expressed as: $$\left(\frac{dg}{dT}\right)_p = -\Delta s$$

The relation between Gibbs free energy and the reversible cell voltage is given by:

$$\Delta g = -nFE$$

Combining both equations the equation for a reversible cell voltage ($E_T$) is found as

$$\left(\frac{dE}{dT}\right)_p = \frac{ds}{nF}$$

Rewriting this equation and substituting $dE=E_T-E^0$ and $dT=T-T_0$ final equation is found:

$$E_T = E^0 + \frac{\Delta s}{nF}\left(T - T_0\right)$$

For the hydrogen-oxygen fuel cell, the term $\Delta s/(nF)$ is negative because $\Delta s$ is negative, thus the reversible cell voltage decreases with increasing temperature.

$$\text{Anode}: H_2 \rightarrow 2H^+ + 2e^- \qquad\qquad HOR\,(\text{Hydrogen Oxidation Reaction})$$
$$\text{Cathode}: \frac{1}{2}O_2 + 2H^+ + 2e^- \rightarrow H_2O \qquad\qquad ORR\,(\text{Oxygen Reduction Reaction})$$
$$\text{Overall}: H_2 + \frac{1}{2}O_2 \rightarrow H_2O$$
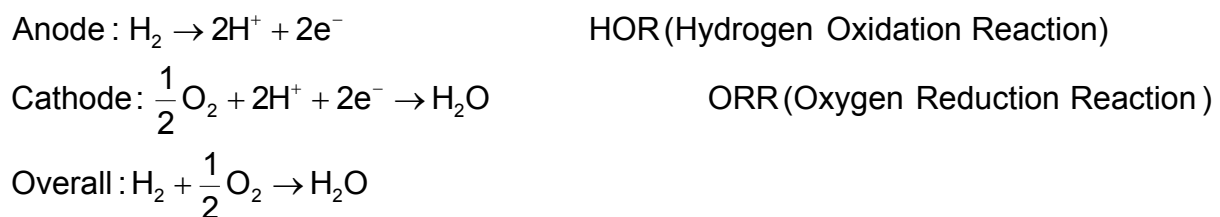
An important issue for this type of fuel cell is water management, because water is necessary for maintaining the high ionic conductivity of a membrane and finally high overall efficiency. In a PEFC, water is produced on the cathode. Protons are produced on the anode and pass through the membrane. During the proton motion molecules of water are also transported, this phenomena is known as electroosmotic drag. Dry gases, high reactants flow and high temperature result in water deficiency and consequently in a dramatic loss of performance due to low conductivity of the

membrane. In order to support a proper water content, hydrogen or both reactants are humidified. When the production and supply of water are higher than elimination from the system, the surplus of water may lead to flooding of the electrode or electrodes, causing problems for gas diffusion, finally reducing the performance.
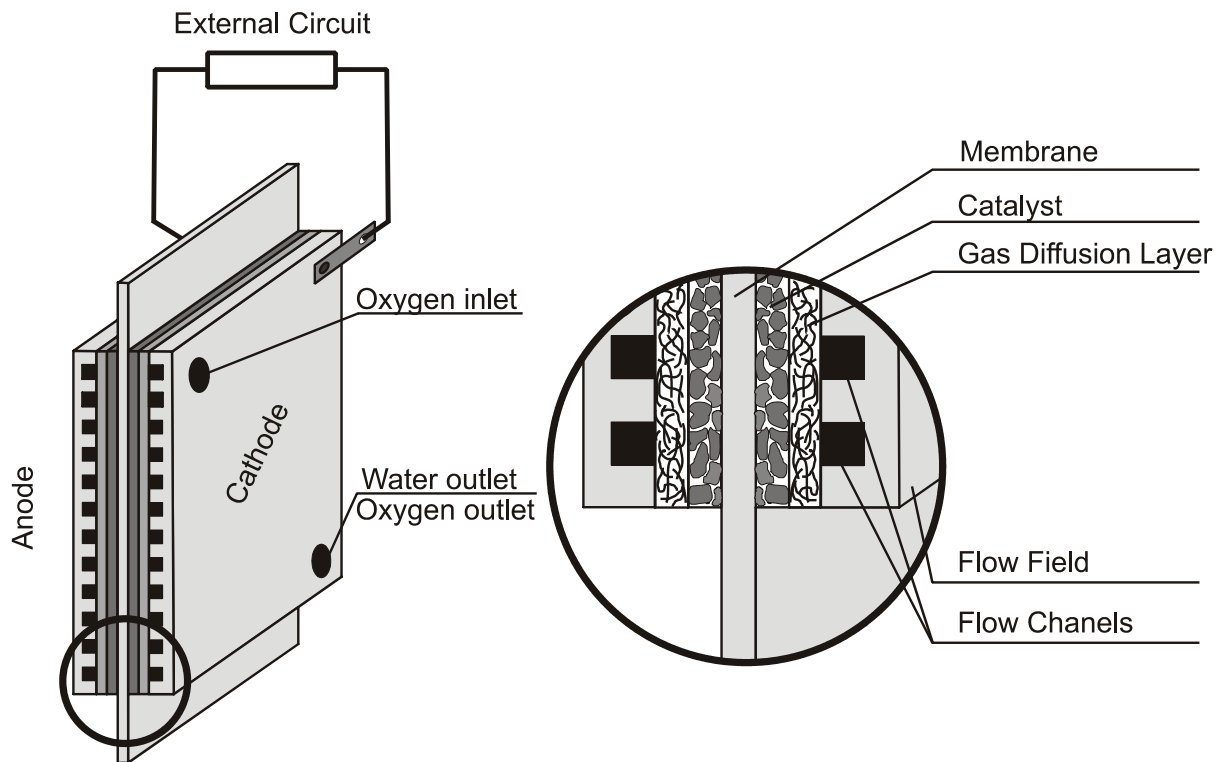


**Fig. 1: Polymer Electrolyte Fuel Cell (PEFC). Hydrogen inlet and outlet are located on the anode side.**

Other types of fuel cells are solid oxide fuel cell (SOFC), direct methanol fuel cell (DMFC, subcategory of PEFC), molten carbonate fuel cell (MCFC), alkaline fuel cells (AFC), and phosphoric acid fuel cells (PAFC). SOFC is a high temperature fuel cell, operating above 600 ºC. Since high temperature internal reforming can be performed in a fuel cell, thus a wide range of fuels can be used including hydrogen, carbon monoxide and light hydrocarbons. All high temperature fuel cells are solutions for stationary applications, which operate continuously. Fast start up now is a problem for SOFC, due to the fact that the fuel cell has to reach high operation temperature, the fast warm-up can cause mechanical stress and damage to the fuel cell components.

For automotive applications PEFC is the best solution, operating at temperatures between 60 and 120 ºC. High power density, fast start, and low time to reach the full operating power make them competitive among others fuel cell solutions for this application.

DMFC also can be considered as a power source for automotive application, but durability and power density are not yet sufficiently developed. Nowadays DMFC's are considered as portable power sources for a growing market of portable electronic devices.

**Table 1: Types of fuel cells, type of electrolyte, types of fuel, operating temperatures.**

| Fuel Cell Type | Type of Electrolyte | Fuel Type | Operating Temperature / ºC |
|---|---|---|---|
| PEFC | Polymer electrolyte (solid acid) | $H_2$ | 80 |
| DMFC | Polymer electrolyte (solid acid) | $CH_3OH$ | 80 |
| AFC | Liquid KOH (in matrix) | $H_2$ | 60-220 |
| MCFC | Molten Carbonate | $H_2$, $CH_4$ | 650 |
| PAFC | Liquid $H_3PO_4$ (in matrix) | $H_2$ | 200 |
| SOFC | Solid Oxide | $H_2$, $CH_4$, CO | 600-1000 |

Generally, fuel cells offer a better efficiency than internal combustion engine because they are not limited by the Carnot cycle. In an internal combustion engine, as in a typical thermal engine, only a part of the heat is converted into mechanical work. The difference between the delivered (dQ) and the given off head is the work (dW) that can be used, the given off head is lost. Therefore, in case of heat a engine, there is always waste heat, which must be given off. In order to achieve an efficiency of 0.8, the heat engine should operate at a temperature difference ($T_H$-$T_L$) equal to 1000 K (where the engine rejects heat at 200 K ($T_L$)). The high temperature is difficult to achieve from material reasons.

The fuel cell efficiency is expressed as a ratio of obtained energy from the process and total energy delivered as a fuel.

$$\eta = \frac{\text{obtained energy}}{\text{total energy}} = \frac{dQ}{dW} = \frac{T_H - T_L}{T_H}$$    Carnot cycle efficiency

Where:

dQ – is the heat delivered to the thermal engine

dW – is the work extracted from the thermal engine

$T_H$- Temperature of a heat source

$T_L$ – Temperature of a heat "sink" – waste heat

From thermodynamics, the available electrical work of a fuel cell is limited by Gibbs Free Energy ($\Delta G$).

$$\eta_{th} = \frac{\text{obtained energy}}{\text{total energy}} = \frac{\text{electrical work}}{\Delta h} = \frac{\Delta g}{\Delta h}$$    Fuel cell efficiency

Where:

$\Delta g$ – Gibbs Free Energy of the process (molar)

$\Delta h$ – Enthalpy of the process (molar)

When liquid water is produced in a fuel cell, the standard enthalpy of the reaction in a hydrogen/oxygen fuel cell is $\Delta h^0$=-286 kJ/mol. Standard Gibbs Free Energy of the reaction in the hydrogen fuel cell is $\Delta g^0$= -237.3 kJ/mol.

$$\eta_{th} = \frac{-237.3 \, kJ/mol}{-286 \, kJ/mol} = 0.83$$    Efficiency $H_2/O_2$ fuel cell

Therefore, to achieve the same theoretical efficiency (about 0.8) for fuel cell is less difficult than for a heat (internal combustion) engine.

There are four major efficiency losses: activation losses, ohmic losses, mass transport and fuel utilization losses. Activation losses are caused by activation overpotentials. The sluggish ORR reaction occurs at the cathode and due to poor kinetics, this is the reason of a drop of the operating voltage.
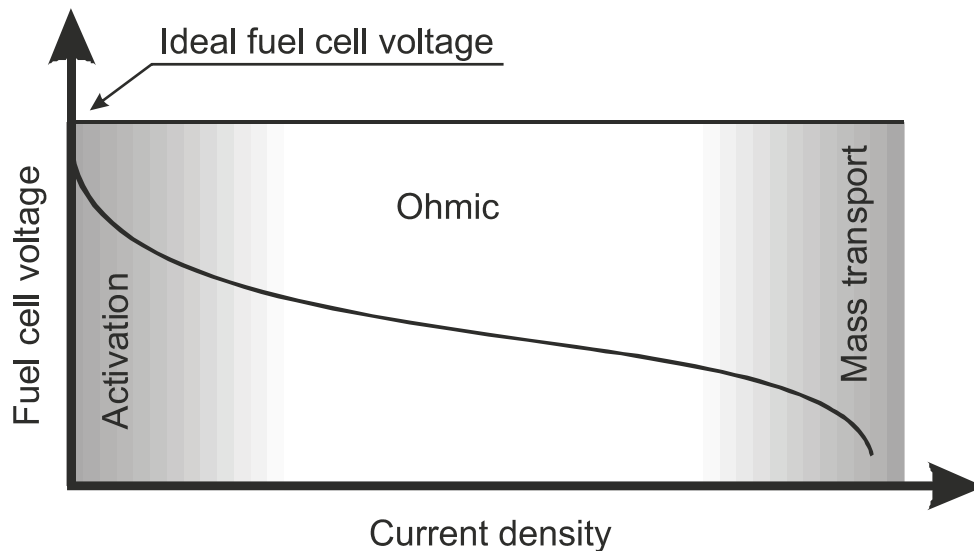
**Fig. 2: Fuel cell polarization curve. Regions of a polarization curve with marked higher contribution losses. The ideal fuel cell voltage is 1.2 V.**

While the anode reaction HOR is relatively fast, it does not create significant activation overpotential. The drop of potential due to overpotential is visible on a polarization curve when the fuel cell is loaded. The operating voltage drops significantly (Fig. 2). Ohmic loses are caused by the resistivity of the membrane, of interfaces, of the electrode, the GDL, bipolar plate, and all electric connections. Therefore, the membrane resistivity as well as the membrane-electrode interface has a major influence on fuel cell efficiency. By a reduction of bulk and interface resistivity improvement a higher efficiency can be achieved. The ohmic loss is expressive in the linear part of the polarization curve (Fig. 2). Mass transport losses occur when the consumption of a fuel or an oxidant (or both) is faster than the fuel transport and a shortage of the fuel in a catalyst layer takes a place. In the polarization curve this is shown as a strong drop of cell voltage at high value of current density (Fig. 2). The energy loss by ohmic loses as well as by activation losses is converted to heat, which is responsible for a fuel cell warming, therefore the fuel cell needs cooling. Generally, the fuel can not be utilized to 100% because of thermodynamic efficiency, fuel crossover and necessity for purging, from time to time, in order to remove accumulated inert gases like nitrogen at the cathode side.

Membrane resistance and interfacial properties between electrode and membrane influence on the ohmic resistance region. The overall fuel cell efficiency, containing all efficiencies, is expressed as:

$$\eta = \eta_{th} \cdot \eta_{voltage} \cdot \eta_{fuel}$$

Component efficiencies are given as:

$$\eta_{voltage} = \frac{V}{E}$$

$$\eta_{fuel} = \frac{i/nF}{v_{fuel}}$$

$$\eta_{th} = \frac{\Delta g}{\Delta h}$$

Where:

$\eta_{th}$ – Thermodynamic efficiency

$\eta_{voltage}$ – Voltage efficiency

$\eta_{fuel}$ – Fuel utilization efficiency (oxidant)

E – Thermodynamically reversible voltage

V – Real operating voltage

i – Current generated by the fuel cell

$v_{fuel}$ – Rate of fuel supplied into the fuel cell

The overall fuel cell efficiency is a product of constituent efficiencies such as: thermodynamic efficiency, voltage efficiency (contains activation losses), ohmic losses, and mass transport losses. Fuel utilization is generally very high and the possible losses are caused by purging, leakages and fuel (oxidant) crossover.
Presented fuel cell efficiency applies only to a single cell, for a larger device (stack) additionally energy losses like energy demand for a compressor, energy for a cooling system, must be taken into account[1].

### 1.1. Overview of Membranes for Polymer Electrolyte Fuel Cell

A membrane for PEFC must be a proton conductor, gas separator, and electronic insulator in parallel. The idea to use a polymer membrane in a fuel cell was described for the first time by Grubb[2]. Proton conductivity, necessary for proton transport from

anode to cathode, is achieved by attaching protogenic groups to a polymer chain. For example, sulfonic acid groups are attached to a perfluorinated backbone in Nafion®, which is a commercially available membrane.

Moreover, a polymer membrane has to meet several requirements, particularly when used to high performance applications such as in an automotive power trains:

- low cost material

- high proton conductivity

- high durability

- sufficient mechanical resistance

- good interface to an electrode

- water management

The cost of proton conducting membranes is a crucial factor for the commercialization of fuel cells. Perfluorinated membranes like Nafion®; however, being almost ideal for many applications, suffer from a complicated synthetic route[3] and in consequence, reduction of production cost is difficult. Nafion® was developed by DuPont in the middle 60's as the first commercial ionomer. The very first use of Nafion® was as a membrane for electrolyses in chlor-alkali production. Nowadays, Nafion® is a benchmark for ionomers; properties like durability, conductivity are usually referred to Nafion®. In the literature, there are described alternative membranes based on hydrocarbon polymers or partially fluorinated polymers are very competitive in terms of production costs and raw materials costs.
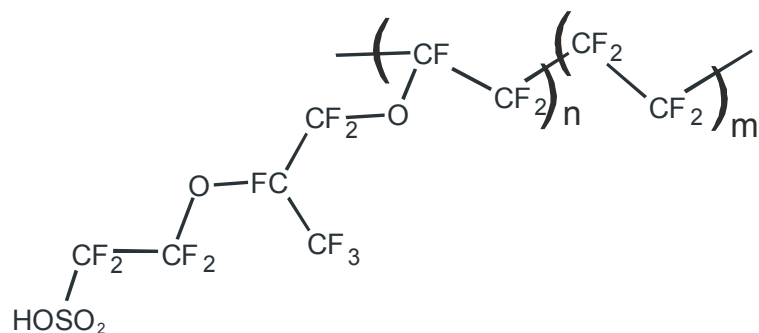


**Fig. 3: Structure of Nafion ®.**

## 1.2. Classification of Polymer Electrolyte Membranes

Fuel Cell membranes can be divided into two categories, firstly with respect to the type of the protogenic group, secondly with respect to the type of the polymer backbone, where the protogenic group is attached. The backbone polymer is responsible for mechanical strength, chemical stability, gas permeability, and partially the water management. The type of protogenic group provides ionic conductivity and influences the water content. The polymer backbone can be fully fluorinated (Nafion®, Flemion® Asahi), partially fluorinated (ETFE grafted with polystyrene and subsequently sulfonated), and non fluorinated (hydrocarbon, aliphatic or aromatic).

## 1.3. Protogenic Groups

A protogenic group is a group with acidic properties, of which there are many groups with different acidities. Weak acid groups, like the hydroxyl group exhibits very high $pK_a$ so that the concentration of dissociated acid groups is low and as a result proton conductivity is low.

In proton conducting membranes usually sulfonic acid groups are attached to an aromatic, aliphatic, or perfluorinated backbone. Since electronic effects are responsible for acidity of the acid group, the acidity of the sulfonic acid as well as the carboxylic acid group changes depending on electronic properties of attached groups. For example, when the sulfonic acid is attached to the trifluoromethyl group, then the pKa value is the lowest (-13) (trifluoromethanesulfonic acid) acid). For the commercially available ionomer Nafion®, where a sulfonic acid group is attached to a perfluorinated chain, the pKa value is also very low (-5.45 to -9). In analogy, carboxylic acid groups, being attached to a perfluorinated chain, exhibit comparatively high (pKa = 0.52) acidity, which is very close to the pKa value of benzensulfonic acid. Carboxylic groups attached to hydrocarbon backbone provide insufficient proton conductivity and therefore have no practical application as a membrane for PEFC.

Polybenzoimidazoles doped with phosphoric acid are examples of membranes where the doping acid is not covalently bound to a polymeric backbone. A polymeric matrix doped with phosphoric acid is not sensitive to humidification and during the fuel cell operation the conductivity does not drop down, as long as the gases are dry.

**Table 2: Acids and their pKa values measured at 25 ºC in water.**

| Name | Reference | Structure | pKa |
|---|---|---|---|
| trifluoromethanesulfonic acid | 4 | $CF_3SO_3H$ | -13 |
| benzensulfonic acid | 5 | $PhSO_3H$ | 0.70 |
| trifluoroacetic acid | 5 | $CF_3COOH$ | 0.52 |
| methanesulfonic acid | 5 | $CH_3SO_3H$ | -2.6 |
| phosphoric acid | 5 | $H_3PO_4$ | 1.3 |
| imidazole | 5 | (see below) | 6.99 |
| acetic acid | 5 | $CH_3COOH$ | 4.76 |
| sulfuric acid | 5 | $H_2SO_4$ | -3 |
| Nafion® | 6 | Fig. 3 | -5.45 to -9 |
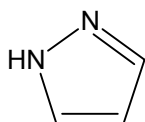
**Fig. 4: Structure of imidazole.**

However, the performance at lower temperature than the boiling point of water is not feasible, because liquid water will leach out phosphoric acid from the matrix[7].

Many different polymers can be used as the base film for polymer electrolyte membranes. The backbone provides important properties including durability, mechanical strength, wetting properties, gas permeability, and surface energy. In the literature as well as on the market there are many polymeric systems successfully used for design of polymer membranes. Aromatic polymers are very often used to synthesize ionomers, aromatic backbone offers chemical stability and aromatic moiety makes those polymers amenable to sulfonation. Polyetherketone, polysulfones, polyphenylenes[8] as well as their derivatives were used for the synthesis of proton conducting membranes (Fig. 5). Aromatic polymers, with aromatic rings in the chain, are synthesized by step-grow polymerization and by subsequent solvent casting of a material in the film form.

Another important category of membranes are radiation grafted membranes. The synthetic approach is to grow a polymer chain by radical polymerization from a polymeric backbone, which plays the role of a multifunctional macroinitiator.
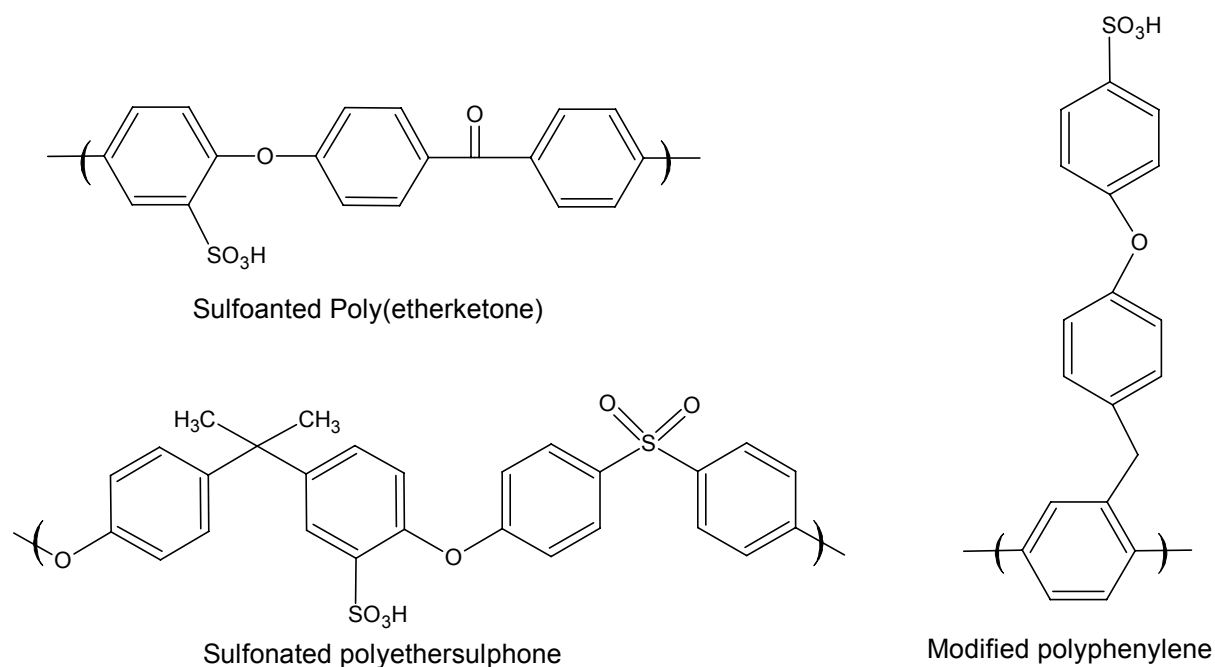
**Fig. 5: Examples of different aromatic ionomers.**

Various types of monomers and base polymer films can be employed in this method. There are several backbone polymers, which are distinguished as non-fluorinated, partially-fluorinated and perfluorinated. Radiation grafted membranes, due to versatility of the synthesis method and of good fuel cell performance of synthesized membranes are an alternative to commercial high cost membranes[9].

## 1.4. Radiation Grafted Membranes

Radiation grafting is a versatile method for the modification of polymers; even highly resistant fluoropolymers can be easily modified by the use of radiation[10]. In the process of radiation grafting there are two main reactions, initiation of the polymeric backbone, and growing of polymer chain from the polymeric backbone. There are two major types of grafting techniques, a simultaneous grafting and preirradiation grafting technique[11]. In the simultaneous method the irradiation and growing of polymers are performed at the same time. Radiation continuously initiates a polymeric backbone, while polymer side chains grow from an initiated backbone. In preirradiation method[12], irradiation is followed by grafting reaction. In this method grafting and irradiation processes are separated in time. Therefore, the irradiated
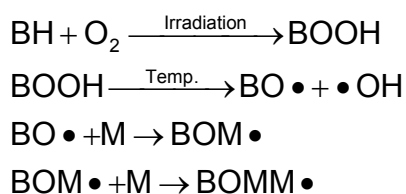
20

base film can be stored in a deep freezer (at -75°C) even a few months without any loss of its ability for initiation. After irradiation, the base film is immersed in a monomer solution and activated thermally to grow side chains. In principle any kind of high energy radiation can be used, X-ray, gamma, UV[13] was reported, also an electron beam can be used for irradiation[14,15,16]. Irradiation can be performed in vacuum, inert gas atmosphere ($N_2$, Ar) or in the presence of air (peroxy/hydroperoxy method). In simultaneous grafting method, radiation induces, in parallel, homopolymerization of the monomer and chain growth on the backbone polymer. In consequence, a higher amount of homopolymers than in the preirradiation technique is formed.

Usually, the active species during the simultaneous irradiation are the radicals, however, creation of cations in non-aqueous systems was also reported. Several monomers, such as α-methylstyrene, vinyl ethers, which do not usually homopolymerize initiated radically, as a proof for an ionic mechanism, were grafted[17].

$$B \xrightarrow{\text{Irradiation}} B\bullet$$
$$B\bullet + M \rightarrow BM\bullet$$
$$BM\bullet + M \rightarrow BMM\bullet$$
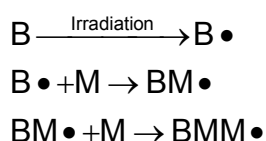
**Fig. 6: Mechanism of continues radiation grafting or preirradiation grafting of films irradiated in oxygen-free atmosphere (or vacuum). B – polymer backbone, M – monomer, ● –radical.**

It is commonly accepted that in the preirradiation method performed in the presence of air, peroxy groups are created. Later, those hydroperoxy groups can be activated thermally like a typical free radical initiator to start graft copolymerization.

$$BH + O_2 \xrightarrow{\text{Irradiation}} BOOH$$
$$BOOH \xrightarrow{\text{Temp.}} BO\bullet + \bullet OH$$
$$BO\bullet + M \rightarrow BOM\bullet$$
$$BOM\bullet + M \rightarrow BOMM\bullet$$

**Fig. 7: Mechanism of preirradiation grafting where samples were irradiated in the presence of oxygen. B – polymer backbone, M – monomer, ● – radical.**

In vacuum or inert atmosphere, irradiation produces radicals, which are stable for a longer time. An irradiated base polymer can be stored for weeks or months after irradiation at -80 °C until it is used[10].

Typically, radiation grafting is performed in systems where monomers are diluted with a suitable solvent. The role of the solvent is to reduce the quantity of the monomers and to increase the graft level of the product. The most favorable solvent for radiation grafting of styrene onto FEP is a mixture of isopropanol and water since with this solvent the highest graft levels can be obtained. The positive solvent influence on graft level was arranged in the following series[18].

**Isopropanol/Water > Isopropanol > Acetic Acid > Methanol > THF > Cyclohexane > Toluene**

Temperature enhances the rate of polymerization enabling reduction of a grafting time. Additionally, an increase of temperature enhances termination reaction and as a consequence membranes with high graft levels can not be synthesize. Simultaneous grafting is performed usually at room temperature, whereas the temperature range for preirradiation grafting is between 40-90 °C.

Preirradiation dose has a substantial influence on graft level. The higher the dose, the higher the obtained graft is.

The method of radiation grafting offers a unique opportunity of polymer modification having already the final physical shape.(e.g. films, tubes). Therefore, this method was early recognized as a convenient way for manufacturing of different types of membranes for diverse membrane applications such as: ion exchange, dialysis[19], electrodialysis[20], ultrafiltration[21], gas separation[22], reverse osmosis[21]. Basically, the monomer styrene is grafted onto a perfluorinated, partially fluorinated or non-fluorinated backbone and subsequently sulfonated. The synthesized material possesses proton conductivity provided by the sulfonic acid groups and good mechanical properties. Therefore, radiation grafted membranes were recognized as a suitable material for PEFC[12].

## 1.5. Properties of Polymer Electrolyte Membranes

Polymer electrolyte membranes can be characterized with respect to many properties, such as conductivity, ion exchange capacity (IEC), water uptake (swelling), hydration number and fuel permeation. Mechanical properties are also very important parameters because a membrane must be durable enough for a fuel cell assembly and further operation. During operation, the membrane is exposed to a mechanical stress due to varying humidity, difference in oxidant and fuel pressure, and temperature.

**IEC:**

Ion exchange capacity (IEC) is defined as a number of mols of acid groups per mass unit of a membrane. IEC is a vital component of conductivity, a membrane with higher IEC value will provide higher conductivity, so that IEC reflects the concentration of charge carriers calculated per mass unit.

**Conductivity:**

Conductivity is the most important parameter for classification of a membrane for the fuel cell application. A membrane should exhibit conductivity in the order of 100 mS cm$^{-1}$ for a thickness of 25-50 μm (ohmic resistance 50 mΩ cm$^2$) or more[23]. Conductivity is a function of the charge carriers concentration (per volume) and charge mobility and by increasing one of them, conductivity will increase. It should be noted that conductivity is a function of water content and decreases when the water content of the membrane decreases. Loss of water becomes more severe at higher temperatures, especially above the water boiling point, and as a result the membrane provides very low conductivity.

**Swelling:**

Water swelling is the amount of water (%) that a membrane can swell and swelling is expressed as ratio of the swollen water to the dry membrane:

$$Swelling = \frac{\text{mass of swollen water}}{\text{mass of a dry membrane}} \cdot 100\%$$

Swelling is a parameter describing the content of water in a membrane, which has a strong influence on membrane conductivity[24].

The hydration number is expressed as the average number of water molecules per single acid group. This parameter is a combination of IEC and swelling, and knowing both of them the hydration number can be calculated as follows:

$$\text{Hydration number} = \frac{\text{Swelling} \cdot 10}{\text{IEC} \cdot \text{M}_{\text{Water}}} = \frac{\text{number of water molecules}}{\text{number of acid molecules}}$$

Where:

$M_{Water}$ – Molecular Weight of Water

$IEC$ –Ion Exchange Capacity in mEq/g

In order to describe surface properties of a membrane, the free surface energy can be estimated for both, polar and non-polar components. Surface free energy is used to evaluate membrane hydrophilicity on the surface. The most suitable technique for this purpose is contact angle measurement enabling estimation of both polar and non-polar component. Membrane surface free energy describes interfacial properties of a membrane[25,26].

## 1.6. Degradation of Styrene Based Membranes

A membrane in a fuel cell is exposed to an aggressive oxidative environment, during the operation the membrane degrades, which is observed by an increase in resistance, leading to membrane failure. Degradation of the polymer membrane is attributed to the oxidative species hydroperoxy (HOO●) and hydroxy (HO●) radicals. There are two possible sources of hydroperoxy and hydroxy radicals. First, on the anode, radicals are generated on the catalyst surface in the reaction of hydrogen with oxygen that diffuses through the membrane from the cathode side[27,12]. Second, the radicals are generated at the cathode during the electrocatalytic oxygen reduction[28]. Hydrogen peroxide is believed to cause the membrane damage being a source of radicals (HOO● and HO●) during a decomposition reaction. There is an evidence of hydrogen peroxide presence in the product water of PEFC[29,30]. Degradation of membranes based on styrene sulfonic acid, in the presence of hydroxy and hydroperoxy radicals, was investigated by La Conti[31] and Roduner[32,33,34].
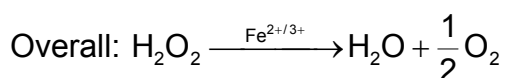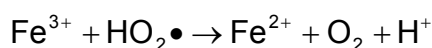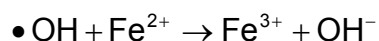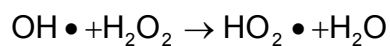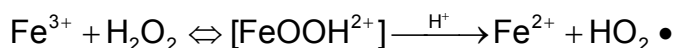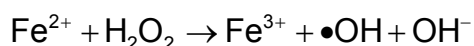
not observed
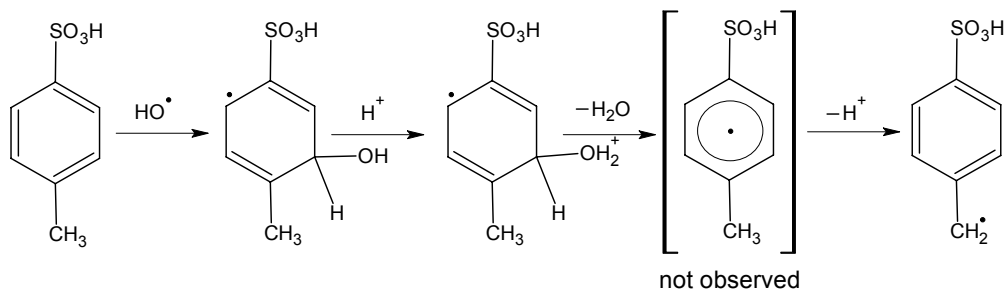
**Fig. 8: Mechanism of *para*-toluene sulfonic acid degradation[33].**

The model compound, *p*-toluenesulfonic acid and hydrogen peroxide were photolized by a high pressure mercury lamp, products were investigated directly with EPR (electron paramagnetic resonance) spectroscopy. Several structures, being products of the reactions, were detected.

The presented mechanism is now widely accepted as a degradation mechanism for membranes based on polystyrene sulfonic acid. In sulfonated polystyrene, α-hydrogen is the most susceptible place for hydrogen displacement, the mechanism proposed by Roduner, suggests that the radical attacks the ring.

The radical attack leads to creation of a radical on a polymer chain, further break down of carbon-carbon bond occurs, which results in a chain scission reaction. Consequently, a polymer fragment is cut off and is easily removed from the membrane. In this process the membrane loses conductivity by a loss of proton conducting component (styrene sulfonic acid).

$$Fe^{2+} + H_2O_2 \rightarrow Fe^{3+} + \bullet OH + OH^-$$

$$Fe^{3+} + H_2O_2 \Leftrightarrow [FeOOH^{2+}] \xrightarrow{H^+} Fe^{2+} + HO_2 \bullet$$

$$OH \bullet + H_2O_2 \rightarrow HO_2 \bullet + H_2O$$

$$\bullet OH + Fe^{2+} \rightarrow Fe^{3+} + OH^-$$

$$Fe^{3+} + HO_2 \bullet \rightarrow Fe^{2+} + O_2 + H^+$$

Overall: $H_2O_2 \xrightarrow{Fe^{2+/3+}} H_2O + \frac{1}{2}O_2$

**Fig. 9: Fenton's mechanism.**

Roduner investigated the model compound *para*-toluene sulfonic acid, however, in case of a styrene based polymer fuel cell membrane the character of degradation is not well known. Decay of the polymer chain can occur according to a zip-like mechanism, the attacked by a radical polymer chain loses fragments (monomer units). The product of the degradation is a low molecular weight species containing aromatic rings and sulfonic acid groups, therefore a radical can cleave several repeating units. In the other proposed mechanism, a radical causes a chain scission, the product of degradation is a relatively short oligomer. Unlike in the zip-like mechanism, the radical causes only one chain scission.

Until now, the treatment with the Fenton's reagent mostly has been used as an ex-situ evaluation of membrane stability[35,36,37,38]. The Fenton's reaction is a decomposition of hydrogen peroxide catalyzed by $Fe^{2+}$ or $Fe^{3+}$ cations, in which hydroperoxy and hydroxy radicals are generated as the byproducts, wherein both radicals degrade a membrane. It is believed that the mechanism of degradation by Fenton's reaction is similar to the degradation mechanism in a fuel cell. The main problem of Fenton's test is to set reproducible conditions, such as iron cation concentration, hydrogen peroxide concentration, etc. Additionally, temperature, pH, and presence of light play a significant role. Moreover, a membrane, being a strong cation exchanger, can capture iron ions from the solution, so that the concentration of iron ions in the membrane can be higher than in the solution. Hence, the use of pure hydrogen peroxide at temperature of about 60 ºC and a concentration of $5\%_{w/w}$ was suggested in order to eliminate the problem of iron migration from the solution to the membrane. Application of methods like thermogravimetry analysis (TGA) is not suitable for an evaluation of membrane stability because of the different nature of the degradation process. The best real life test is a fuel cell experiment, however, long time of testing reaching even thousands hours causes this kind of tests to be time consuming and expensive, consequently high throughput cannot be achieved. In the fuel cell, the membrane is not degraded uniformly over the area, some regions show a higher tendency for degradation than the others (fuel and oxidant inlets). Moreover, there are many parameters influencing the fuel cell test, during the testing time power cuts or apparatus failure can have a significant influence. Other factors, such as MEA preparation, type of electrodes, parameters of operation, such as current density, stoichiometry, and humidification, have a significant influence on fuel cell performance and membrane degradation. In conclusion, a fuel cell test is a good

real-life test, but it can not be applied as a high throughput method for the evaluation of different membrane types.

## 1.7. Selection of Alternative Monomers for Radiation Grafted Membranes

There is a large number of monomers that can be grafted onto preirradiated polymeric backbones, each radically polymerizable, and also monomer systems that can be copolymerized by a radical mechanism[59]. From the view point of the PEFC membrane research, only those monomers are important, which can provide proton conductivity directly or after a simple modification. The most popular monomer for cation exchange membranes is styrene, the benzene ring of styrene can be easily sulfonated or undergo any other electrophilic substitution reaction. However, easily available and prone to modification, styrene, when polymerized and sulfonated, is susceptible for degradation under fuel cell conditions. Uncrosslinked styrene based membranes, where styrene was grafted onto FEP base film and sulfonated, perform only about 50 hrs[12], after this time heavy loss of polystyrene sulfonic acid is observed. The membranes were grafted from a 50 μm thick FEP film irradiated with a dose of 60 kGy, the grafting was performed at 60 ℃, and the graft level was about 20%. Fuel cell test was carried out at 60 ℃ with full humidification (both hydrogen and oxygen humidified). After the fuel cell test the membranes were investigated by FTIR and the backbone polymer was found intact. In order to improve the stability of styrene based radiation grafted membranes, a bi-functional monomer acting as a crosslinker is used for the grafting reaction with styrene[39]. Typically, technical grade of divinylbenzene (DVB) with a purity of about 80% is used. Crosslinking improves the durability of a membrane significantly and then performance times of 4000 - 8000 hrs[40] can be achieved. The way, how a crosslinker influences the membrane durability, is not well known. Three different effects can be responsible for improvement of membrane stability. The crosslinker reduces diffusion into a membrane and, therefore, the access of species, responsible for degradation, to the membrane is limited. The single chain scission in a crosslinked structure does not cause a cleavage of a long chain like in an uncrosslinked membrane. A molecule of the crosslinker can stop degradation of a polymer chain, if the mechanism of degradation is of "zip" type, if the process of degradation cleave unit by unit.

Styrene sulfonic acid is very susceptible towards attacks of hydroperoxy radicals, this mechanism is described in the next chapter.
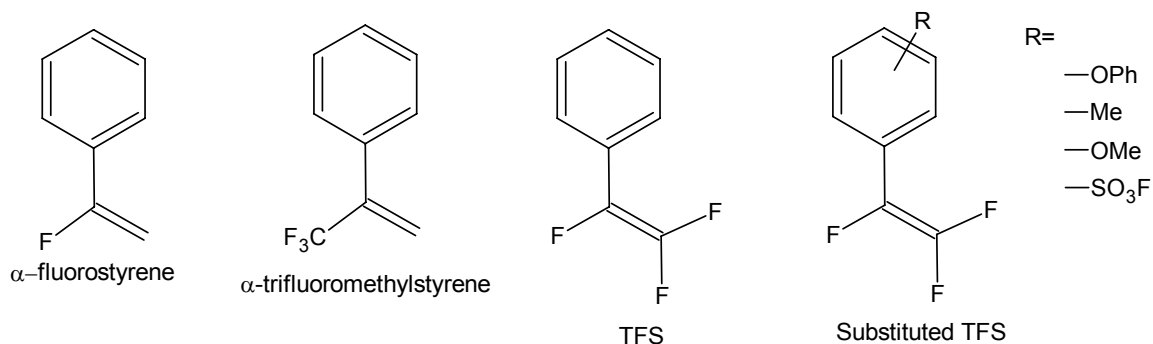


**Fig. 10: Fluorinated styrene derivatives.**

The styrene fluorinated homologue *α,β,β*-trifluorostyrene (TFS) seems to be a good replacement for styrene. TFS was synthesized for the first time by Cohen[41] *et al* in 1949. This monomer, grafted onto fluorinated backbone like FEP or PTFE and sulfonated, shows much better durability in the fuel cell[42]. Unlike styrene, TFS has no hydrogen atom in the vinyl group, which makes it much less prone to oxidative attack. Apart from advantages of TFS based membranes, there are several disadvantages of TFS for larger scale application. The reason of having low interest on TFS for membrane synthesis are as follows: Difficult and expensive synthesis, tendency to irreversible dimerization[43], poor homopolymerization yield[44], slow homopolymerization[45], difficulties with sulfonation[46]. However Ballard Power Systems (Burnaby, Canada) applied TFS derivatives such as para-methyl, -methoxy, or -phenoxy-TFS in BAM® grafted PEM[47,48]. The use of para-sulfonylfluoride-TFS in grafting reaction eliminates sulfonation and makes the process simpler. It was reported that BAM® type membranes showed better performances in a fuel cell than Nafion®[49]. Fluorinated styrenes such as TFS, *α*-fluorostyrene and *α*-(tri-fluoromethy)styrene[50] are known in the literature[51,52]. There are several methods of synthesis described as well as attempts of polymerization by different mechanisms (radical, ionic). From the practical point of view, an alternative monomer to styrene should be a cheap, commercially available monomer like styrene. The synthesis of fluorinated monomers is a step generating high costs due to the complicated chemistry and multi-step synthesis. In Paul Scherrer Institut (Villigen, Switzerland) work performed by Steuernagel[53] towards the synthesis of TFS and halogen

derivatives of styrene was carried out, wherein the high cost of TFS and derivatives was confirmed. TFS derivatives with pendant sulfonic acid group, connected in *para* position of the aromatic ring, with –$CF_2$-$CF_2$- bridge, were also grafted and tested in the fuel cell by Alkan Gursel *et al*. The performance was better than for Nafion 112® and performance time until failure was 524 hrs[54]. Consequently, the focus on non-fluorinated monomers, styrene derivatives, is advised for a reduction of fuel cell membranes costs.

Monomers with aromatic rings are of special interest, because an aromatic ring can be easily sulfonated with the known procedure. Additionally, an aromatic monomer should not have any hydrogen in α-position to an aromatic ring, which would result in low stability of the polystyrene sulfonic acid[34]. The monomer α-methylstyrene (AMS) is a good candidate for the replacement of styrene in radiation grafted membranes because:

- AMS is available at low prices (36 chf/L from Aldrich).
- The α-position is protected by methyl group.

AMS grafted onto PTFE was demonstrated as a material for a membrane in a zinc/ferricyanide battery by a comparison with styrene grafted onto PTFE. AMS membrane performed 200 hrs without any significant lost of mass while, the styrene based membrane showed up to 17% mass loss[55]. AMS is a commercial monomer with wide range of applications[56], copolymer with acrylonitrile (AN) is a heat resistant thermoplastic with higher thermal resistance than copolymer of styrene and acrylonitrile. BASF produces poly(AMS-co-AN) with the commercial name Luran® KR 2556 with a recommendation for impact and thermo resistant applications[56]. The AMS monomer is also used for the improvement of styrene by a copolymerization[57]. The resultant copolymer has better thermal properties then styrene alone. AMS is an electron donating monomer, with electron withdrawing monomers it forms a charge transfer complex (CTC). A CT complex of those two monomers exhibits a high ability for polymerization, even without an initiator[58]. For example, AMS and maleic anhydride (MAH), both monomers are almost not homopolymerizable, but copolymerize readily with a tendency to form perfectly alternated copolymer poly(AMS-alt-MAH)[59].

Radical polymerization of AMS, however difficult, can be performed in emulsion systems[60]. It was previously reported that for radical homopolymerization of AMS a temperature below 61 ºC is required, since at higher temperatures adverses the reaction, and depolymerization is observed[61]. This temperature is called ceiling temperature, above which the reaction changes direction due to thermodynamic reasons. However, homopolymerization of AMS with a radical mechanism is possible, yet the rate is very low, making the reaction not favorable.

Despite the problems with the radical polymerization of α-methylstyrene, homopolymerization with both cationic and anionic mechanisms can be carried out with high conversion and much faster than the radical polymerization.

For the synthesis of preirradiation grafted membranes, it is very important to have a polymeric system, which can be radically polymerized, because, polymerization according to the ionic mechanism is difficult to perform. Cationic grafting can be initiated by gamma irradiation, and the simultaneous technique of grafting must be employed. Additionally, cationic polymerization is extremely sensitive to residual impurities, in particular water, therefore, typical for ionic polymerization strict measures must be undertaken. In the literature, radiation grafting of AMS, vinyl n-butyl ether and isobutylene onto polyethylene was reported[17].

In order to make AMS useful for radiation grafted membranes, another monomer must be introduced to prevent the limiting effect of the ceiling temperature and the poor kinetics of homopolymerization. AMS can be copolymerized radically with plenty of vinyl monomers[62], including even with those, which do not undergo radical homopolymerization like maleic anhydride (MAH).

The use of AMS for the synthesis of radiation grafted membranes was already suggested in the literature. Preirradiation grafting of AMS with acrylonitrile onto ETFE was studied by Becker[63], however, the testing of the resultant membranes in fuel cells was not performed. A higher stability of ETFE-*g*-(AMSSA-co-AN) than ETFE-*g*-SSA was verified by a comparative test with Fenton's reagent.

Among a variety of monomers able to copolymerize with AMS, attention should be paid on styrene, since styrene can be sulfonated, and resulting in a higher ion exchange capacity and consequently contribution to conductivity. Unfortunately, styrene possesses a hydrogen atom in α-position so that it is prone to oxidative attack of hydroperoxy radicals. On the other hand, MAH, after hydrolysis, would contribute two carboxylic acid groups per monomeric unit of MAH, but weak acid

groups do not significantly contribute to conductivity. As proposed already, acrylonitrile does not contribute any charge carriers like a sulfonated ring does. By analogy, an acrylonitrile homologue methacrylonitrile seems to be an attractive comonomer for AMS because:

- Homopolymerization rate constant is 1000 lower than AN[62].
- Methyl group can provide additional stability.
- MAN was not found to be carcinogenic like AN.
- Copolymerization of AMS with MAN is known in the literature[64,65].

In the work of Becker[63] the strong dependency of composition (AN content) on graft level caused a predominant homopolymerization of AN in the first period of reaction. Consequently, molar ratio of AMS/AN increases with time of reaction. That can be explained that AN initiates the reaction and grafted chains are rich in AN, at the beginning of the process. The use of copolymer with lower homopolymerization can force higher AMS content in the graft copolymer.

The methyl group of MAN can provide a steric protection of a copolymer chain against a radical attack, resulting in higher stability. Radical copolymerization of AMS and MAN was described already in the literature[66,67]. Moreover, the nitrile group gives a possibility of elemental analysis of nitrogen and easy FTIR analysis for quick analytical routines. Finally, MAN was selected as a comonomer for radiation grafted-membranes based on AMS in this work.
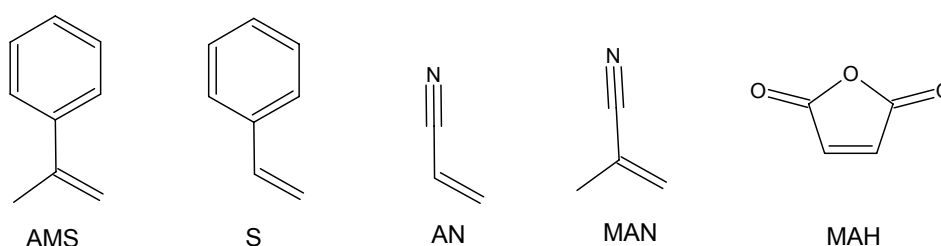


**Fig. 11: Structure of α-methyl styrene (AMS), styrene (S), acrylonitrile (AN), methacrylonitrile (MAN) and maleic anhydride (MAH).**

Crosslinking provides a higher durability of styrene based radiation-grafted membranes operated in a fuel cell[40]. For further improvement, crosslinkers, multi

functional monomers were selected for radiation grafted membranes based on AMS and MAN. DVB is a standard vinyl crosslinker, used not only for the fabrication of radiation-grafted membranes, but also crosslinking of ion exchange resins and solid supports for solid phase organic chemistry. Triallylcyanurate was proposed as an alternative crosslinker for radiation-grafted membranes[39]. As the third crosslinker 1,3-diizopropenylbenzene (DIPB) was selected, because it is similar to AMS, it joins both properties as difunctional monomer (crosslinker) and has a protected α-positions like AMS. DIPB is already known in the literature as a difunctional monomer, it was used for crosslinking in radical polymerization[68]. Cationic UV-initiated homopolymerization of m-DIPB gives a linear polymer (Poly[1,6-(1,3,3-trimethylindanyl)]. Anionic homopolymerization and copolymerization with AMS gives a linear product, where the second double bond of DIPB remains intact[69].



DVB
divinylbenzene
(mixture of isomers)

TAC
triallylcyanurate

*meta*-DIPB
1,3- diisopropenylbenzene
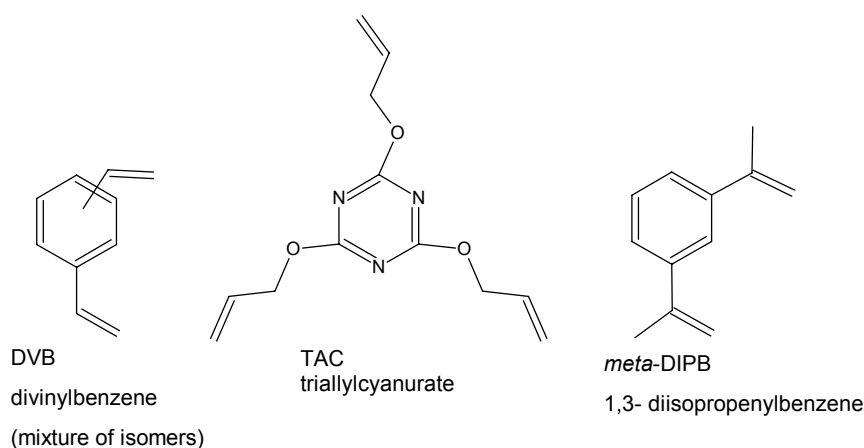
**Fig. 12: Crosslinkers.**

## *1.8. Base Polymers for Radiation Grafted Membranes*

There are many polymers that can be used as the base film for radiation grafting: perfluorinated, partially fluorinated, and hydrocarbon based polymers.

Radiation entails three different processes, chain scission, branching/crosslinking, and partial oxidation. Occurrence of those effects depends on intrinsic properties of the material. For example, polypropylene (PP) treatment causes predominantly branching and crosslinking, but radiation treatment of fluoropolymers leads mainly to chain scissions. Partial oxidation is leading to the creation of peroxy groups and even carboxylic groups while irradiation was carried out in the presence of oxygen (air). Irradiation in an inert atmosphere, like nitrogen, does not produce hydroperoxy

groups but free radicals, which can not recombine because they are immobilized in a backbone. Immobilized radicals cannot recombine with one another, because of the reduced mobility of a chain in solid phase. Crosslinking in hydrocarbon polymers, like polypropylene, is widely applied in industry, since it improves mechanical properties. In irradiated fluoropolymers, chain scission leads to a deterioration of mechanical properties. The best resistance to radiation was found for polyethylene (PE), this polymer can be treated with relatively high dose of 100-3000 kGy showing discoloration in contrast to polytetrafluoroethylene (PTFE), which, treated with a maximum dose of 80-600 kGy, exhibits disintegration.

PTFE is the first discovered and commercialized fluoropolymer. Nowadays PTFE is produced in a large scale, this is because PTFE offers superior oxidative stability among polymers as well as a high servicing temperature (260-300ºC). Unfortunately, PTFE is not processable by injection-molding extrusion to form a desired product, the high crystallinity reaching 90% and relatively high molecular weight are reasons for its extremely high viscosity ($10^{10}$-$10^{12}$ Pa·s)[70]. PTFE films are produced by skiving of billets, not as usually by extrusion for thermoplastics. High cristallinity is a real problem in grafting modification techniques and it was overcome by heating of PTFE film close to melting temperature and crosslinking with irradiation. The crosslinking freezes the amorphous state of a polymer, so that after cooling down the polymer can not produce the crystalline phase[71].

Since PTFE is processable only with special techniques, there is a demand for easy processable materials with similar properties like PTFE. Poly(tetrafluoroethylene-*co*-hexafluoropropylene) (FEP) is a perfluorinated polymer, which meets most of the requirements of PTFE, can be processed. The methyl $CF_3$ groups are distributed statistically, preventing excessive crystallization, finally FEP exhibits a lower crystallinity than PTFE and can be easily processed by extrusion and injection-molding. Generally, properties of FEP are similar to those offered by PTFE with the exception of the high servicing temperature, which is 204 ºC. FEP is considered to be a very good backbone polymer for a synthesis of radiation grafted membranes. A high range of extruded films is available on the market[70].

In a variety of perfluorinated polymers two poly(tetrafluoroethylene-co-perfluoropropyl vinyl ether), PFA, and poly(chlorotrifluoroethylene), PCTFE, should be considered. PFA exhibits very similar properties to PTFE. PFA has very good resistance to oxidative conditions and organic chemicals. PFA is easily processed into films by

conventional methods. An introduction of the "large" chlorine atom into a chain of PCTFE results in a lower tendency for crystallization. PCTFE is resistant to oxidative conditions as well as to ionizing radiation, whereas it is prone to an attack of organic chemicals. Both have been described as backbones for radiation grafting[70].

Another family of fluoropolymers are the partially fluorinated polymers, where not all hydrogens were replaced by fluorine. ETFE is a copolymer of tetrafluoroethlylene with ethylene, a copolymer is produced by the radical mechanism, due to the fact that ethylene cannot homopolymerize, and the product is an alternated copolymer. ETFE offers good mechanical properties after a radiation treatment. After grafting, grafted films inherit excellent mechanical of the backbone polymers (Table 3). The necessary dose to graft ETFE is lower than for FEP and PTFE.

The base polymer has a strong effect on the grafting process, and in consequence, on the final product. First of all, the irradiation has an influence on the base film, reducing mechanical properties, by chain scissions and oxidation reaction. Secondly, irradiation causes different quantities of active centers, being able to the initiation of polymerization. In addition, monomer swelling by the backbone is an important parameter. Different base polymers irradiated at the same dose grafted at the same parameters yields different graft levels (Table 3). Finally, the backbone has an influence on oxidative stability of the radiation grafted product (membrane) and the stability can be classified as follows[73].

**High Stability  PTFE, PFA  >  FEP  >  ETFE  >  PVDF  Low Stability**
**(Oxidative Stability)**

Fluorinated base polymers used for radiation grafted membranes offer the best oxidative stability compared to partially fluorinated, the worst oxidative stability was observed for non-fluorinated backbones, like PE. Despite a lower oxidative stability, membranes based on partially fluorinated polymers, after grafting, exhibit much better mechanical properties (tensile strength, elongation at break). These aspects were investigated by many researchers[72,73]. Thus, in this work, FEP as a backbone, offering high oxidative stability and acceptable mechanical properties, was chosen as a model backbone for grafting AMS and MAN in order to obtain membranes for fuel cell applications.

**Table 3: Properties of selected fluoropolymers. Grafting was performed after irradiation with a gamma source (dose 20 kGy in air, monomers Styrene/DVB at constant parameters: temperature, film thickness). Elongation at break was measured for irradiated samples with gamma rays in the air and the dose of 20 kGy[73].**

| Polymer | Crystallinity / % | Elongation at the Break / % | Graft Level / % (irradiated) | Elongation at the Break / % (irradiated) |
|---------|-------------------|------------------------------|-------------------------------|--------------------------------------------|
| PTFE | 38 | 350 | 16 | 10 |
| FEP | 26 | 320 | 44 | 120 |
| ETFE | 34 | 430 | 52 | 380 |
| PVDF | 46 | 240 | 78 | 160 |

**Table 4: Different base polymers used for a radiation grafting.**

| Name | Abbreviation | Structure |
|------|--------------|-----------|
| **Perfluorinated polymers** | | |
| Polytetrafluoroethylene | PTFE | $-(CF_2-CF_2)_n-$ |
| Poly(tetrafluoroethylene-co-hexafluoropropylene) | FEP | $-(CF_2-CF_2)_n(CF_2-CF(CF_3))_m-$ |
| Poly(tetrafluoroethylene-co-perfluooropropyl vinyl ether) | PFA | $-(CF_2-CF_2)_n(CF_2-CF(OC_3F_7))_m-$ |
| Poly(chlorotrifluoroethylene) | PCTFE | $-(CH_2-CF(Cl))-$ |
| **Partially fluorinated polymers** | | |
| Polyvinylidene fluoride | PVDF | $-(CF_2-CH_2)_n-$ |
| Poly(vinylidene fluoride-co-hexafluoropropylene) | PVDF-co-HFP | $-(CF_2-CH_2)_n(CF_2-CF(CF_3))_m-$ |
| Poly(ethylen-co-tetrafluoroethylene) | ETFE | $-(CH_2-CH_2)_n(CF_2-CF_2)_m-$ |
| Polyvinyl fluoride | PVF | $-(CF_2-CHF)_n-$ |
| **Hydrocarbon polymes** | | |
| Polyethylene | PE | $-(CH_2-CH_2)_n-$ |
| Polypropylene | PP | $-(CH_2-CH(CH_3))_n-$ |

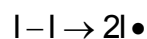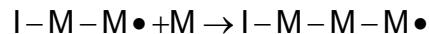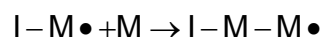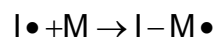# 2. Polymer Chemistry Methods

## 2.1. Polymerization

The radical polymerization is a chain reaction of monomers to grow a chain. The chain is initiated by the radicals produced from the decomposition of an initiator. Initiation can be provided also by electromagnetic initiation (UV, gamma radiation, X-ray), thermal autoinitiation[74], and ultrasound initiation[75].

The radical polymerization consists of mainly three kinds of reaction, initiation by the radical, propagation by reacting with monomer, chain transfer reactions, and finally chain stopping reactions, such as recombination or chain transfer to a non-active radial.
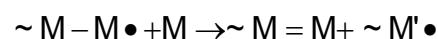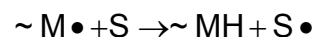
**Initiation:**

$I-I \rightarrow 2I\bullet$

**Propagation:**

$I\bullet + M \rightarrow I-M\bullet$
$I-M\bullet + M \rightarrow I-M-M\bullet$
$I-M-M\bullet + M \rightarrow I-M-M-M\bullet$

**Chain transfer:**

$\sim M\bullet + S \rightarrow \sim MH + S\bullet$
$\sim M-M\bullet + M \rightarrow \sim M = M + \sim M'\bullet$

**Termination:**

$\sim M\bullet + \sim M\bullet \rightarrow \sim M-M \sim$
$\sim M\bullet + \sim M\bullet \rightarrow \sim M = M + \sim M$
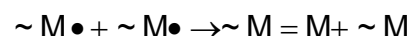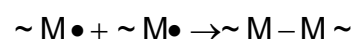
**Fig. 13: Mechanism of radical polymerization.**

Chain transfer to a monomer causes the initiation of a new chain, since chain transfer to the solvent can lead to chain termination or to a new chain with a part of a solvent. Chain transfer to a polymer involves branching and, in consequence, the product polymer is not linear but branched.

## 2.2. Copolymerization

The free-radical copolymerization is known as a reaction of two monomers, together forming a copolymer consisting of units from both monomers. The copolymer exhibits

properties combining those from parent monomers. This technique enables tuning of polymeric material properties by modification of composition. By the use of different monomers, new tailor made materials can be synthesized. In practice, copolymers have great meaning for industry, rather than homopolymers. The most well-known copolymers are ABS (acrylonitrile-butadiene-styrene) terpolymer. Since in copolymerization more then one monomer takes part in a reaction, thus a variety of products with respect to the monomer distribution along the chain can be synthesized. Following types of copolymers can be distinguished:

In random copolymers, the monomers are distributed statistically, no regular arrangement can be distinguished.

$\sim A - B - A - B - B - A - A - A - B - B - A - B - A \sim$

**Fig. 14: Random copolymer.**

Alternating copolymers contain a perfectly, or almost perfectly, alternating structure. Some pairs of monomers possess natural tendency to form alternating copolymers such as AMS and maleic anhydride.

$\sim A - B - A - B - A - B - A \sim$
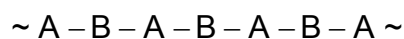
**Fig. 15: Alternating copolymer.**

Block copolymers are characterized by a highly organized structure, where regular blocks or groups of monomer can be distinguished along a polymer chain.

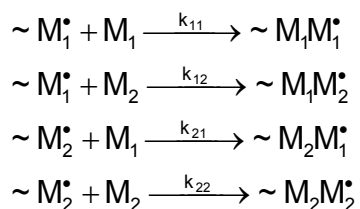$\sim A - A - A - B - A - A - A - B - A - A - A - B \sim$
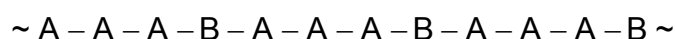
**Fig. 16: Block copolymer.**

In graft copolymers, a linear main chain called as the backbone can be distinguished from side chains attached to the backbone. Graft copolymers are highly branched, usually not soluble, depending on their degree of branching (Fig. 17).
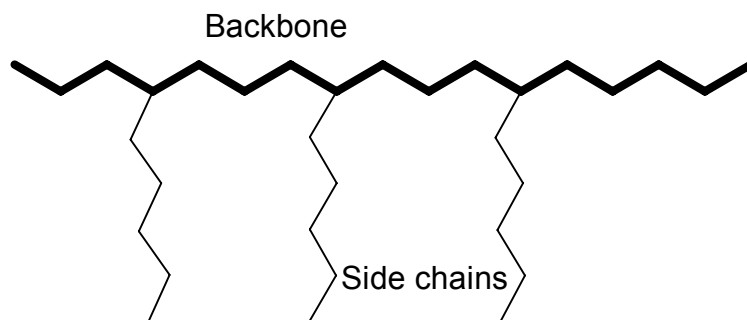
**Fig. 17: Graft copolymer.**

Radical copolymerization is carried out as a simultaneous polymerization of two (or more) monomers; however, there are also other methods. Since some monomers are more reactive than the others, differences between feed composition and copolymer composition are expected. In a simple homopolymerization two species are present, a monomer and a radical (active polymer chain). As the reaction proceeds, monomer molecules are attached to the radical increasing the chain length. In a copolymerization, the situation is more complicated, since two monomer species can react with one of two different chain ends. The four following equations, which describe a copolymerization, are given below:

$$\sim M_1^\bullet + M_1 \xrightarrow{k_{11}} \sim M_1 M_1^\bullet$$
$$\sim M_1^\bullet + M_2 \xrightarrow{k_{12}} \sim M_1 M_2^\bullet$$
$$\sim M_2^\bullet + M_1 \xrightarrow{k_{21}} \sim M_2 M_1^\bullet$$
$$\sim M_2^\bullet + M_2 \xrightarrow{k_{22}} \sim M_2 M_2^\bullet$$

The process of copolymerization is described by four kinetic constants, neglecting for simplicity termination reactions. The constant $k_{11}$ or $k_{22}$ are constants of homopolymerization of the two monomers $M_1$ and $M_2$, but since in the reaction there are two monomers, a cross reaction is possible. Therefore, constants $k_{12}$ and $k_{21}$ represent reaction of the radical originating from the monomer $M_1$ reacting with a monomer $M_2$, and radical $M_2$ reacting with monomer $M_1$, respectively.

Each chain terminated with a radical can react either with a monomer of the same type or with the other monomer. The reactivity of the active chain depends only on the properties of the last unit. This model was developed in the early 1940 by Mayo and it is called Mayo-Lewis[76] model or the terminal model. Nowadays, the terminal

model is widely applied to study copolymerization and the reactivity ratios are available for many monomer pairs or they can be estimated from the Alfrey-Price Q-e scheme[62]. The most important information obtained from the terminal model is the relation between monomer feed composition and a copolymer composition. The model is based on mechanistic relation of kinetic rate constants and its derivate as:

$$-\frac{d[M_1]}{dt} = k_{11} \cdot [M_1^\bullet] \cdot [M_1] + k_{21} \cdot [M_2^\bullet] \cdot [M_1] \qquad \text{EQ: 1}$$

$$-\frac{d[M_2]}{dt} = k_{12} \cdot [M_1^\bullet] \cdot [M_2] + k_{22} \cdot [M_2^\bullet] \cdot [M_2] \qquad \text{EQ: 2}$$

Dividing equation 1 by 2, the equation for instantaneous copolymer composition is found:

$$\frac{d[M_1]}{d[M_2]} = \frac{k_{11} \cdot [M_1^\bullet] \cdot [M_1] + k_{21} \cdot [M_2^\bullet] \cdot [M_1]}{k_{12} \cdot [M_1^\bullet] \cdot [M_2] + k_{22} \cdot [M_2^\bullet] \cdot [M_2]}$$

The concentrations of radicals $M_1^\bullet$ and $M_2^\bullet$ can be calculated by a steady-state assumption for each of them separately.

$$k_{21} \cdot [M_2^\bullet] \cdot [M_1] = k_{12} \cdot [M_1^\bullet] \cdot [M_2]$$

$$\frac{d[M_1]}{d[M_2]} = \frac{\dfrac{k_{11} \cdot k_{21} \cdot [M_2^\bullet] \cdot [M_1]^2}{k_{12} \cdot [M_2]} + k_{21} \cdot [M_2^\bullet] \cdot [M_1]}{k_{22} \cdot [M_2^\bullet] \cdot [M_2] + k_{21} \cdot [M_2^\bullet] \cdot [M_1]}$$

Simplification of the equation by dividing of the right side by $k_{21}$ [M_2*][M_1] gives a equation without radical concentrations.

$$\frac{d[M_1]}{d[M_2]} = \frac{\dfrac{k_{11} \cdot [M_1]}{k_{12} \cdot [M_2]} + 1}{\dfrac{k_{22}}{k_{21}} \cdot \dfrac{[M_2]}{[M_1]} + 1}$$

Defining reactivity ratios as:

$$r_1 = \frac{k_{11}}{k_{12}} \text{ and } r_2 = \frac{k_{22}}{k_{21}}$$

Multiplying the denominator and the numerator by the concentration of both monomers and introducing a definition of monomer ratios, the final copolymerization equation is obtained.

$$\frac{d[M_1]}{d[M_2]} = \frac{[M_1] \cdot ([M_2] + r_1 \cdot [M_1])}{[M_2] \cdot ([M_1] + r_2 \cdot [M_2])}$$

$d[M_1]/d[M_2]$ is the ratio of monomers consumed from the feed solution, thus it is the ratio of monomers entering the copolymer at the moment. The concentrations can be replaced by molar fractions. The copolymerization equation describes the instantaneous feed solution composition and copolymer composition. The composition of the feed mixture changes with the time of reaction, because the monomers are not equally consumed. For the composition calculation the equation has to be integrated either numerically or analytically.

The terminal model enables easy calculation of a copolymer composition by use of published literature reactivity ratios, even for multi-monomer systems. In the idealized terminal model, several influences were neglected, for instance:

- side chain reactions such as: termination, chain transfer
- influence of the penultimate unit
- solvent (polarity) influence

Although, some solvent effects on copolymer composition were found for radical copolymerization[77].

## 2.3. Other Grafting Techniques

Apart from radiation induced grafting, which is very convenient from a practical point of view, there are other methods for grafting of polymers. Basically, in order to graft a
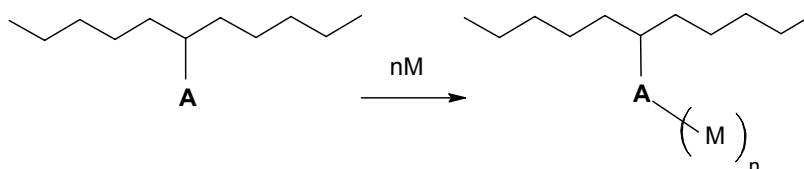
polymer, an active group needs to be created by a chemical reaction. There are three approaches of grafting[77]:
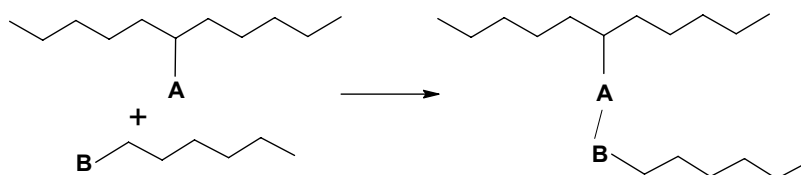


**Fig. 18: Grafting "onto" the backbone by reaction of two polymers.**

Grafting onto is a reaction between two polymer chains by reactive groups on side chains and a backbone.



**Fig. 19: Grafting "from" the backbone. The side chains grow from a backbone.**

When a polymer backbone plays the role of a multi-functional macro-initiator, a polymerization reaction is initiated. The side chains grow from a backbone.
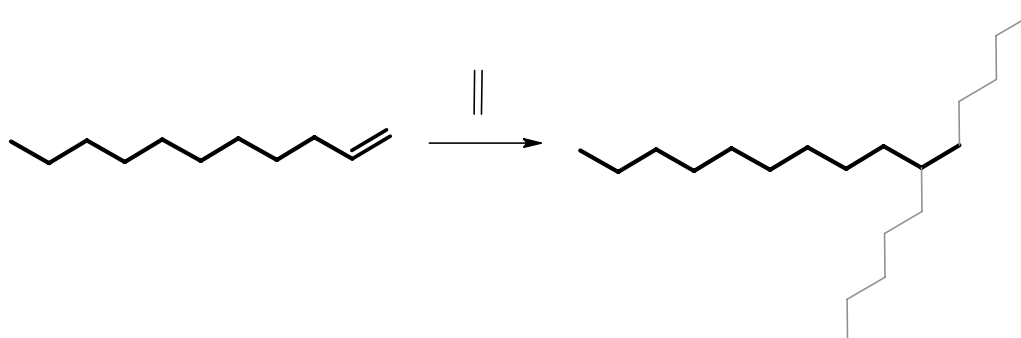


**Fig. 20: Grafting "through" the backbone.**

In this approach of grafting, the side chains with active bi-functional groups like double bond are necessary. The growing chain of the backbone reacts with a double bond of a side chain, forming a graft copolymer. In this method, side chains have to be introduced into the reaction mixture.

## 2.4. Chemical Grafting

Chemical grafting is known as the grafting initiated by a chemically created active center. In this method, the backbone plays the role of macroinitiator with a large number of initiating sites. A polymer backbone must be chemically prepared by chemical treatment to create active groups, later acting as initiators. Finally, grafting is carried out by activation of these groups, and side chains grow from the backbone[14].

## 2.5. Chain Transfer Grafting

Chain transfer grafting uses chain transfer reaction to graft a polymer onto a backbone. A polymer backbone is mixed with an initiator and a monomer and the reaction is initiated. During the reaction, a monomer polymerizes, some radicals are transferred to the backbone starting the polymerization from the backbone and leading to a grafted polymer. During the grafting reaction a high yield of homopolymer is formed, since the reaction of homopolymerization initiated by the initiator and only a small fraction of monomer is grafted to the polymer[78].

## 2.6. Grafting by Controlled Radical Polymerization

Today, in polymer science the development of controlled radical polymerization (CRP) is observed. The use of CRP in grafting gives a better control over grafted side chains, therefore a graft copolymer with a narrow distribution of side chain lengths can be synthesized as well as it is a new tool to synthesize side chains with a block structure[14]. There are several methods to control growing chains ATRP, RAFT, etc.

## 2.7. Ionic Grafting

A polymer backbone can be grafted by an ionic mechanism, if the cationic or ionic active center is created. Gamma radiation initiated cationic grafting was reported and monomers, hardly homopolymerizable according to a radical mechanism, were grafted on many kinds of polymeric backbones by this method. A group able to start an ionic polymerization can be chemically created and chemically activated. This

process requires typical conditions, like for ionic homopolymerization: water free conditions, inert atmosphere and high purity must be strictly provided[17].

## 2.8. Nano and Micrografting

Radiation grafting was used for patterning with lateral dimensions as small as 100 nm were grown onto ETFE backbone. In order to graft a polymer as a microstructure, the pattern is written by either electron beam or X-ray on a backbone. Subsequently, an irradiated backbone is exposed to a monomer solution to perform polymerization from the backbone. After the grafting, growth of the polymer occurs only on the irradiated area and the polymer chains forms "brush-like" structures on backbone surface. The covalently bound polymer to the backbone can be further modified chemically to obtain desired properties or functionality[79,80].

Micrografting is an interesting complementary tool for nanotechnology as well as a potential method for combinatorial chemistry and screening technologies in life science.

# Experimental

## 3. Grafting

### 3.1. Monomers

Methacrylonitrile (MAN) 99% (GC), stabilized with 50 ppm monomethyl ether hydroquinone; α-methylstyrene (AMS) 99% (GC) 15 ppm 4-(tert-butyl)catechol, divinylbenzene (DVB) technical grade (mixture of isomers: 56,3% meta, 24.4% para and 20% of ethylvinylbenzene) stabilized with 0.1% 4-(tert-butyl)catechol; 1,3-diisopropenylbenzene (DIPB) 97% (GC), unstabilized.

All monomers were purchased from Aldrich. Monomers were used as they were received, without removal of inhibitor 4-(tert-butyl)catechol for grafting. For the synthesis of copolymers poly(AMS-co-MAN), monomers were washed with an aqueous solution of sodium hydroxide (2%), dried with calcium oxide and distilled under vacuum.

### 3.2. Chemicals

Analytical reagent grade isopropanol, acetone, dichloromethane, toluene, and methanol were purchased from Fisher Scientific. Water was purified by a Seralpur® PRO 90 CN system and the conductivity of the purified water was < 0.1 μS/cm. Potassium hydroxide and potassium chloride were analytical grade and purchased from Merck (pro analysi). Chlorosulfonic acid 98% was purchased from Fluka.

### 3.3. Irradiation of Films

Backbone polymer (FEP) poly(tetrafluoroethylene-co-hexafluoropropylene) (Teflon® FEP 100A) films of 25 μm thickness were purchased from Du Pont (Delaware, USA). The films were cut into pieces of 13 × 13 cm and two holes were made in the parallel line of the extrusion direction. The mass of the film sheet was ca. 0.9 g per 13 × 13 cm sheet. The films were washed in ethanol (technical grade), dried in vacuum at 80 ºC, transferred to polyethylene zip lock bags and sealed.

Electron-Beam irradiation was performed at Studer AG, (Däniken, Switzerland) with an electron accelerator manufactured by IBA SA (Louvain-La-Neuve, Belgium). The accelerating voltage was 1.05 MV. Irradiation doses were controlled by radiochromic film dosimeters manufactured by Far West Technology Inc. (Californa, USA) containing an organic dye tris{4-[bis(2-hydroxyethyl]amino)phenyl} acetonitrile dispersed in 50 μm thick polyamide films. Samples were spread on a conveyer tray and passed under the electron beam. The radiation dose was maintained by the velocity of the conveyer under the radiation source. After irradiation, films were packed into a thermally insulated box together with dry IEC and shipped to the laboratory. In the laboratory, films were stored at -80 ºC until they were used.

## 3.4. Graft Copolymerization of AMS/MAN

Films were loaded to trap-tube reactors, subsequently the reactors were filled with the grafting solution. In order to remove oxygen, reactors were purged with nitrogen (at 10 NL/h) for one hour and than the reactors were sealed and placed into a heating water bath (60 °C). After the reaction, the grafting solution was removed and then the reactor with the product was washed twice with acetone. Grafted films were removed from reactors and dried in a vacuum oven at 80 ºC for 3 hrs.

During the reaction 0.9 g base film increases its mass as a consequence of grafting reaction. The mass increase for a film grafted with a graft level of 40 % is equal to 0.54 g. In this case the grafting solution was depleted from the monomers by 0.54 g, assuming the average density of monomers is 0.85 g/cm$^3$, the volume of consumed both monomers is 0.64 cm$^3$. Further, comparing with 18 cm$^3$ of both monomers in a grafting system, it was calculated that only 3.5 % of monomers was consumed during the grafting reaction, therefore, changes of concentration in the liquid phase can be neglected.

## 3.5. FTIR Spectroscopy

The mid-IR spectra were measured at 2 cm$^{-1}$ resolution with a PerkinElmer FTIR System 2000 spectrometer. Samples were either free-standing grafted films or prepared as KBr pellets. Films were 3 times folded in order to enhance intensities of important bands for a qualitative analysis. KBr pellets were prepared by a standard

technique where 3-5 mg of a sample was compounded and pressed with 300 mg of KBr.

The curve-fitting GRAMS/AI software (v.7.01) from Thermo Electron Corporation (Waltham, USA) was used to fit all vibrational spectra, and the fitted peak shapes were taken to be a mixture of Gaussian and Lorenzian forms. All spectra were well defined, and consistent fits were obtained without fixing any fitting parameters for the analysis of the radiation-grafted films. The applied software supports the Levenberg-Marquart algorithm for peak deconvolution[81].

Membranes were converted into a salt since the acid form of the membrane swells water from the air which affects the FTIR spectra. For this purpose, membranes were immersed into 0.5 M aqueous solution of KCl, dried and the spectrum was recorded.

## 3.6. Elemental Analysis

Elemental analysis of nitrogen was performed in order to find a calibration curve for a quantitative FTIR method. Samples of poly(AMS-*co*-MAN) were analyzed for their nitrogen content. The apparatus LECO CHN-900 (LECO Corporation, St. Joseph, MI, USA) was used for the analysis. Accuracy of the method and equipment is about 0.3% absolute.

## 3.7. Membranes

Grafted films were sulfonated according to the following procedure to convert them into membrane form: Six films were rolled and bound together with the PTFE tape. Solution of chlorosulfonic acid was prepared by mixing of 30 $cm^3$ of chlorosulfonic acid and 650 $cm^3$ of dichloromethane. Films were submerged in the solution in vertical position. Sulfonation was carried out in a tube shape vessel for 6 hrs at room temperature.

The films were taken out with tweezers, washed once with water, and immersed in aqueous solution of sodium hydroxide (0.4%) for 6 hrs. Membranes were rinsed with water and placed in 2 M aqueous solution of sulfuric acid for 6 hrs, in order to retrieve the acidic form of a membrane. After removal on the acid, membrane conditioning was performed by heating the membrane in distilled water at 80 ºC for a minimum 6 hrs. Water was replaced until the pH-value the reached range of 6-6.5.

## 3.8. Ion Exchange Capacity and Swelling

Ion exchange capacity was measured with acid-base titration and swelling with gravimetric analysis. The percent swelling is the percent difference between the mass of the water-swollen membrane and its dry water-free form (salt form), and the IEC is the number of moles of acid groups per unit mass of membrane. The IEC and swelling measurement were carried out as follows:

Six disks (diameter 20 mm) were cut off a membrane, the wet mass ($m_{wet}$) of two discs was determined by weighing, each of two disks was placed in a 50 cm$^3$ beaker filled with 0.5 M KCl, the beakers were covered with Parafilm® and allowed to be stirred with a magnetic bar over night. An amount of the beaker was titrated with 0.05 M KOH to estimate the volume ($V_{KOH}$) for sodium hydroxide necessary for neutralization of the liberated HCl. After titration the weight of a sample ($m_{salt}$) in salt form (dry state) was estimated. The dry mass ($m_{dry}$) representing a dry membrane in the acid form was calculated as follows:

$$m_{dry} = m_{salt} - 38.1 * 0.05 * V_{KOH}$$

The IEC was calculated according to the followed formula:

$$IEC = 0.05 \cdot \frac{V_{KOH}}{m_{dry}} \cdot 1000$$

Swelling was calculated using the following formula:

$$Swelling = \frac{m_{wet} - m_{dry}}{m_{dry}} \cdot 100\%$$

Three titrations were performed for each membrane sample.


## 3.9. Conductivity

Discs (6 pcs) of the fully swollen membrane (diameter 20 mm) were assembled between platinum contact discs in the conductivity cell. To provide a good contact between disc and membrane a mechanical load was applied.

The membrane conductivity was recorded at ambient temperature (21 ºC) by impedance spectroscopy using the Zahner IM6/IM6e equipment and the conductivity cell (Fig. 21). Measurements were performed in the galvanostatic mode at zero current and an amplitude of 5 mV in the frequency range from 1 to 50 kHz. The

membrane resistance was determined by extrapolating the high frequency end of a Nyquist plot to the real axis, whereby a linear regression with the values of the ten highest frequencies was made.
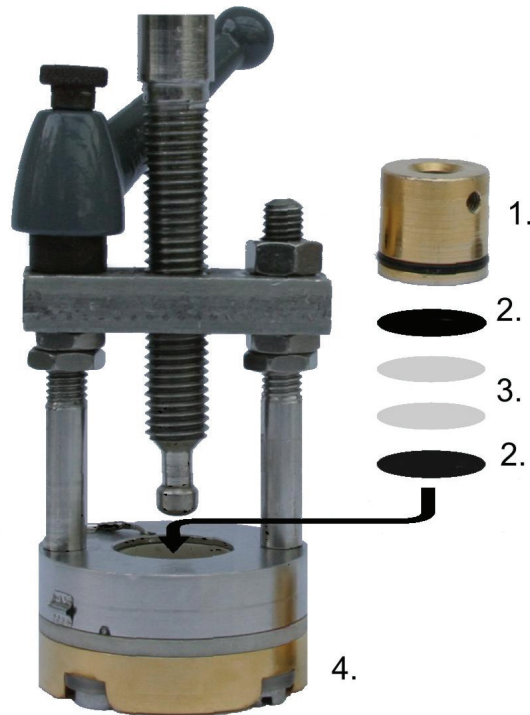


**Fig. 21: Conductivity cell and its assembly. (1) piston, (2) platinum discs, (3) stack of membranes, (4) cell body.**

The measurement was performed for 2, 3, 4, and 5 membrane discs in order to estimate the contact resistance between a membrane and a platinum contact discs. It was assumed that the contact resistance between membranes is negligible. For the estimation of the contact resistance (membrane to platinum disc) the resistivity was plotted against number of membranes, which gives a linear correlation. A value of the resistivity extrapolated to the number of membranes equal to zero, is the contact resistance. Resistivity of a membrane was calculated by a linear fit, where the slope gives the membrane resistance. Thickness measurement for the calculation of conductivity was carried out 5 times using an equipment delivered by Heidenhain Corporation (Schaumburg, USA) type VRZ 403 (read out) and MT12B (sensor) taking the average of five values.

# 4. Fuel Cell Tests

## 4.1. Durability and Performance Test

The MEAs were assembled using Elat type carbon cloth electrodes from E-TEK (Somerset NJ, USA) with a Pt loading of 0.6 mg cm$^{-2}$ (20% Pt/Vulcan XC72) without hot pressing and Nafion® impregnation. The experiment with membrane No. M5 was carried out with E-TEK electrodes with a Pt loading of 0.4 mg cm$^{-2}$. The MEAs were assembled into graphite single cells with an active area of 30 cm$^2$. The flowfields were shaped with serpentine flow channels. The cells were operated in the temperature range from 60 to 80 ºC using hydrogen and oxygen as a fuel and oxidant, respectively. Humidity and flow stoichiometry of both gases were controlled. The gas pressure at outlet ports was 1 bar$_a$. The cell was operated at a constant current density of 500 mA cm$^{-2}$.
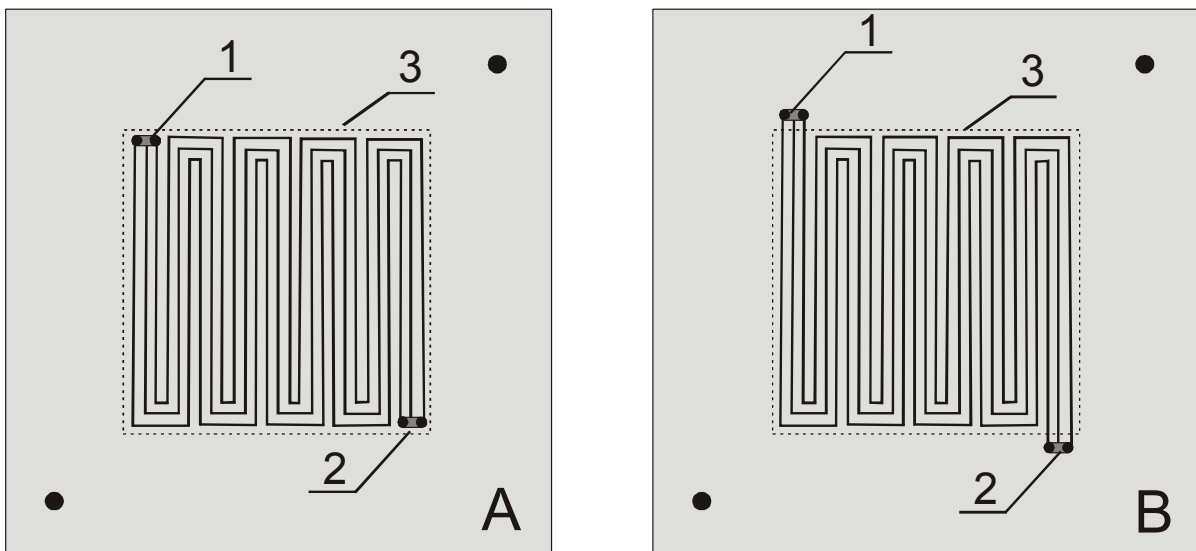


**Fig. 22: Flowfield with "normal" gas inlet (A) used for experiments: M1, M2, M3, M4, M6 and flowfield with hidden (B) gas inlet used for experiment M5. (1) inlet, (2) outlet, (3) active area (within dashed line).**
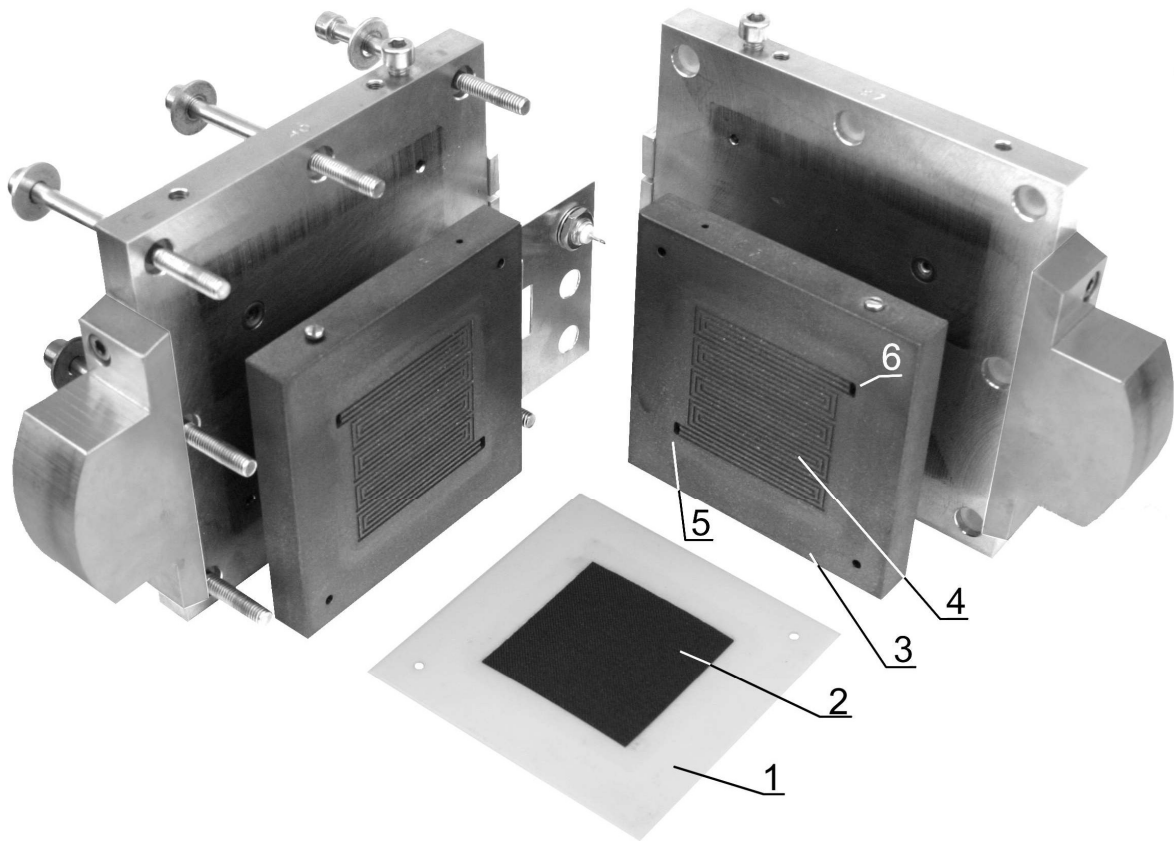
**Fig. 23: Fuel cell assembly. (1) gasket, (2) MEA, (3) flowfield, (4) channels, (5) and (6) gas inlet and outlet.**

## 4.2. In Situ Ohmic Resistance

The *in situ* membrane resistance was measured during fuel cell experiments using the current pulse method. Sequences of current pulses of 5 A generated by a fast pulse generator (rise time <10 µs, pulse duration 10 ns, built at PSI), were superimposed to the DC current delivered by the fuel cell. The rising edges (current switched off at t=0) of the resulting transient of cell voltage were sampled by a fast digital oscilloscope and evaluated in a time window of 400-880 ns. The membrane resistance was calculated by the Ohm's law. Transient heights of 10 mV (corresponding to 2 mOh ms and 56.6 mOhm $cm^2$, respectively, for 29.16 $cm^2$ cells) is resolved with an accuracy better than 5%. Details of this method are described elsewhere[82,83,84].

# 5. Post Mortem Analysis

For the *postmortem* analysis, the electrodes have to be peeled off the membrane and the surface of the membrane has to be cleaned from remaining particles of the electrode, since those particles may make the further measurements difficult. Since the MEA is very fragile and the membrane may be brittle in dry state, the MEA was conditioned very carefully in water at 80 ºC for 5 hrs without stirring. After the conditioning, the electrodes were peeled off from the membrane, in cases when it was not possible the MEA was submerged in water and subsequently, treated with ultrasound then the electrodes were separated from the membranes. When black spots from the electrodes remained on the membrane surface, an additional washing stage with ultrasound was applied for about 2 hrs or longer. With the described method all MEA's were successfully disassembled, even hot-pressed ones.

## 5.1. Degree of Degradation

The average membrane degradation was estimated by an acid-base titration of the membrane after separation of the active area from the rest of the membrane by cutting off the edge. Before the titration of both parts, the active area and the edge were exchanged in 2 M sulfuric acid for 6 hrs and deacidified in a beaker with water at 80 ºC. Water was exchanged until a pH value of 6-6.5 was reached. The loss of IEC in the active area was calculated according to the formula:

$$IEC\,Loss = \frac{IEC_{Active\,Area}}{IEC_{Pr\,istine\,Sample}} \cdot 100\%$$

The accuracy of this method was found to be +/- 5% absolute.

## 5.2. Degradation Analysis with FTIR

After fuel cell testing of the radiation grafted membranes the backbone remains intact, and degradation is only observed for the grafted component[85]. This offers the opportunity to use FTIR spectroscopy to analyze the grafted component.

Membranes were exchanged in 0.5 M KCl, dried in vacuum, and the FTIR spectra was recorded with conventional FTIR spectrometer. A peak for benzene ring at 1009 cm$^{-1}$ was intergraded. The degradation was calculated as follows:

$$\text{Degradation} = \frac{A_P - A_D}{A_P} \cdot 100\%$$

Where:

$A_D$ – Peak area at 1009 cm$^{-1}$ of an active area

$A_P$ – Peak area at 1009 cm$^{-1}$ of a pristine sample

The peak for a stretching vibration for S=O at 1038 cm$^{-1}$ is not appropriate for the analysis because it is a very intense peak (exceeding 2 absorbance units). The analyzed peak at 1009 cm$^{-1}$ for samples exhibiting high IEC value shows very high intensity reaching 2 absorbance units and consequently, it results in a higher error of measurement.

# Results & Discussion

## 6. Grafting

### 6.1. Preparation of AMS/MAN Copolymers (poly(AMS-co-MAN)

The preparation of poly(AMS-co-MAN) copolymers was performed in bulk. AMS and MAN were purified from stabilizer, distilled under reduced pressure and stored cold prior to their use. The radical initiator AIBN was used as received. Monomer and the initiator were placed in a 2-necked reaction flask, equipped with a gas inlet and outlet, magnetic stirrer, and a water bath. After 90 hrs of reaction time, the polymers were precipitated with methanol, washed, and dried in vacuum.

### 6.2. Spectroscopy of Films and Membranes

Radiation grafted films and membranes are challenging for the component analysis as well as for morphological studies, due to their properties such as insolubility and chemical resistance. The most straightforward characterization methods for those samples are optical methods like FTIR, Raman, UV, and fluorescence spectroscopy. In this study a spectroscopic analysis focused on FTIR was considered as a main tool and Raman spectroscopy was used as the auxiliary technique. UV spectroscopy is not suitable because of the high absorbance obtained. Fluorescence is mentioned as a potential technique for a composition analysis of aromatic crosslinkers, such as DVB and DIPB.

There is no difference between a blend and a grafted copolymer by means of FTIR and Raman spectroscopy since the grafted polymers yield the bands as the blends[86]. That is to say, FEP grafted with styrene (FEP-g-Styrene) gave the same spectrum like blended with polystyrene.

Strong and moderately strong peaks of backbone, due to an extremely high absorbance can not be quantitatively measured by FTIR. Strong vibrations cover some regions of the spectrum, however, apart from the covered regions the observation of vibrations originating from a grafted component is possible. Weak peaks of the backbone can be analyzed and compared with peaks from the grafted

component to analyze a composition (graft level). The most important vibrations identified[87] in AMS/MAN membranes and films are given as follows:

**FEP**

1385-1052 cm$^{-1}$ C-F, strong

982 cm$^{-1}$ weak

**Membranes (FEP-g-poly(AMSSA-co-MAN))**

3800-3000 cm$^{-1}$ OH, stretch, strong

3150-2813 cm$^{-1}$ C-H, stretch, strong,

2235 cm$^{-1}$ CN, stretch, moderate

1600 cm$^{-1}$ aromatic ring

1635-1540 cm$^{-1}$, aromatic band strong

1039 cm$^{-1}$ S=O, stretch, very strong

1009 cm$^{-1}$ aromatic ring (sulfonated)

**Films (FEP-g-poly(AMS-co-MAN) )**

3150-2813 cm$^{-1}$ C-H, stretch, strong

2230 cm$^{-1}$ CN, stretch, moderate

1600 cm$^{-1}$ aromatic ring, moderate

1580 cm$^{-1}$ aromatic ring, moderate

Based on vibrations for the benzene ring at 1600 cm$^{-1}$ and the nitrile group at 2235 cm$^{-1}$ a method for analysis can be found, due to the fact that both vibrations do not overlap with the backbone.

The strong vibrations for S=O at 1039 cm$^{-1}$ and the benzene ring at 1009 cm$^{-1}$ can be used for an analysis of membrane degradation after a fuel cell test.

### 6.3. Quantitative FTIR Analysis

FTIR is the most convenient method, for the analysis of the composition of a grafted film with respect to AMS and MAN content. For the FTIR analysis, characteristic vibrations for AMS (1600 cm$^{-1}$) and methacrylonitrile (2235 cm$^{-1}$) were selected and the ratio method was employed[86]. Since the peak at 1600 cm$^{-1}$ overlaps with the

peak at 1580 cm$^{-1}$, the peak deconvolution was applied in order to obtain the area of the peak at 1600 cm$^{-1}$. The ratio method combines a relationship between weight ratios of AMS to MAN in the copolymer and peak areas in FTIR spectrum, respectively. In order to obtain an analytical equation to calculate the weight ratio, the factor F must be determined. For this purpose, the following method is proposed:

- Preparation of the homopolymer blends, and the use of the blends with known composition as standards for FTIR analysis.
- Preparation of several copolymers, measurement of the composition with an other method (e.g. elemental analysis), to use the copolymers as a FTIR standard.

PolyAMS and polyMAN are non-miscible homopolymers and the method based on homopolymer blends is difficult to apply, since incompatibility can influence the composition of prepared blend. The method is based on the standards prepared with different AMS content. AMS content was estimated by an elemental analysis of nitrogen. The elemental analysis data was used to calculate the content of AMS and MAN in copolymers.

$$\frac{w_{AMS}}{w_{MAN}} = \frac{A_{1600}}{A_{2235}} \cdot F$$

Where:

$w_{AMS}$ – weight of AMS

$w_{MAN}$ – weight of MAN

$A_{1600}$ – Peak area for AMS at 1600 cm$^{-1}$

$A_{2235}$ Peak area for MAN at 2235 cm$^{-1}$

F- Constant

After the FTIR spectra were recorded, the peaks were integrated and the peak ratio was plotted against the monomer ratio in the copolymer. The weight ratios obtained previously by elemental analysis of AMS/MAN vs. peak ratio are presented in Fig. 24.

$$\frac{w_{AMS}}{w_{MAN}} = \frac{A_{1600}}{A_{2235}} \cdot F$$

F=2.37352

R=0.99804

St.Dev.=0.03962
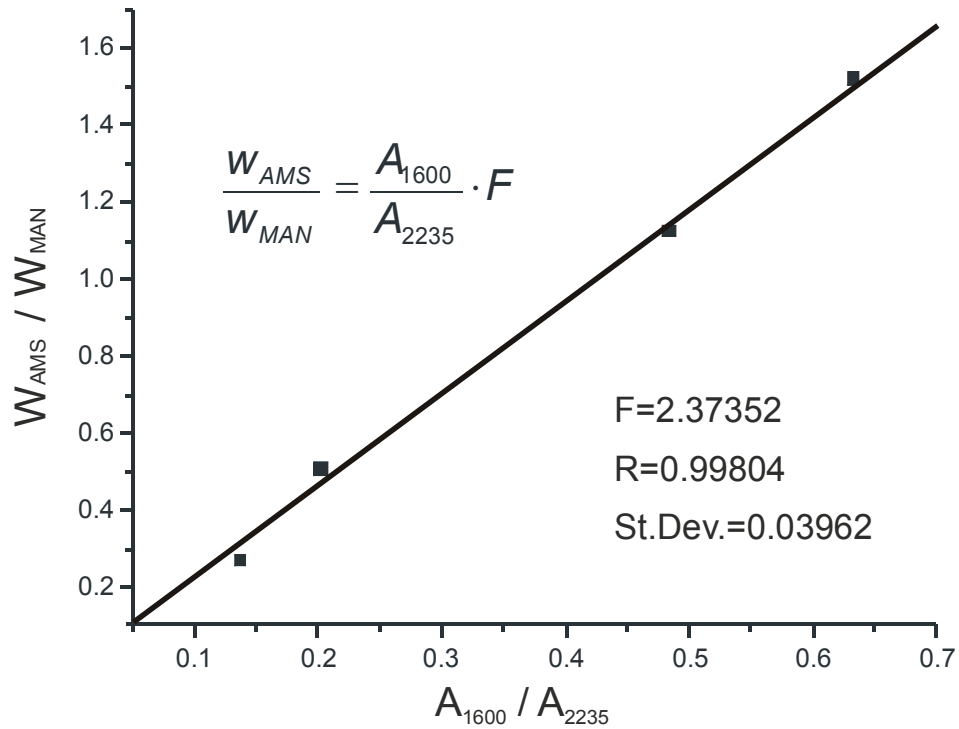
**Fig. 24: Calibration curve for a composition analysis of AMS/MAN copolymers.**

The ratio can be converted to a weight fraction by the equation:

$$X_{AMS} = \frac{R}{R+1} \quad \text{where: } R = \frac{w_{AMS}}{w_{MAN}}$$

The total AMS content in grafted film is given by:

$$C_{AMS} = X_{AMS} \cdot GI$$

Where:

GI- graft level

## 6.4. Solvent Influence on Grafting AMS/MAN

Grafting of AMS/MAN was performed in four different solvents: isopropanol, isopropanol-water, toluene, and methanol. The influence of solvent type and concentration of monomers was studied on both AMS content and the graft level. Grafting time of 22 hrs, molar AMS/MAN ratio of 1.5, and preirradiation dose of 25 kGy were maintained constant.
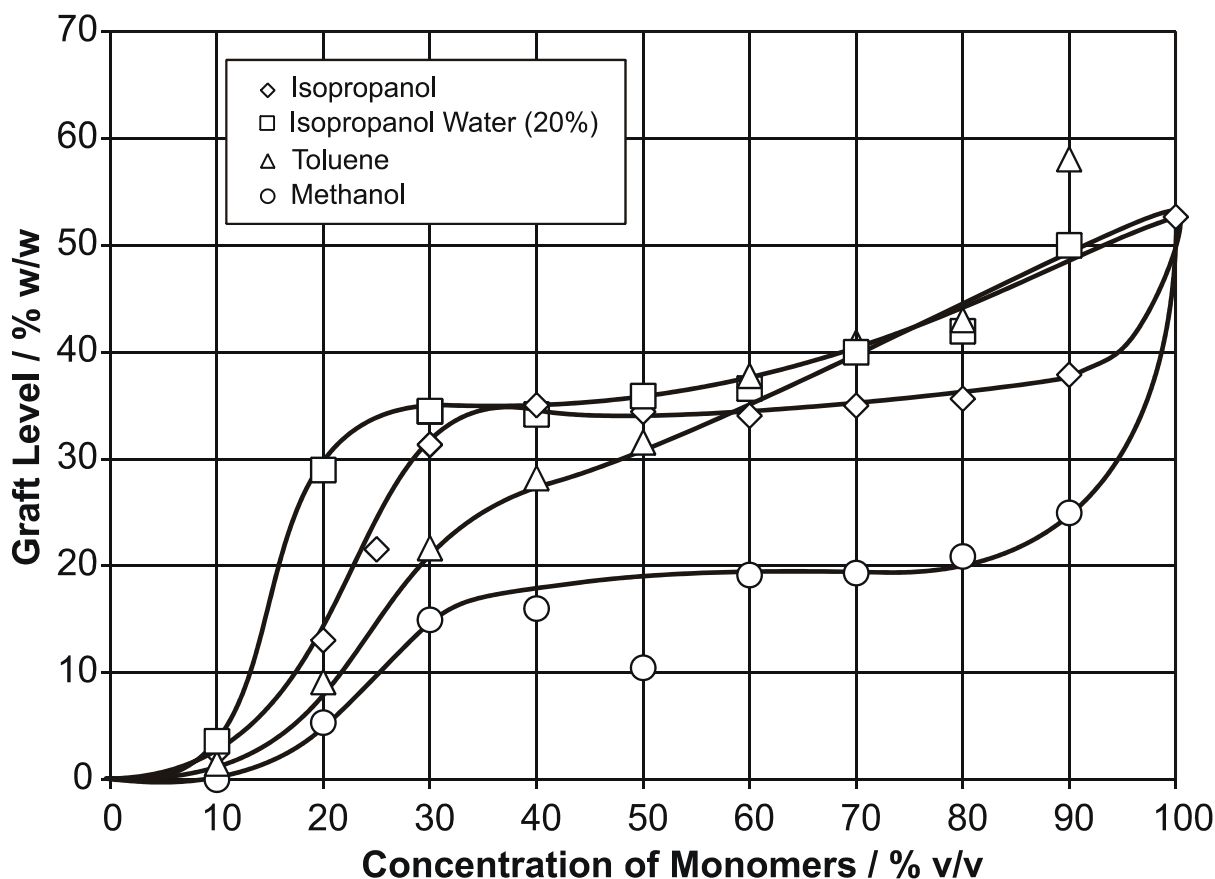
**Fig. 25: Grafting of AMS/MAN from FEP in four different solvents at different concentration of both monomers (monomers = AMS+MAN). Temp. of grafting 60°C. Time 22 hrs. $R_m$=1.5.**

Graft levels as function of monomers concentration and solvent type were plotted for different solvents in Fig. 25. Grafting in the isopropanol-water solvent system yielded the highest graft levels at low concentration of monomers (lower than 35%). An increase of graft level is caused by a partitioning effect, wherein water, as a non-solvent for both monomers, influences the partitioning of monomer between two phases, a liquid and a solid phase. Addition of water increases the concentration of monomers in the solid phase. Therefore, the graft levels at low concentration of monomers are the highest for a low concentration of monomers. Graft levels obtained in isopropanol-water are higher for concentration of monomers higher than 40%, due to the fact that water increases more the concentration of AMS in the solid phase then MAN. An increasing concentration of AMS causes a decrease of the graft level, because AMS reacts slower. Further, chain transfer to a monomer (AMS) is responsible for chain termination.

The lowest graft levels over the whole range of concentrations were obtained using methanol. Those graft levels were even lower than values determined for toluene. However, Rager[18] reported the opposite trend for styrene grafting from FEP films. For AMS/MAN system chain transfer to methanol is stronger than in case of styrene, which results in faster chain termination.
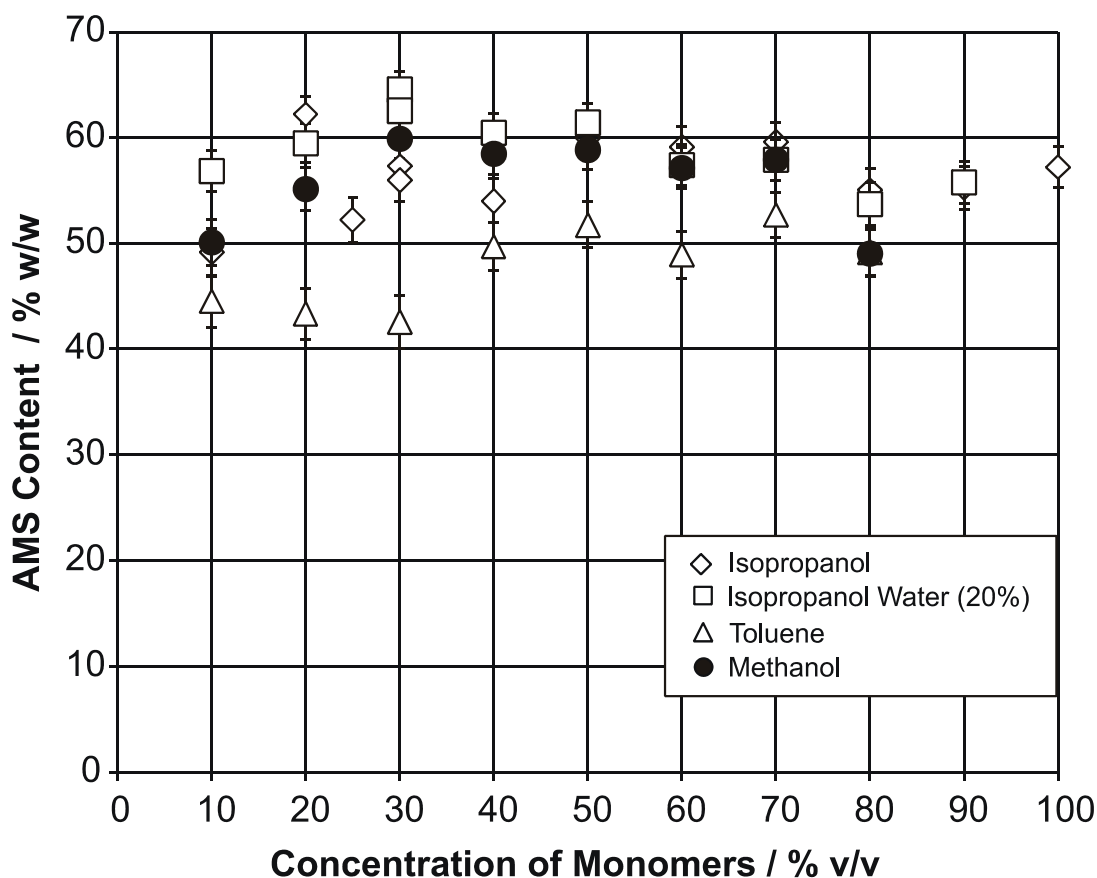


**Fig. 26: AMS content in grafted films with respect to solvent type and monomer concentration. Error bars represent standard deviation.**

The AMS content in grafted films was analyzed by FTIR spectrometry. In Fig. 26 the content as a function of monomer concentration for the four solvents is presented. The isopropanol-water mixture gave the highest AMS concentration (64%), when concentration of monomers was equal to 30%. For all solvent systems, with increasing monomer concentration, the AMS content tends to approach the value obtained without a solvent. As the monomer concentration increases, the solvent effect is less observable, since the solvent is present in a lower fraction in the grafting mixture. The lowest AMS concentration was obtained for toluene. The difference of

AMS concentration in samples grafted in toluene and those grafted in isopropanol and toluene is 20%$_{w/w}$. The observed effects, altering the AMS content, are attributed to a partitioning of monomers between the liquid phase – grafting solution and the solid phase – grafted film. A polar solvent like isopropanol or methanol increases the effective concentration of AMS-monomer in the film during the grafting reaction. The effect is even stronger when a non-miscible (with monomers) solvent, a polar solvent like water is added. AMS as a hydrocarbon monomer is less polar than MAN containing the polar nitrile group. Therefore, water as a polar solvent increases the concentration of AMS monomer in a grafted film (solid phase) to a higher extent than MAN.

Since the monomers were used without removal of the inhibitor, a partitioning of the inhibitor is another effect, which increases the graft level for a series of grafted films, when water was present in the grafting solution. The inhibitor, being a polar phenol derivative, accumulates in the liquid phase (grafting solution) leaving the phase of the reaction free from inhibitor, as a consequence a higher graft level is obtained.


## 6.5. Kinetics of AMS/MAN Grafting

The investigation of variation of graft level with time was performed for two different mixtures, either using an isopropanol/water mixture or isopropanol only as a solvent at the temperature of 60 ºC. Results are displayed in the Fig. 27. The data obtained for samples grafted in the presence of isopropanol/water at the temperature of 50 ºC are included as well for comparison.

After 65 hrs of grafting reaction, saturation could not be achieved since the curves did not level off showing that the grafting reached a maximum. A water containing grafting solution showed a dramatic increase of grafting rate at the early phase of grafting (the first 10 hrs of reaction), as compared with the experiments carried out without water as well as at a lower temperature (50 ºC).

At the mentioned early phase of grafting (10 hrs), there is no difference between the series grafted with the same non-aqueous condition (composition of the grafting solution), but at the lower temperatures 60 and 50 ºC. Further, with increasing reaction time, the samples grafted at lower temperature exhibited higher graft levels. The difference in graft level of samples with different composition of grafting solution is increasing with time of reaction time. This effect is explained by a recombination of

radicals. At lower temperature, the recombination reactions are not significant, having a lower influence on the final graft level. At 60 ºC, termination by recombination is favored, due to a higher concentration of radicals, thus the final graft level is lower as compared to the data set grafted at 50 ºC.

At very early phases of the reaction, occurring in the first few hours, an inhibition period was not detected and the reaction starts immediately, producing a grafted film. The retardation time is observed for a system containing a free radical inhibitor (t-butyl-cathechol), then for the first hours of reaction the formation of a grafted film could not be observed. This showed that the investigated grafting systems are not susceptible to the low concentration of a free radical inhibitor, as it is present in commercially available monomers.

The samples from three grafting experiments were analyzed with FTIR for their AMS content in order to study the dependence between the graft level and the AMS content (Fig. 28). The investigation of grafted films for the composition by FTIR analysis revealed a relatively constant concentration of AMS in the grafted films. At the early phase of grafting (<10 hrs) the concentration of AMS in films seems to be lower than in the terminal phase (after 30 hrs). The effect of changing the concentration with time of grafting can be related to the fact that MAN reacts first, being initiated by active radicals from the base film, later a copolymer AMS-co-MAN is formed.

This type of behavior was described by Becker[36] for ETFE grafted with AMS and AN. It was found that the composition of the grafted material changes from a low to a high concentration of AMS in films. It was suggested that AN initiates the reaction and forms short chains of a homopolymer, then both monomers can form a copolymer. However, there is a significant difference between MAN and AN in terms of the kinetic constant of homopolymerization; that is to say, the kinetic constant for MAN is 1000 times lower than for AN. Since the tendency for homopolymerization is reduced, the effect is expected to be minor.
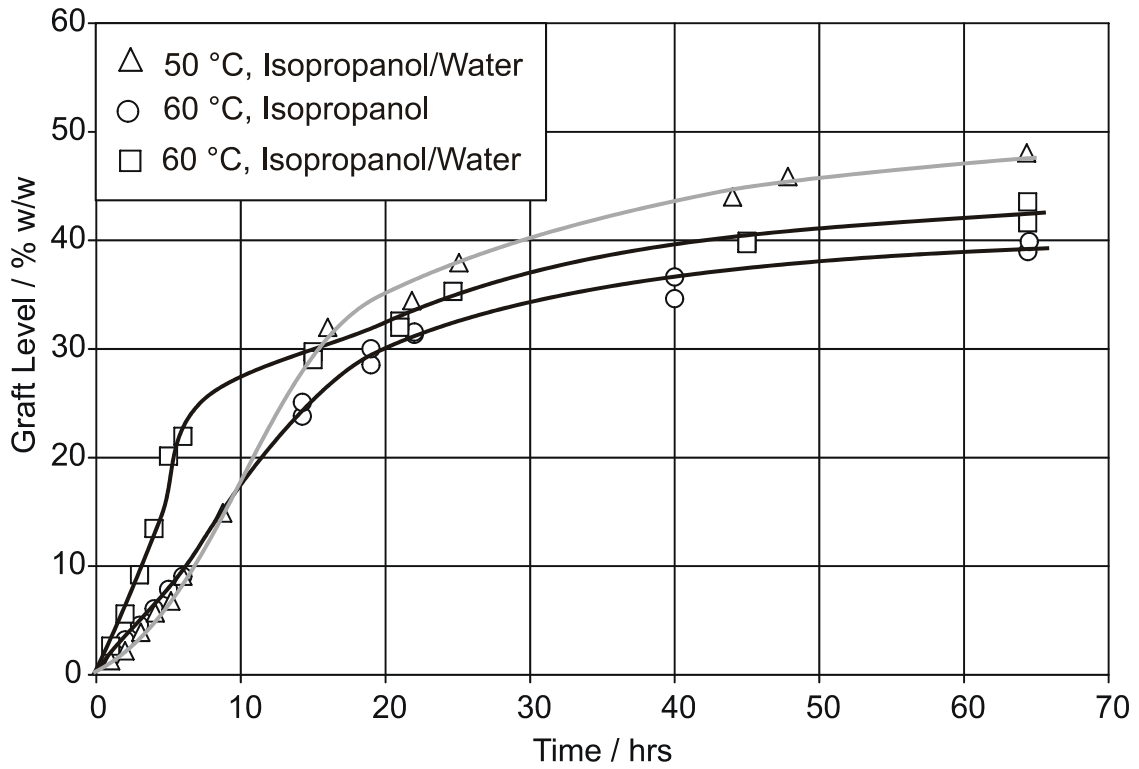
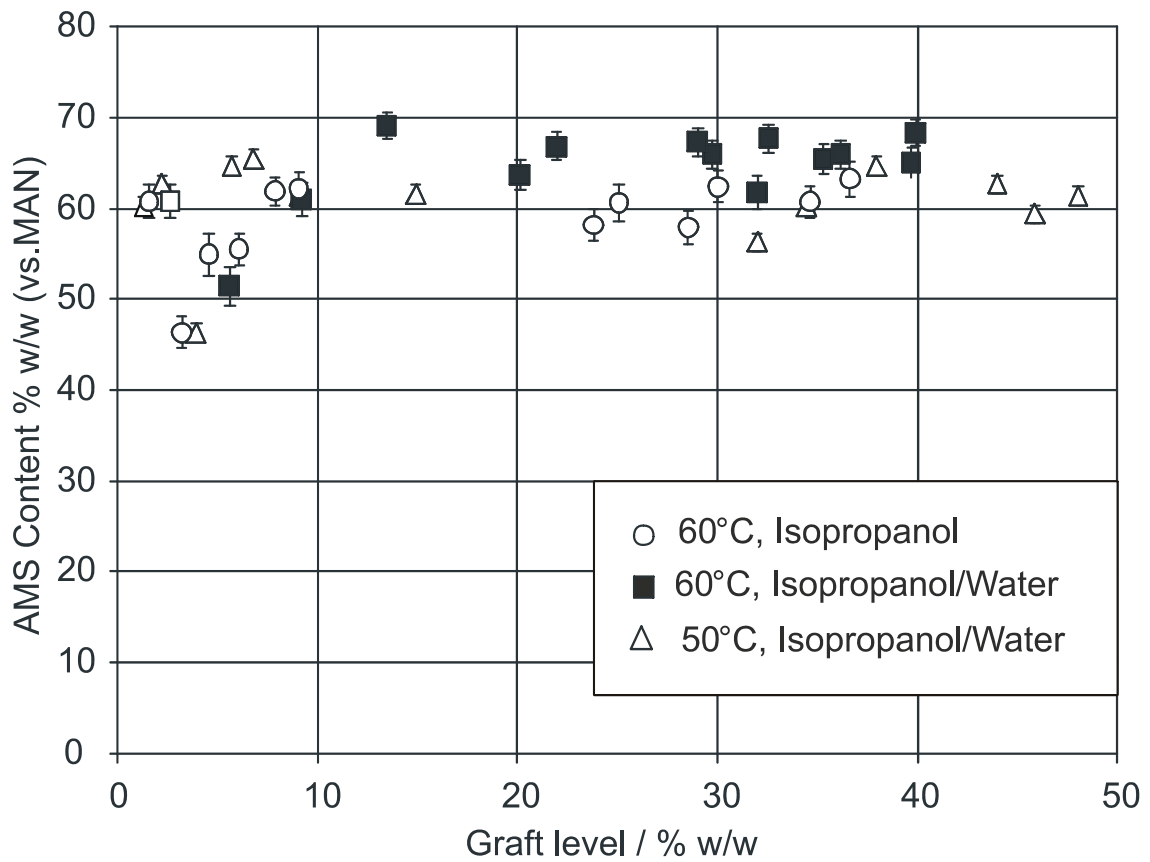**Fig. 27: Kinetic profile of grafting of AMS/MAN membranes.**



**Fig. 28: Content of AMS in grafted films as a function of a graft level (vs. Styrene). Error bars represent standard deviation.**

## 6.6. AMS/MAN Graft Copolymerization (Mayo-Lewis plot)

The Mayo-Lewis plot was used to study the graft copolymerization of an AMS/MAN monomer system. Reactions were carried out using the following experimental conditions: Monomer concentration of 30%$_{v/v}$ in grafting solution, temperature of 50 ºC, two solvent systems: isopropanol-water and isopropanol, reaction time of 65 hrs. The AMS content with respect to the MAN was varied. The Fig. 29 presents the AMS content (with respect to MAN) in a graft copolymer measured by FTIR spectroscopy.

**Table 5: Literature reactivity ratios for AMS and MAN.**

| Set | AMS | MAN | Reference | Remarks |
|-----|------|------|-----------|---------|
| 1 | 0.15 | 0.21 | 62 | |
| 2 | 0.54 | 0.38 | 88 | 60°C, toluene, 10% conversion |
| 3 | 0.06 | 0.28 | 67 | Copolymerization in emulsion |

The literature data, the relationship calculated on the basis of reactivity ratios, were added to the Fig. 29, from the comparison (Table 5). The data were collected from various publications, wherein for the estimation of reactivity ratios different procedures and experimental condition were used. In consequence, a strong discrepancy is observed. However, as shown by Johnston and Rudin[88], the system AMS/MAN matches very well to the Mayo-Lewis model (the Terminal Model). The Mayo-Lewis model can be used for the modelling of graft composition, since in the studied system conversion of monomers to polymer is very low and usually does not exceed 3% (for a Graft Level c.a. 50%). In graft copolymerization, a difference between the data obtained in isopropanol-water mixture and isopropanol only was observed. The presence of water in the grafting solution leads to a higher AMS concentration in the copolymer, compared to the value in isopropanol. The elevated AMS concentration is attributed to the partitioning effect, which is described in the previous chapter.
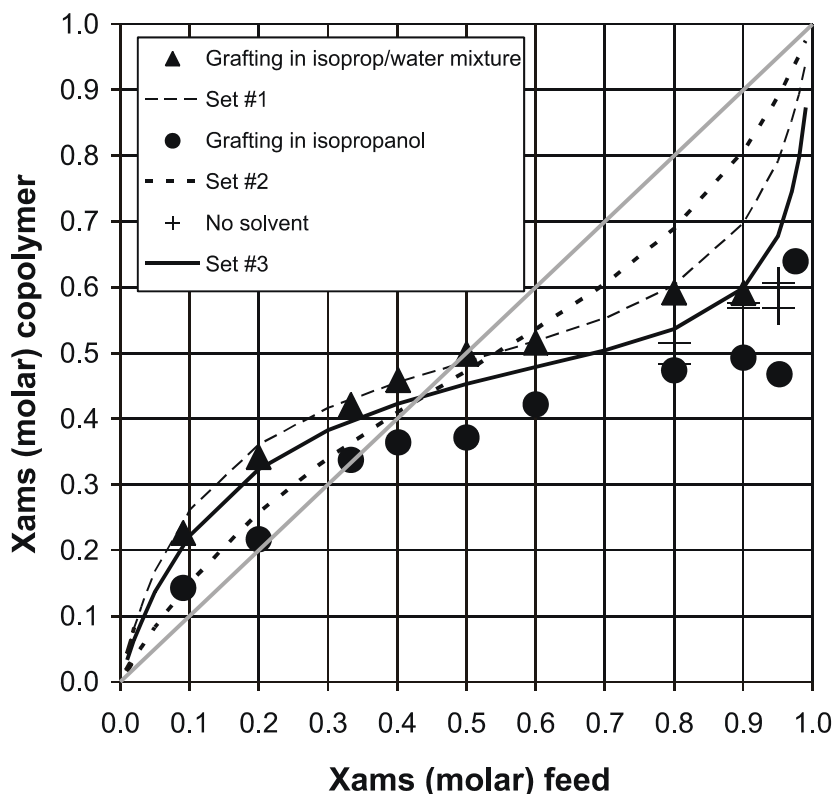
**Fig. 29: Mayo–Lewis copolymerization plot for the copolymerization of AMS and MAN represents the relation between the feed composition of the reacting mixture and the composition of the copolymer. Lines – literature data. Points – experimental data.**

An increase of AMS concentration in the grafting mixture, however, increases the AMS concentration in the copolymer, together with a significant reduction of the graft level. A low graft level is attributed to the termination by a chain transfer to a monomer (AMS) as well as slow addition of AMS monomer to an active polymer chain with an AMS unit. The previously described composition of the grafted film in terms of the AMS content vs. MAN does not reflect the practical needs, because a high concentration of AMS vs. MAN content at low graft level will not provide a sufficient conductivity. The variation of the graft level as a function of AMS in the grafting solution should be taken into account, since an increased AMS concentration in grafting solution strongly reduces the graft level, due to chain transfer. In Fig. 30 graft level and AMS vs. MAN content as a weight fraction are displayed as a function of AMS monomer content in the grafting solution. Two sets of experiments were performed in isopropanol/water mixture (20%) and isopropanol only. The concentration of monomers was 30%$_{v/v}$. Grafting was performed at 50 °C for 65 hrs. There is a significant difference in AMS content of the copolymer between a series

grafted with and without water addition, as it was shown above. In fact, for a fuel cell membrane graft levels between 20 to about 35% of graft level are recommended. Membranes with low graft do not provide sufficient conductivity while membranes with higher graft levels exhibit poor mechanical properties making it impossible to prepare a MEA.

The high dependency of AMS monomer concentration of the grafting solution on graft level was determined (Fig. 30). Moreover, the water content of the grafting solution has a profound influence on graft level. For instance, for $X_m=0.1$, the amount of MAN is higher then of AMS, the difference between series of data is 80% of graft level. For a AMS molar fraction in the grafting solution equal $X_m=0.6$ ($R_m=1.5$) the difference is the smallest so that the graft level is not sensitive for the addition of water. Further, the sensitivity increases, enabling to reach graft level of more than 20% at $X_m=0.9$. For a comparison, grafting without water at the same AMS fraction yields lower graft levels than 10%.
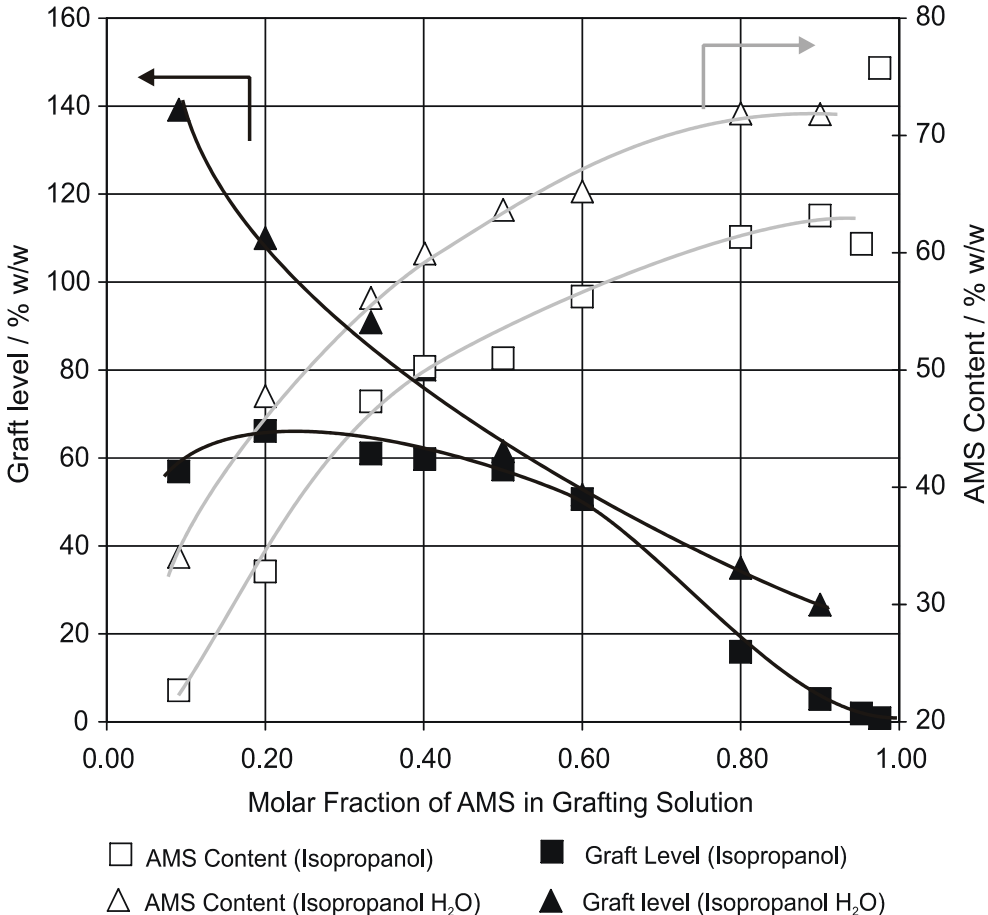


Fig. 30: The influence of AMS in grafting solution on graft level and AMS content in the films.

## 6.7. Crosslinking

In order to improve the membrane oxidative stability, which results in a longer performance time in the fuel cell, the introduction of a crosslinker was performed. Two crosslinkers were studied, well known divinylbenzene (DVB) and a DVB homologue, with the α-positions protected by methyl groups, meta-diisopropenylbenzene (DIPB). It was found that the crosslinker decreases the graft level, which is shown in Fig. 31. In this experiment, grafting of AMS/MAN from FEP was performed at different feed concentration of a crosslinker. Another goal of this experiment was to fabricate crosslinked membranes for the fuel cell experiment, and to validate a concept of crosslinking to extend the lifetime of membranes.

The addition of a crosslinker, at higher concentration (content $> 1\%_{v/v}$), reduces the graft level due to the formation of a crosslinked structure, which serves as a barrier for monomer diffusion. A crosslinked film, being a non-elastic structure, swells lower amounts of monomers. At lower crosslinker content, in the presence of water in grafting solution (content $> 1\%_{v/v}$), a higher graft level than for uncrosslinked samples was observed. The increase of graft level is attributed to the following effects. First, the crosslinking immobilizes the growing polymer chains reducing their mobility, thus a reaction of active chain recombination is reduced, and finally the polymer chains can reach higher length. The second effect can be related to reactivity. At lower crosslinker concentration, crosslinking does not influence neither the monomer diffusion nor the structure elasticity. Therefore, a more reactive crosslinker can increase the graft level. Both crosslinkers DVB and DIPB exhibit the same effect of crosslinker addition, because DIPB is a derivative of DVB with blocked α-positions by a methyl group, which sterically reduces double bond reactivity. Both, the reactivity of DIPB and the effect on graft level, should also be lower. Intriguing is the fact that the increase of graft level occurs only when water was added to the grafting solution. For grafting without water the graft level decreases monotonously as the crosslinker content increases. This observation was found for both series of crosslinking with DVB and DIPB.

Until now, DIPB has not been employed as the crosslinking agent for the preparation of radiation grafted membranes. The presence of DIPB in a grafted membrane was confirmed by FTIR spectroscopy (Fig. 32), at the end of the finger print IR region, the peak at 800 cm$^{-1}$ increases with the concentration of DIPB in the grafting solution.

However, not investigated in this work, there is an adverse effect of a crosslinker to the mechanical durability, as the crosslinker content increases mechanical properties deteriorate. For all highly grafted samples (crosslinker concentration > 5) brittleness was observed. A membrane with insufficient mechanical durability will break during a MEA assembly or during the fuel cell operation. The broken membrane causes gas crossover and an experiment must be terminated.
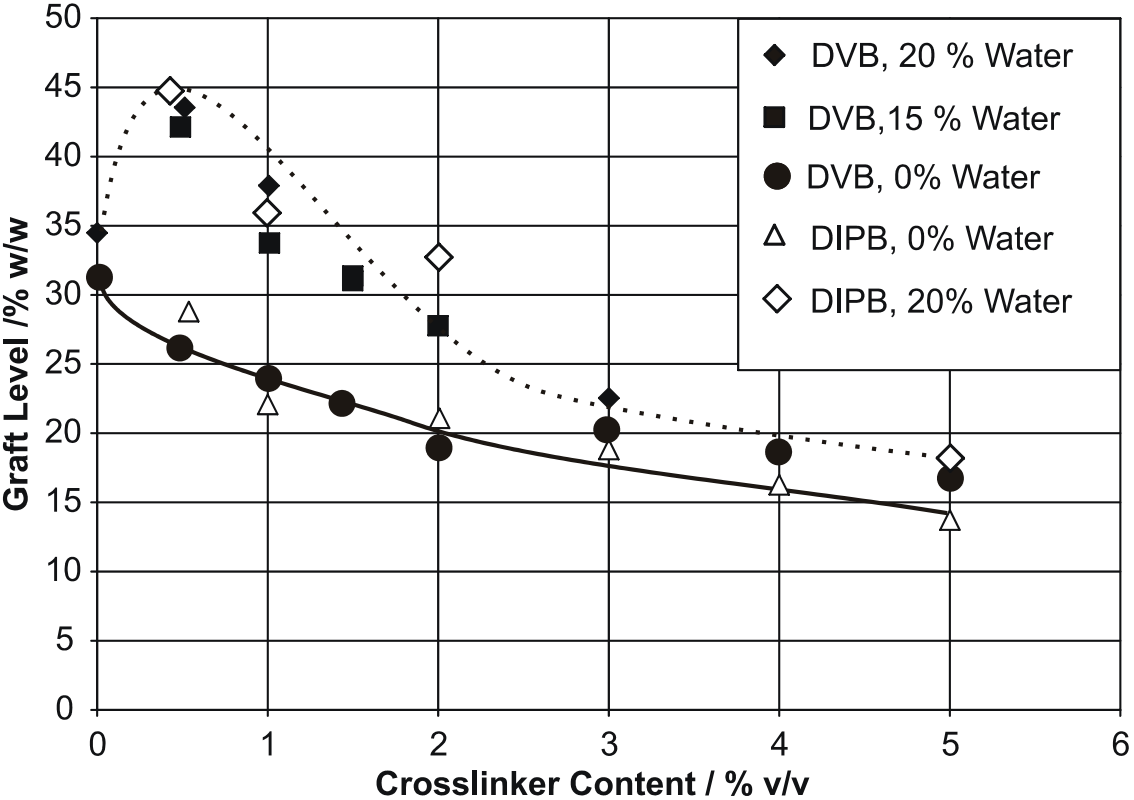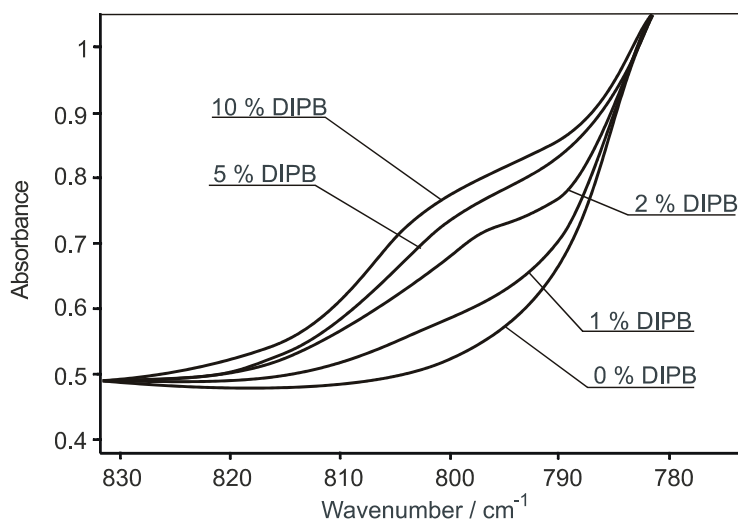


**Fig. 31: Influence of the crosslinker concentration on graft level. Comparison of two crosslinkers DVB and DIPB grafted in the presence or absence of water.**

66

**Fig. 32: FTIR spectrum of the samples grafted with different DIPB concentrations (% v/v) in a grafting solution. The peak at 800 cm$^{-1}$ increases with a crosslinker (DIPB) concentration.**

## *6.8. Membranes*

In this part properties of AMS/MAN membranes are studied in order to select samples for a fuel cell tests as well as to investigate material properties. The membranes have a graft level from 17.8 to 36.7% and the AMS content from 8.9 to 23%$_{w/w}$.

The IEC has been found to be strongly dependent on AMS content and the measured IEC was in agreement with theoretically predicted values, however, some deviation was observed. The swelling of AMS/MAN membranes has been found to be higher than for styrene membranes.

# 7. Properties and Characterization

The results of the variation of IEC with the change of AMS content in samples are presented in Fig. 33. As a reference, the theoretically predicted IEC value was added. Prediction was made assuming that there is only one sulfonic acid group per each benzene ring of AMS (continuous line). The graft level does not reflect the concentration of sulfonic acid groups, because MAN is included in the graft level, the membrane properties are related to the AMS content in a grafted film. The samples with the AMS content of around 10%$_{w/w}$ exhibit higher IEC values than the theoretically predicted IEC. In conclusion, samples with lower AMS content are

sulfonated with more sulfonic groups than one per benzene ring. The effect is opposite in the case of samples with higher AMS content, where the sulfonation did not reach the theoretically predicted value of IEC. This effect may be understood from the fact that at high graft AMS contents, domains of poly(AMS-co-MAN) in FEP due to steric reasons are less susceptible for sulfonation.

In Fig. 34, there are three sets of data, values for AMS/MAN membranes, values for FEP-SSA membranes and literature data[89]. The two sets of data for styrene based membranes, from two different laboratories, are in agreement. The effect of IEC on swelling for AMS/MAN membranes was found more significant than for uncrosslinked styrene membranes, as it is shown in Fig. 33. Such behavior may be attributed to the fact that the nitrile group of MAN is polar. At the same IEC both membranes will have the same number of aromatic units, which undergo sulfonation. AMS/MAN membrane has the polar methacrylonitrile units in grafted side chains, which do not contribute protogenic groups. The polar MAN unit renders the membrane more hydrophilic and as a result the swelling is more than twice higher with respect to styrene in the IEC range from 1.0 to 1.4 mEq/g.
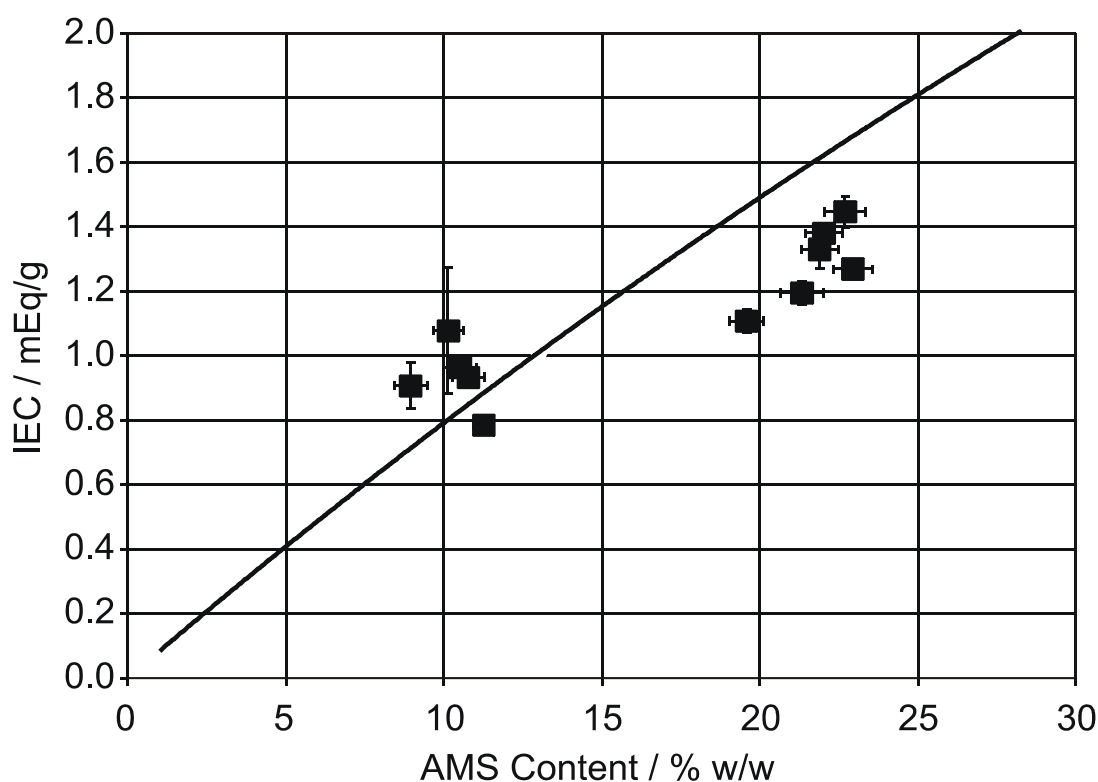


**Fig. 33: IEC values for different AMS contents. The solid line represents the theoretically predicted IEC value. Experimental data are plotted as filled squares. Error bars represent standard deviation.**
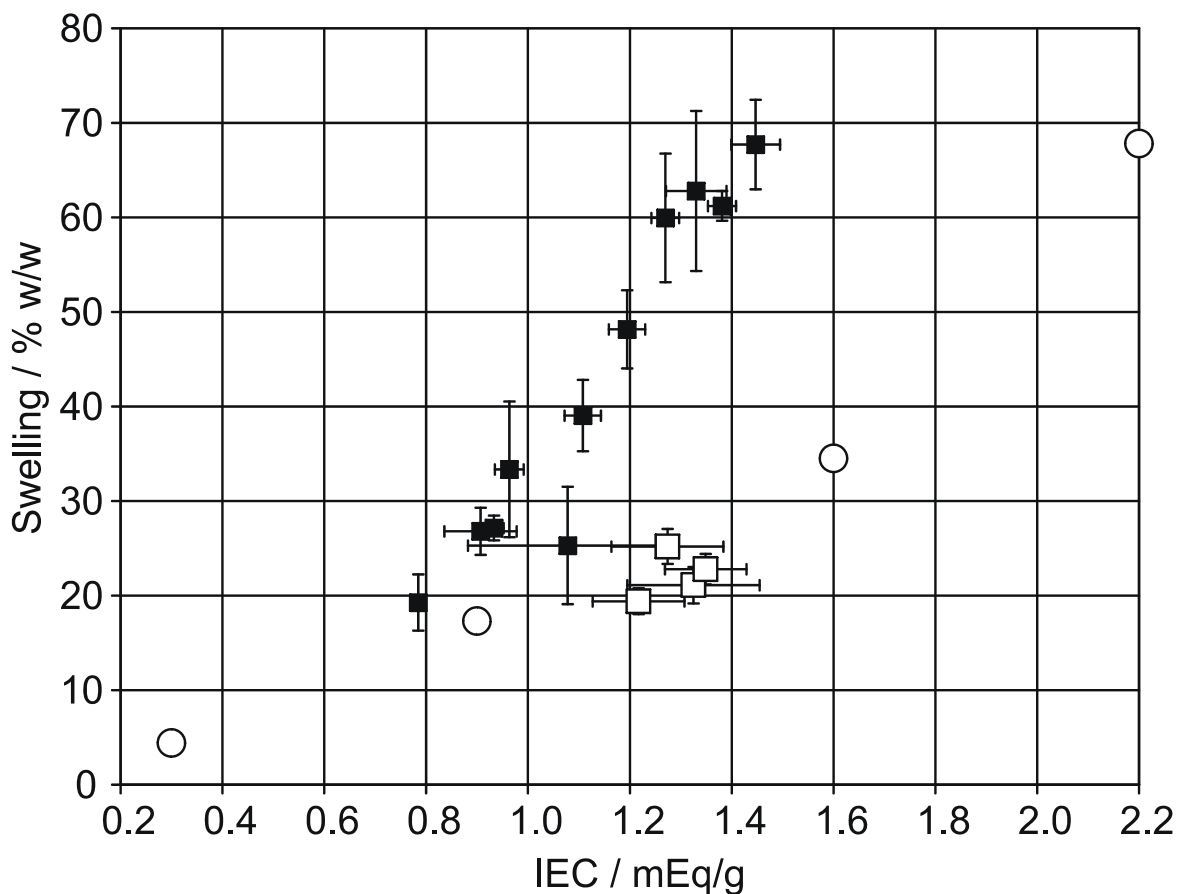
**Fig. 34: Swelling as a function of IEC for AMS/MAN membranes (■), styrene membranes (□), literature data[89] (○). Both membranes were prepared by grafting from FEP 25 µm. Error bars represent standard deviation.**

## 7.1. Conductivity

Conductivity changes can be achieved by increasing or decreasing the graft level, or by an increase of the relative AMS content in a graft copolymer. In the first case, the graft level content of both AMS and MAN, is increased. As a second option, by increasing AMS concentration, at the same graft level, it is possible to achieve a higher conductivity, but practically the AMS concentration can not be increased more than 72%$_{w/w}$ vs. MAN. The absolute AMS content in membranes can be adjusted between 10-22%$_{w/w}$ of AMS in a graft copolymer. In Fig. 35 the relation between AMS content in the graft copolymer (film) and the conductivity is displayed. Additionally, points representing graft levels of investigated samples are also added for a comparison. The best range of graft levels for uncrosslinked membranes is between

69

20-35%$_{w/w}$. The membranes grafted with 20% are mechanically robust to assembly a MEA but the conductivity is only about 40 mS/cm. With increasing graft level mechanical properties deteriorate, however at the graft level of 35 % the membrane still can be used to assemble a MEA. The highest achieved conductivity for membranes grafted with 35% of total graft level and with about 22%$_{w/w}$ of AMS was 120 mS/cm and this seems to be the highest conductivity possible.
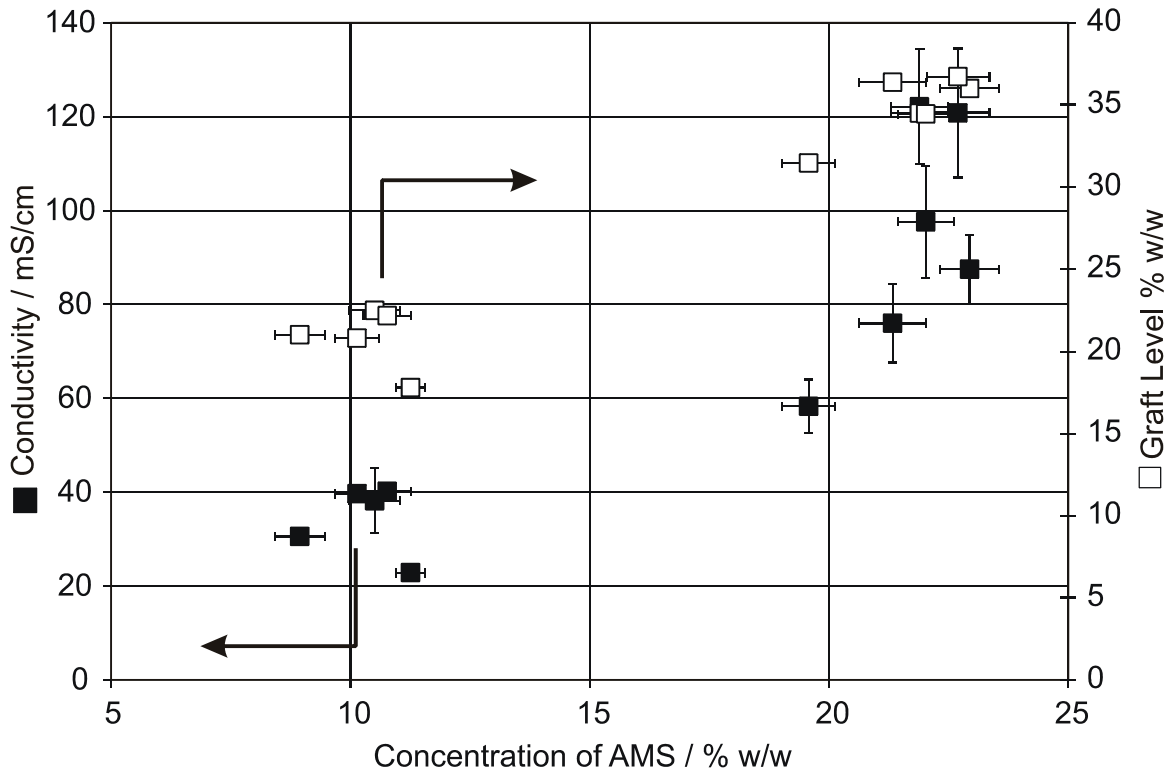


**Fig. 35: Conductivity as a function of AMS content in AMS/MAN uncrosslinked membranes. Error bars represent standard deviation.**

# 8. Crosslinked Membranes

Crosslinking improves membrane performance and durability in a fuel cell, however, reduces membrane conductivity as well as swelling and IEC. The dense structure of a crosslinked membrane is not as flexible as an uncrosslinked one, therefore a membrane can not expand to allow higher water uptake. The crosslinked structure reduces proton mobility, because the conductivity is a product of charge carrier density and proton mobility, conductivity of a crosslinked membrane is lower than that of an uncrosslinked one. Additionally, a crosslinker molecule (benzene ring) is

70

not sulfonated during the applied process, therefore the crosslinker is a component which does not provide any protogenic group. Consequently, the crosslinked membrane has a lower IEC value and a lower water uptake.

The grafting process proceeds by the front mechanism. It starts at the surface and the reaction front moves to the center of a film. Depending on the parameters of the grafting process, there is a stronger or weaker gradient of graft level in the membrane cross section. The similar effect was described for crosslinked films. Brack *et al*[90] investigated films synthesized by styrene and DVB grafted from FEP and ETFE. The comparison of data obtained from FTIR analysis using transmission mode and surface specific ATR method was used. Results from both methods showed that a higher crosslinker content was found at the surface, measured as the ratio of styrene to double substituted benzenes (isomers of DVB).

The studied membranes were synthesized with different concentrations of crosslinker ranging from 0.5 to 5%$_{v/v}$ in grafting solution. The conductivity of membranes is sensitive to the addition of crosslinker, even the lowest crosslinker content decreases conductivity. The films grafted with DIPB as a crosslinker showed slightly higher conductivity than films crosslinked with DVB and synthesized at the same conditions. A linear correlation between graft level and IEC (Fig. 37) was observed. Due to the different crosslinker content in the grafting solution the samples have different graft levels, the graft level decreases with increasing crosslinker concentration. For samples crosslinked with DIPB and DVB and synthesized without the presence of water, the same slope for both lines were obtained (Fig. 37). For samples crosslinked with DVB in the presence of water, yielded scattered data and lower IEC values are obtained compared to samples synthesized without an addition of water (at the same graft levels).

Since the benzene ring in a crosslinker molecule can not be sulfonated, it can be assumed that samples synthesized in the presence of water are more strongly crosslinked than the samples grafted without water. The stronger crosslinking is assumed by the lower IEC value caused by significant incorporation of the crosslinker (DVB) in the structure. However, due to overlapping bands, DVB was not detected by FTIR.
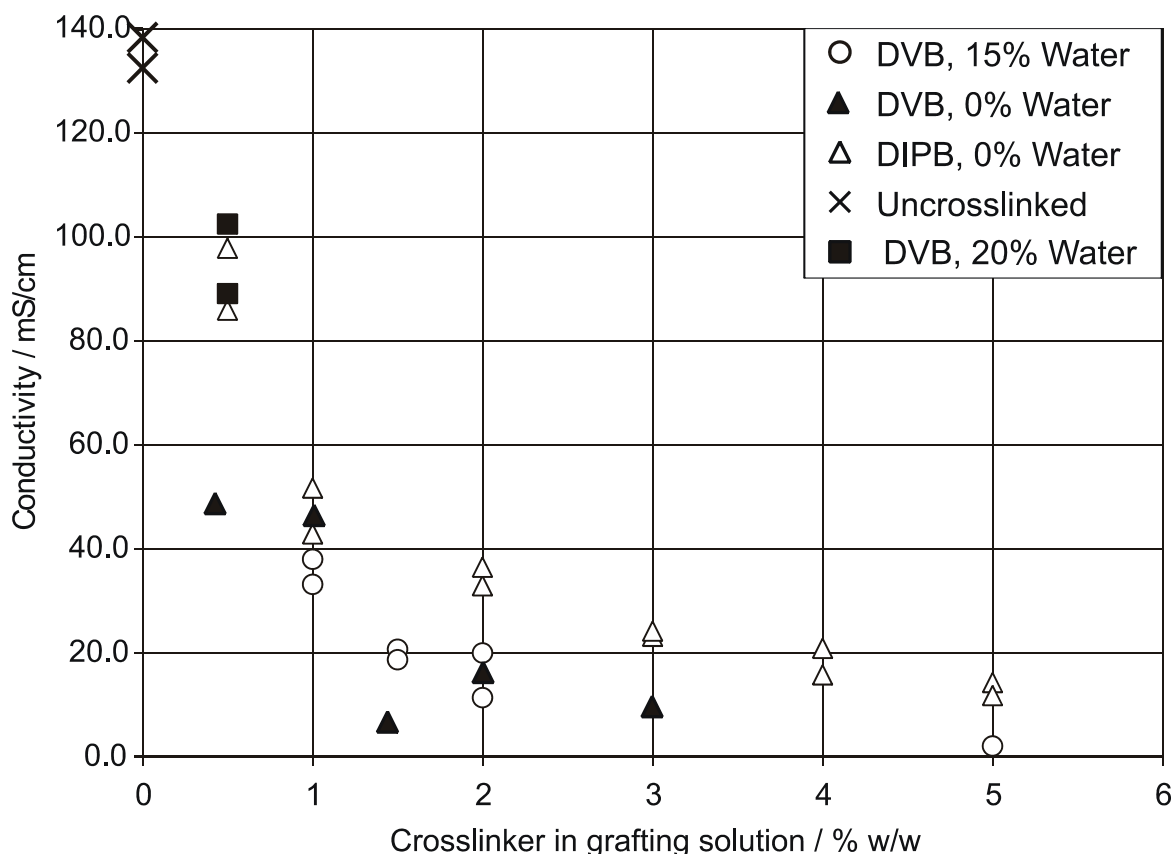
**Fig. 36: Deterioration of conductivity with increasing concentration of a crosslinker in the grafting solution.**

Qualitative analysis of components in a graft copolymer AMS/MAN/crosslinker, wherein the crosslinker is either DVB or DIPB, is not established until now. Therefore, analysis of crosslinker content could not be performed and thus there is no method for quantification of crosslinking. Apparently, the crosslinker content does not represent a full image of crosslinking, because during the reaction of a crosslinker possessing two vinyl groups one may remain intact. The other "pendant" double bond remains intact. For the full analysis of crosslinked material, it is necessary to analyze the amount of pendant double bond to estimate inactive crosslinker species.

Fortunately, swelling is very sensitive to crosslinker addition, even a small amount of 0.5% $_{v/v}$ of DVB in the grafting solution causes a strong loss of swelling. For instance, membranes M3 and M4 (Table 6), were synthesized at the same conditions, except membrane M4 was grafted with 0.5%$_{v/v}$ DVB in grafting solution. Although, graft levels of both membranes are almost identical, the crosslinked membrane exhibit 50% less swelling as compared to the uncrosslinked one.
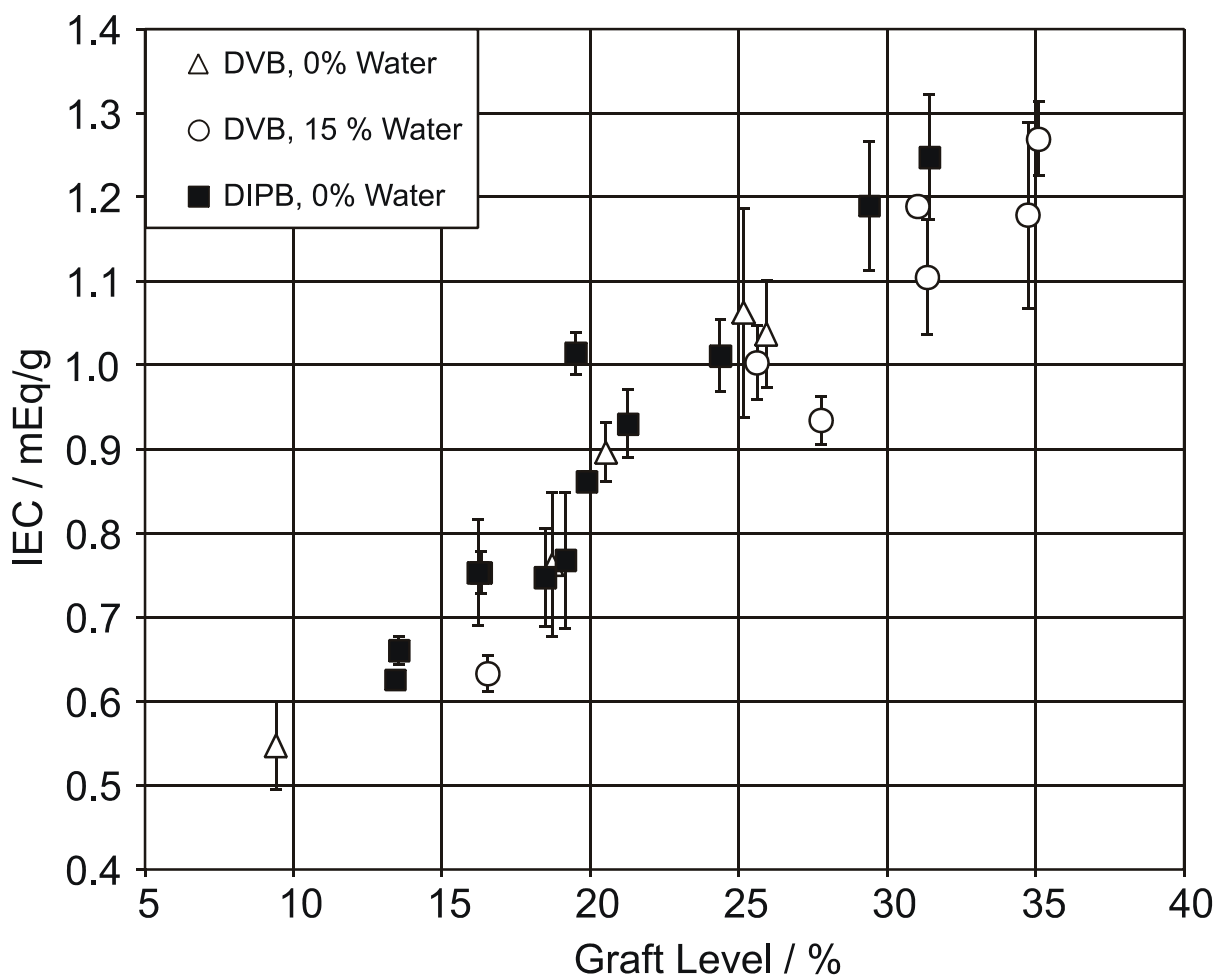
**Fig. 37: Correlation between IEC and Graft level. The concentration of crosslinker was varying from 0.5 to 5%$_{v/v}$ in grafting solution. Error bars represent standard deviation.**

In general, swelling can be used to study the extend of crosslinking of different membranes, while a detailed analysis of the composition, in particular an analysis of the crosslinking agent, is not possible. On the other hand, the value providing information about the concentration of the protogenic group is ion exchange capacity (IEC), expressed in millimols or milliequivlents per mass unit of dry membrane.

Fig. 38 presents swelling data as a function of the IEC for differently crosslinked membranes. Swelling and IEC are used to study the crosslinking efficiency for two different crosslinkers (DVB and DIBP) as well as for samples grafted with different water content. The membranes have graft levels from 9% to 35%.
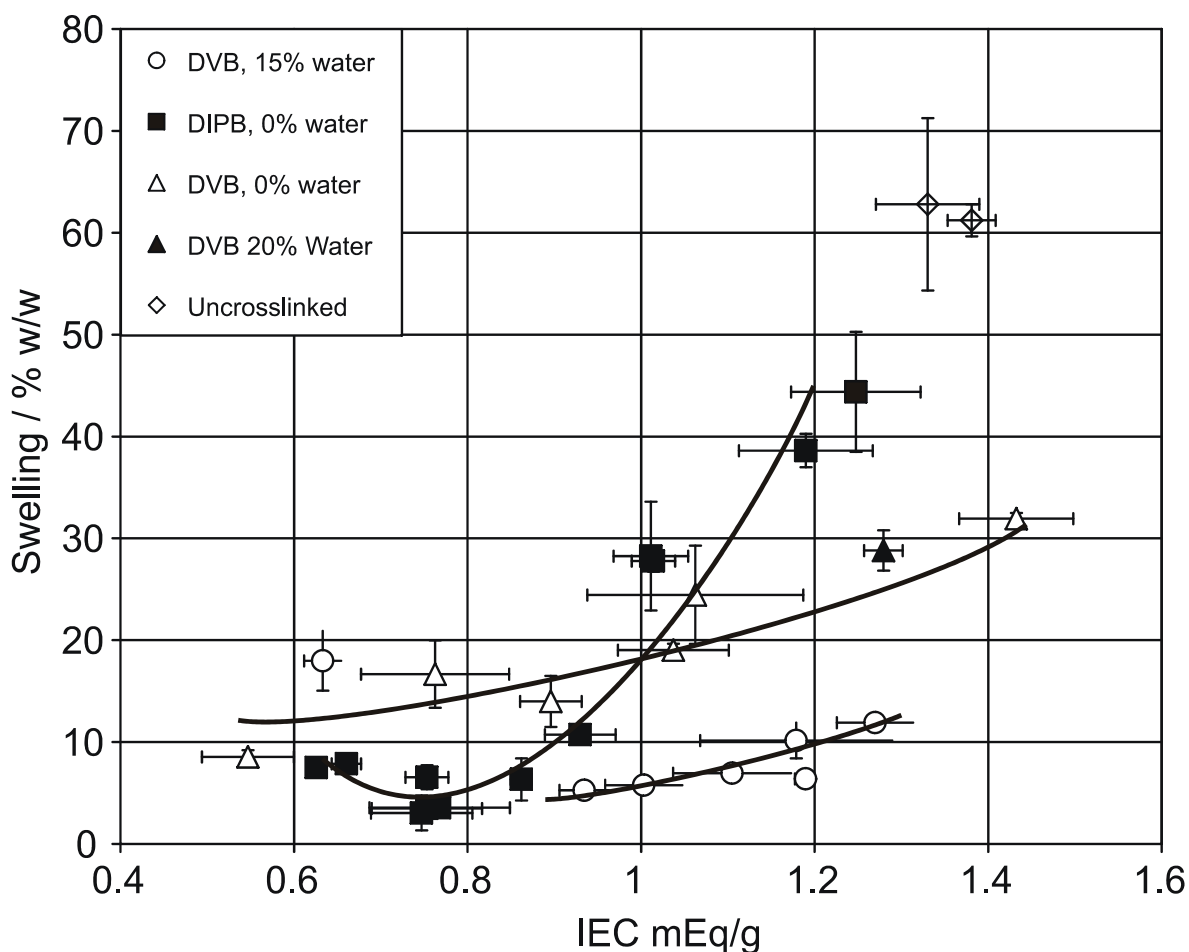
**Fig. 38: Differently crosslinked membranes and their swelling values as a function of ion exchange capacity (IEC). Error bars represent standard deviation.**

The highest swelling and IEC were obtained for uncrosslinked samples. The crosslinking reduces swelling, in the range of IEC from 0.9 to 1.3 mEq/g, the highest effected crosslinking expressed as value of swelling, was observed for samples crosslinked with DVB in the presence of water. The samples crosslinked with DIPB, with an IEC lower than 1 mEq/g, showed significant crosslinking, however, the crosslinking was lower than that of the samples grafted with DVB when water was present in the grafting system. Swelling for DIPB samples was spread from 5 to 45%, wherein a sample with 45% of swelling was crosslinked with 0.5%$_{v/v}$ addition of DIPB in the grafting solution. The samples with 3 and 4%$_{v/v}$ of DIPB allow a minimum of swelling at an IEC equal to 0.75 mEq/g and swelling value of 3.5%. At the highest crosslinker content (5% $_{v/v}$) swelling is slightly higher, reaching a value of 8%. This weak maximum can not be explained until now. However, it can be treated as the line levels off instead of creating a swelling minimum. Membranes crosslinked with DVB,

grafted in the absence of water in the grafting solution, exhibited higher swelling than samples synthesized under the same conditions but crosslinked with DIPB in the studied range of IEC 0.7-1.0 mEq/g. Considering swelling as a value for crosslinking quantification, the samples crosslinked with DIPB reached higher crosslinking than those crosslinked with DVB, while the other synthetic parameters were the same for both sets. Among the samples crosslinked with DVB, those grafted at 15% presence of water in the grafting solution showed lower swelling values and, consequently, higher crosslinking than the samples grafted in the absence of water in the grafting solution. In this case, the higher crosslinking can be explained by a partitioning effect. That is to say, water as a non-solvent for DVB forces a higher concentration of DVB-monomer into a grafted film. Consequently, the DVB concentration in the grafted film is higher and the crosslinking is stronger. The difference between DIPB and DVB is that DIPB as a molecule with steric hindrance, a methyl group, reacts slower than DVB.

# 9. Fuel Cell Tests

The aim of the fuel cell tests was to carry out experiments until membrane failure, as an estimation of durability, as well as to compare performances by means of polarization curves.

Properties of the different types of radiation grafted membranes are displayed in Table 6, including state of the art crosslinked styrene based membranes and uncrosslinked styrene based membranes for comparison. Furthermore, the AMS/MAN membranes have different graft levels and, in consequence, IEC values and conductivities. Among them, there are sets of 2 uncrosslinked as well as 2 membranes crosslinked with DVB. For a comparison of membrane performance, a standard, commercially available Nafion 112® membrane was used. The polarization experiment was carried out at two different temperatures 60 and 80 ºC, respectively, because the uncrosslinked styrene based membrane could not be operated at 80 ºC for a sufficiently long period of time, and therefore it was replaced by Styrene/DVB membrane as a reference. In each membrane test the temperature was increased from, 60 to 80 ºC, according to the temperature profile included in the ANNEX. The fuel cells were started at 60 ºC, and then the temperature was increased to 70 ºC and further to 80 ºC, the longest period of the experiment was carried out at 80 ºC except for membrane M1.

**Table 6: Properties of tested radiation grafted membranes.**

| # | Membrane type | Graft Level / % w/w | IEC mEq/g | Swelling / % w/w | Thickness / µm | Conductivity / mS/cm | Hydration number |
|---|---|---|---|---|---|---|---|
| M1 | FEP-g-SSA | 18.9 | 1.21 +/- 0.13 | 25 +/- 2 | 32 +/- 1 | 104 +/- 6 | 11.5 |
| M2 | FEP-g-(AMSSA-co-MAN) | 20.8 | 1.08 +/- 0.20 | 25 +/- 6 | 39 +/- 1 | 40 +/- 2 | 12.9 |
| M3 | FEP-g-(AMSSA-co-MAN) | 34.5 | 1.38 +/- 0.03 | 61 +/- 2 | 44 +/- 1 | 98 +/- 12 | 24.6 |
| M4 | FEP-g-(AMSSA-co-MAN-co-DVB) | 36.0 | 1.28 +/- 0.02 | 29 +/- 2 | 38 +/- 1 | 89 +/- 8 | 12.6 |
| M5 | FEP-g-(AMSSA-co-MAN-co-DVB) | 25.2 | 1.04 +/- 0.06 | 24 +/- 5 | 37 +/- 1 | 48 +/- 3 | 12.8 |
| M6 | FEP-g-(SSA-co-DVB) | 19.9 | 1.27 +/- 0.01 | 25 +/- 2 | 32 +/- 1 | 42 +/- 2 | 10.9 |
| | Nafion® 112 | N.A | 0.91 | 37 | 50 | 82 | 22.6 |

Additionally, during the experiment, the *in-situ* membrane resistance was monitored, which includes the membrane resistance, the resistances of interfaces between the membrane and the electrodes and the electrode resistance.

## *9.1. Performance in Fuel Cell*

The single cell performance of the different membranes at 60 ºC is displayed in Fig. 40. Uncrosslinked AMS/MAN membranes (M2, M3) showed the better performance than the uncrosslinked styrene membrane (M1). The membrane M2 performed better than M3, due to a lower membrane resistance, obtained by a higher graft level. The difference in polarization between membrane M1, styrene based, and M2, AMS/MAN based can be attributed to the better electrode/electrolyte interface properties. In the Nyquist plot in the Fig. 39 the intercept of the half-circle with the *x*-axis indicates the Ohmic resistance of the electrolyte. The diameter of the half-circle shows the charge-transfer resistance for the electrochemical reaction at the electrode/electrolyte interfaces. Concluding, the higher ohmic resistance of membrane M2 is compensated by the lower charge-transfer resistance of the interface.

At low current density (< 500 mA/cm$^2$) the best performance was observed for the AMS/MAN/DVB membrane (M5), at higher current densities (> 500 mA/cm$^2$) the highest performance was observed for the second AMS/MAN/DVB membrane (M4), it was slightly higher than the performance recorded for Nafion® 112.

At the temperature of 80 ºC, the best performance is archived by the AMS/MAN/DVB membrane M5 (Fig. 41). It should be mentioned that this membrane has a lower graft level then membrane M4 and, as a consequence, lower IEC and swelling values. The performance of M5 is clearly higher then the performance of Nafion® 112 in the current density range from 0 to 800 mA/cm$^2$. *State-of-the-art* styrene/DVB membrane performed very similar to the AMS/MAN membrane (M3). Both membranes M3 and M4, showed the lowest performance at 80 ºC of all tested membranes.

The reason for the better performance for crosslinked AMS/MAN/DVB membranes as compared to uncrosslinked ones seems to be the better membrane-electrode interface. The ohmic resistance of M2 is similar to that of the uncrosslinked membranes M5 and M3 to M4, respectively. Therefore, the higher performance observed in the polarization should be of another origin than membrane conductivity.
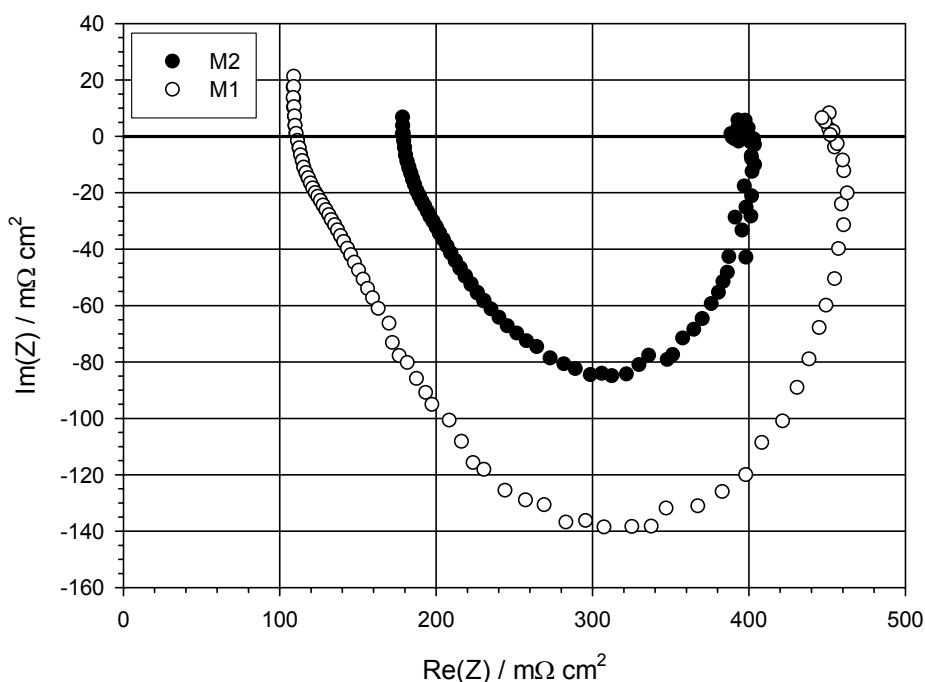
**Fig. 39: Nyquist plots of the impedance data for membranes M1 and M2. Recorded at current density of 500 mA/cm$^2$ , full humidification, temp. 60 °C and time of operation 24 h.**

There are two possible explanations for a superior interface for crosslinked AMS/MAN/DVB membranes. The first, the crosslinker (DVB) promotes polymerization close to the surface of the membrane. Consequently, the surface has higher a IEC and a conductivity. The second, the crosslinker immobilizes the polymer chains on the surface, the chains can not undergo reorientation contacting to the hydrophobic membrane.

With obtained experimental data, it is not possible to conclude unambiguously which effect is responsible for the better interface properties of grafted membranes. Additionally, it is not excluded that both mentioned effects take place.

Generally, the crosslinked membrane with lower graft level (M5) performed better at 80 °C than at 60 °C, which is unusual, because this membrane showed lower conductivity. The key is that the explanation can be in a different synthesis or different water management in the fuel cell. The difference in synthesis between M5 and M4 is that the first one was synthesized without water in the grafting solution.

78
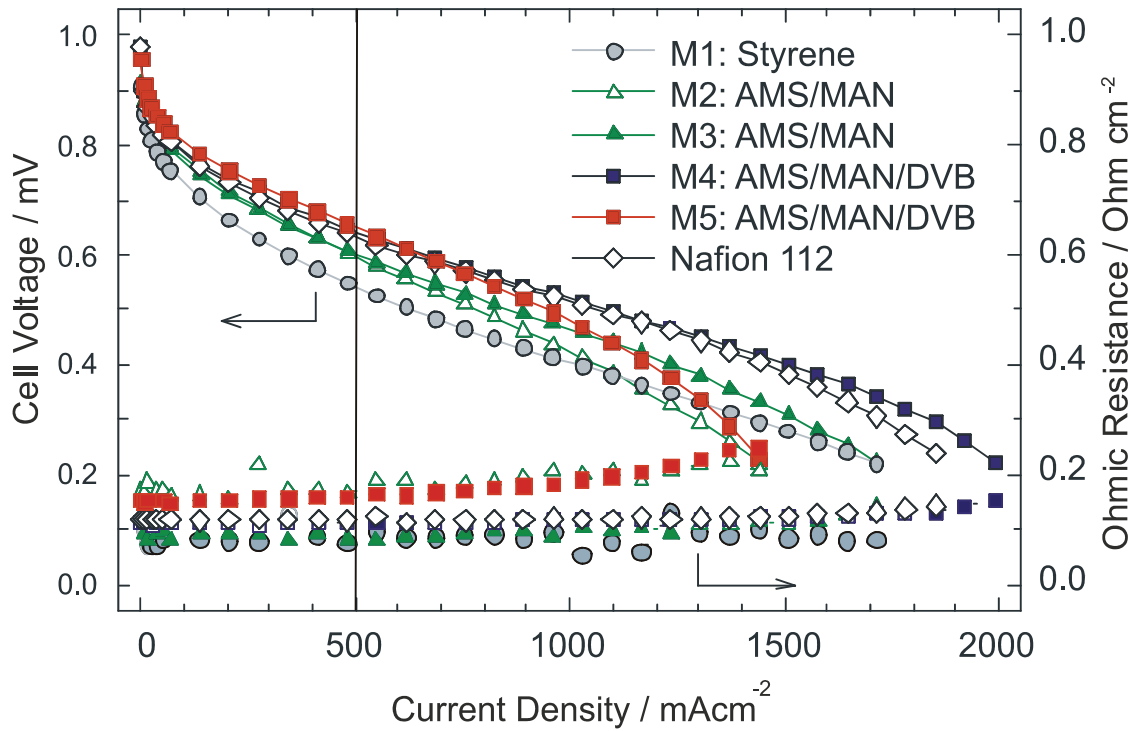
**Fig. 40: Polarization characteristics of different radiation grafted membranes and Nafion 112® as a reference at 60 ºC. Data obtained at the beginning of operation.**
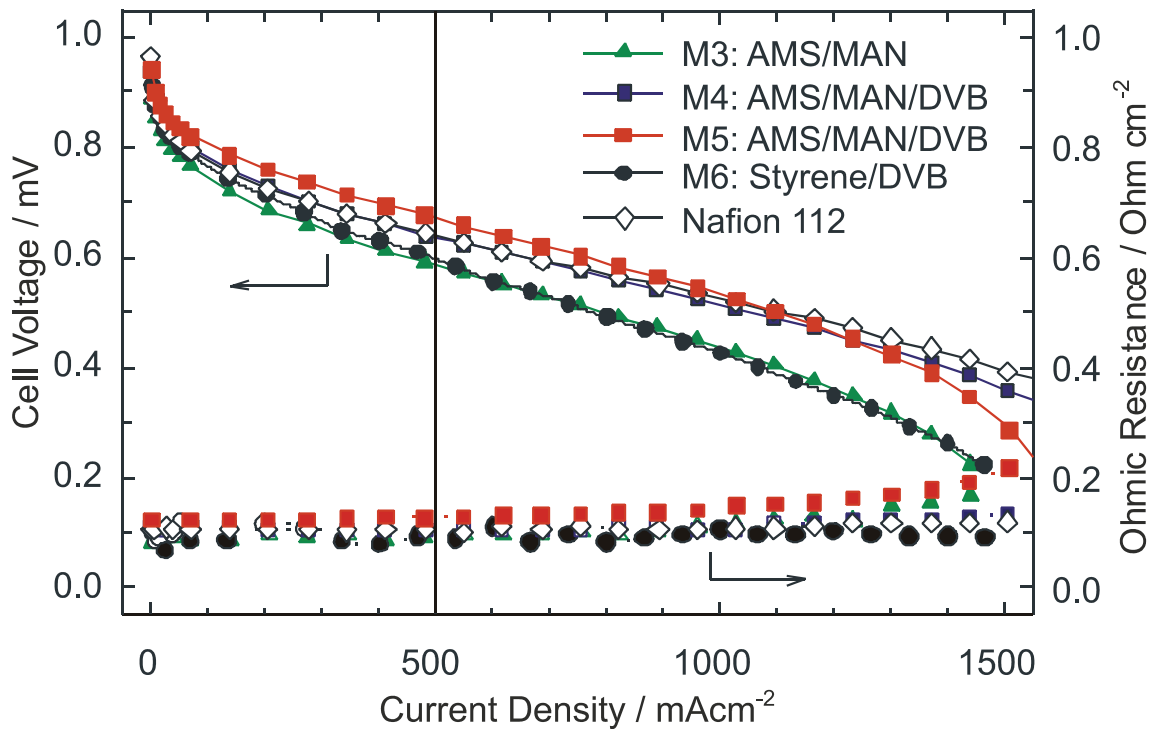


**Fig. 41: Polarization of different radiation grafted membranes and Nafion 112® as a reference at 80 ºC. Data obtained at 100th hour of operation.**

As it was previously discussed, water affects the distribution of monomers, mainly non-polar monomers as DVB and AMS are forced to penetrate into the film during the grafting to an higher extend. Conditions of synthesis have a direct influence on membrane morphology and, consequently, the behavior in a fuel cell is different.

Durability of the membranes was evaluated by running a fuel cell experiment to the membrane failure. The failure was caused by a massive gas crossover close to the oxygen inlet, and after a visual inspection a hole in the membrane was found. The membrane M5 did not fail, the experiment was terminated in order to compare the degree of degradation with the membrane M4.

The obtained results showed that the AMS/MAN/DVB membranes are not yet optimized and further optimization should result in longer durability. The fuel cell test showed a trend between the chemical composition of a membrane and the performance. Change in a parameter of synthesis such as graft level, composition, addition of a crosslinker is reflected during further performance in a fuel cell. The performance of AMS/MAN/DVB membranes was slightly better than that of commercially available Nafion® 112. However, although performance of the tested membrane is satisfactory, durability should be improved. Optimization of the tested membranes was steadily improved by changing synthesis parameters, addition of a crosslinker, and variation of a graft level.


# 10. Post Mortem Analysis of the Fuel Cell Membranes

Post mortem analysis of a membrane is a complementary method to the testing of a membrane in a fuel cell. During the test, the membrane is exposed to aggressive conditions and undergoes various modes of degradation. Degradation modes occurring during the time of performance in the fuel cell are as follows:

- Chemical degradation– damage to the polymer caused by chemical species (radicals),
- Mechanical degradation– stress caused by mechanical forces during swelling and drying cycle, compaction force,
- Thermal degradation– thermal degradation of polymer materials.

Degradation modes are difficult to separate in these experiments. Despite of the difficulties to separate these degradation modes, in some cases, when a chemical degradation was found to be very low, a fuel cell failure can be attributed to the mechanical modes. For example, when cracks or pinholes were found in a membrane, which failed at the beginning of the test and further membrane analysis found no chemical degradation by means of IEC loss. Moreover, the membrane degradation is strongly dependent on the operating conditions, used materials, and fuel cell construction.

The post mortem analysis of membranes, described in this work, focuses on chemical modes, attributed to the loss of a grafted component. The analysis is aimed mainly to compare the degree of degradation for different membranes, in order to confirm or contradict oxidative stability (chemical mode).

## 10.1. Degradation by Means of IEC

Degradation measured by the loss of IEC reflects the chemical degradation mode. For comparison of fuel cells, usually the performance time until failure is taken into account. But to consider membrane stability by means of degradation of IEC, the degradation shown as a percent loss of IEC (Fig. 42), during the experiment, should be compared.

The lowest durability was observed for the uncrosslinked styrene based membrane (M1), only 50 hrs of performance was recorded. Moreover, the membrane showed significant degradation in the active area, 78% of IEC loss was found. Both uncrosslinked AMS/MAN membranes performed slightly longer than 500 hrs, which is, compared to the previous styrene based membranes ten times longer. The membrane (M2) showed higher degradation compared to M3, the IEC loss was found to be 61 and 31%, respectively. This difference in degradation may be understood from the fact that the membrane M3 had a higher graft level than M2. In this case, a postmortem analysis brings the key results to judge about the membrane stability, because by means of performance time membranes were very similar, however the post mortem analysis revealed difference in degradation.

The crosslinked membrane M4 was found to perform twice as long as the uncrosslinked membranes. Measurement of degradation gave a value of 43% of IEC at the end of test, which should not be a reason of failure. The leakage test showed a

strong gas crossover, which is a result of membrane perforation. Further visual inspection confirmed this expectation, a hole close to an oxygen inlet was found. The experiment with the second crosslinked membrane (M5), was discontinued after 1000 hrs of performance, in order to perform postmortem analysis and to compare degradation with the membrane M4. The IEC loss was found to be about 15%, additionally a visible membrane damage was not detected.
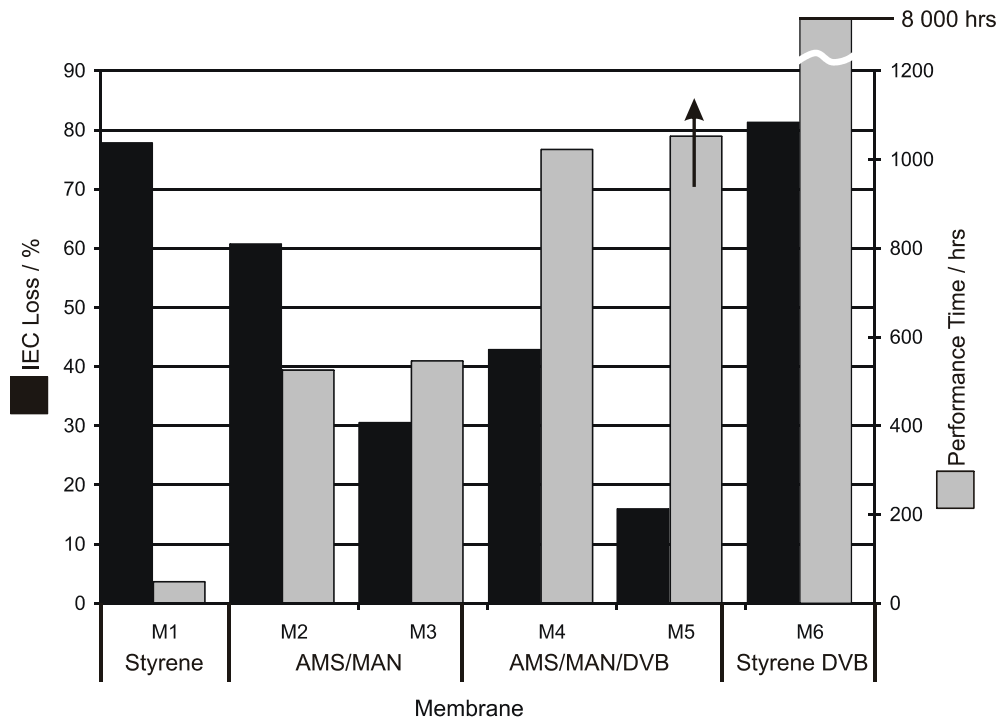


**Fig. 42: Degree of degradation, expressed as loss of IEC and performance time for different radiation grafted membranes. The performance is time until failure of the fuel cell. The experiment with the membrane M5 was terminated by the operator.**


## 10.2. *Locally Resolved Degradation Analysis with FTIR*

The experiment employing FTIR spectroscopy was performed in order to analyze membrane homogeneity after degradation. In contrast to titration, FTIR gives an opportunity for an analysis of particular points or regions of a membrane. The six points on a membrane were selected for spectra recording. At the oxygen inlet, degradation is relatively low for all tested membranes. However, in three cases (M2, M3, M4), formation of a hole was observed leading to a membrane failure as show in the Fig. 44. A membrane perforation leads to a sudden failure, because of a gas crossover. Therefore, in the membrane M5, the gas entrances were changed in order

to protect this area. Previously, the gas entered perpendicular to the membrane surface, in the new modified flowfield gases enter parallel to the membrane surface. It is known that low gas crossovers, pinholes do not cause fuel cell failure. For example, after assembly the membrane M4 showed a gas crossover of about 0.5 $cm^3$/min, despite the crossover this membrane performed over 1000 hrs.

The highest degradation was observed close to the hydrogen inlet, the grafted component is completely depleted in case of membrane M2, and for the other membranes the degradation exceeds 60 % (point #6). Nevertheless, membrane integrity remained intact in the degraded region and is still a barrier for fuel and oxidant crossover. In contrast to the degradation at the oxygen inlet, degradation at the hydrogen inlet leads only to deterioration of membrane performance and does not cause any perforation.

Depicted in Fig. 44 is an image of membrane degradation, which shows the active area and the outer rim. The outer rim is not exposed to the fuel cell environment, during a fuel cell experiment the outer rim is only heated to the temperature of operation. In the active area transparent area (slightly greenish) are significantly degraded, for a point 6 in the membrane M2 the degradation is 100% (Fig. 43). At the border of the outer rim with the active area and the active area there is visible significant degradation. Additionally, dark spots are located randomly around the active area. The degradation pattern is difficult for explanation, because neither current distribution nor humidity distribution, over the area, are not known. In the degraded areas the concentration of degradation species is higher, this can be related either to current density or to humidification aspect.
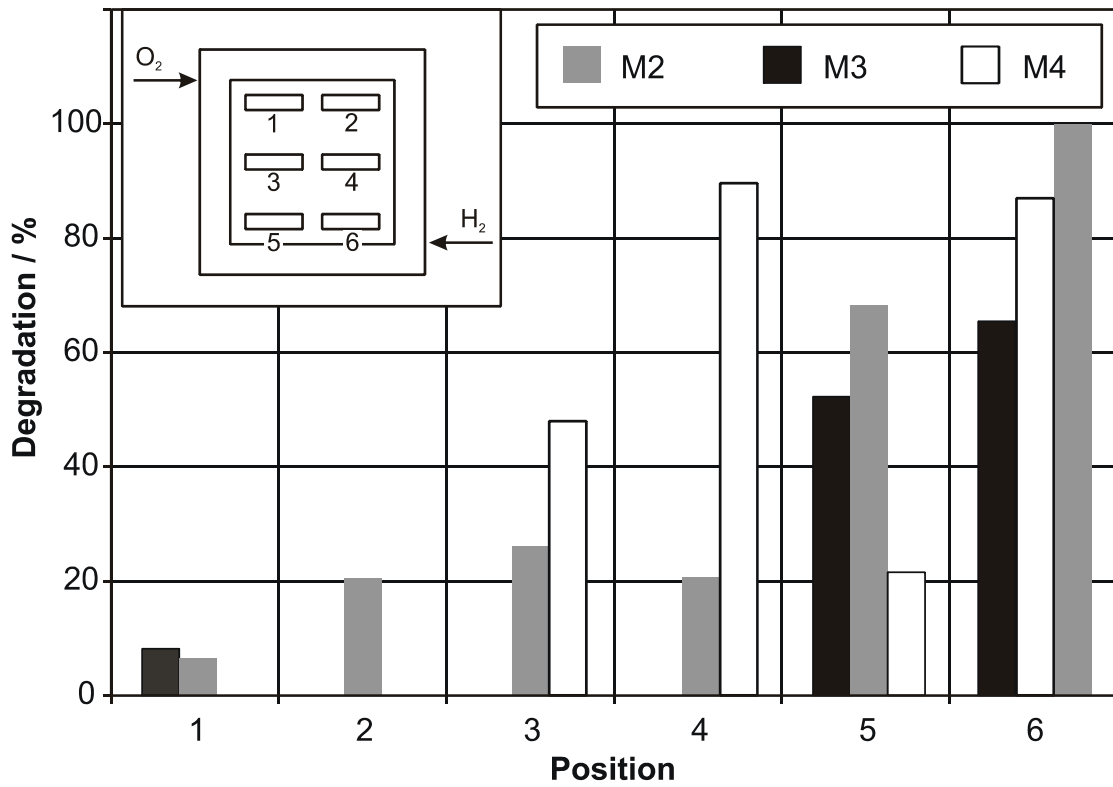
**Fig. 43: FTIR post mortem analysis of membranes. Measurement performed at 6 points of a membrane.**
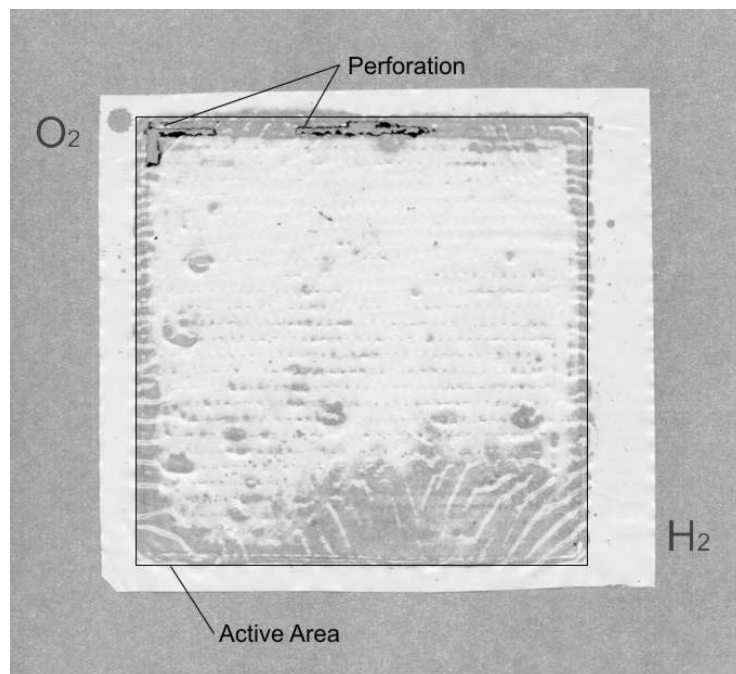


**Fig. 44: Image of the membrane M2. The grey areas within the active area (5.4 × 5.4 cm) represent degradation. A green background was used for a better contrast.**

# 11. Summary

In the scope of this thesis, the new material, FEP-g-(AMSSA-co-MAN), was proposed as a membrane for low temperature fuel cells. The work was carried out in three directions, material discovery, synthetic study, ex-situ characterization and fuel cell characterization.

Currently, for radiation grafted membranes styrene is a very convenient monomer. However, hydrogen at α-position in the styrene molecule is prone to an oxidative attack. Degrading species (radicals) are able to deplete the hydrogen atom and trigger a degradation mechanism. Therefore, a protection of α-position in a molecule of styrene can lead to an improvement of stability. AMS was found as a candidate to replace styrene for the process of synthesis of radiation grafted membranes. Poor kinetics as well as chain transfer to the monomer do not allow to obtain a homopolymer, thus AMS can not be grafted from a backbone according to the preirradiation grafting method. Because the properties of AMS do not exclude a copolymerization, MAN was chosen as a comonomer to enable the membrane synthesis using AMS.

Grafting of AMS and MAN was studied in various solvents. A mixture of isopropanol and water was found to be the best solvent for the grafting of AMS and MAN. The partitioning effect between the film and the grafting solution was found to be responsible for the film composition (AMS/MAN ratio in a grafted film).

Two crosslinkers were successfully used to obtain the crosslinked membranes. DVB and DIPB are suitable for the crosslinking of membranes based on AMS and MAN. The effect of crosslinking was detected by observation of water swelling properties since even small crosslinker addition reduces water swelling.

Membranes synthesized by grafting of AMS and MAN from FEP exhibited superior durability during the fuel cell testing than the state-of-the-art styrene based membranes. The performance time of AMS/MAN membrane was slightly higher than 500 hrs, while the similar styrene based membrane performed only 50 hrs. The work towards crosslinking of AMS membranes was initiated, and improved performance as well as durability of a crosslinked membrane was proved in the fuel cell. Non-optimized, crosslinked membranes showed a twice as high lifetime than the uncrosslinked one.

The membranes were investigated postmortem, after a fuel cell experiment. The postmortem analysis was invaluable for an evaluation of the membrane degradation degree. The postmortem analysis was complementary to the data obtained from a fuel cell experiment, such as performance time. Measurement of the degradation degree showed better stability of AMS/MAN membranes under fuel cell condition.

An application of a comonomer for AMS enabled the grafting, but the MAN is not the only one monomer than can be applied. In the next step, apart from optimization of crosslinked membranes and better characterization, the research should go toward a selection of an alternative to MAN. MAN as a molecule, which can not be sulfonated, reduces the IEC of a membrane. The desired comonomer for AMS should be able to provide also IEC. Successfully, application of AMS and encouraging fuel cell experiment results shed a new light on the synthesis of radiation grafted membranes, because it is possible to synthesize many combination of radiation grafted membranes using AMS and other monomers.

# 12. ANNEX
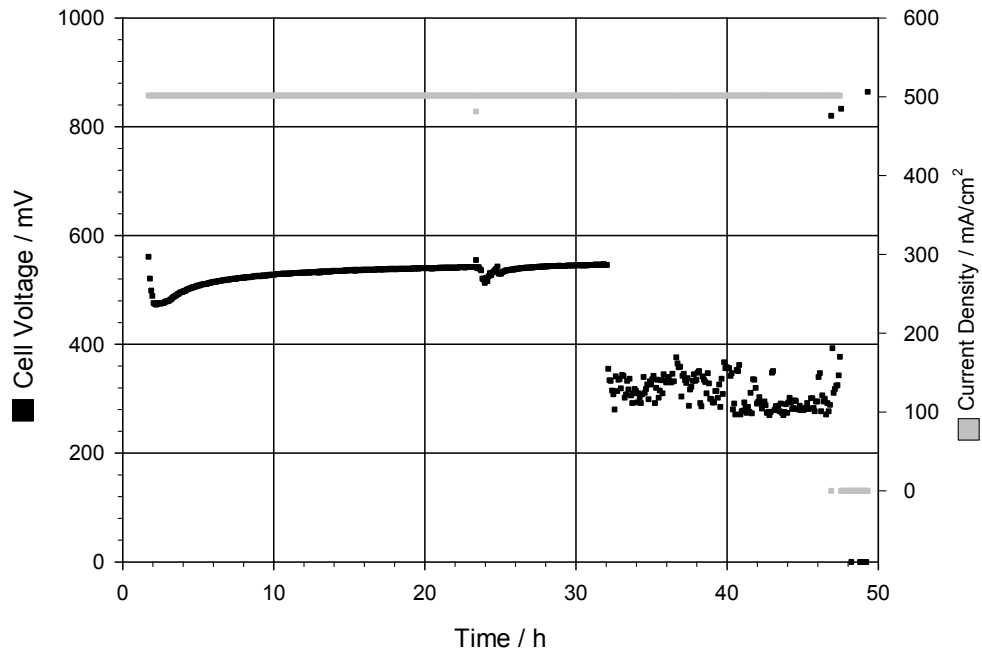


**Fig. 45: Performance of styrene based membrane M1.**
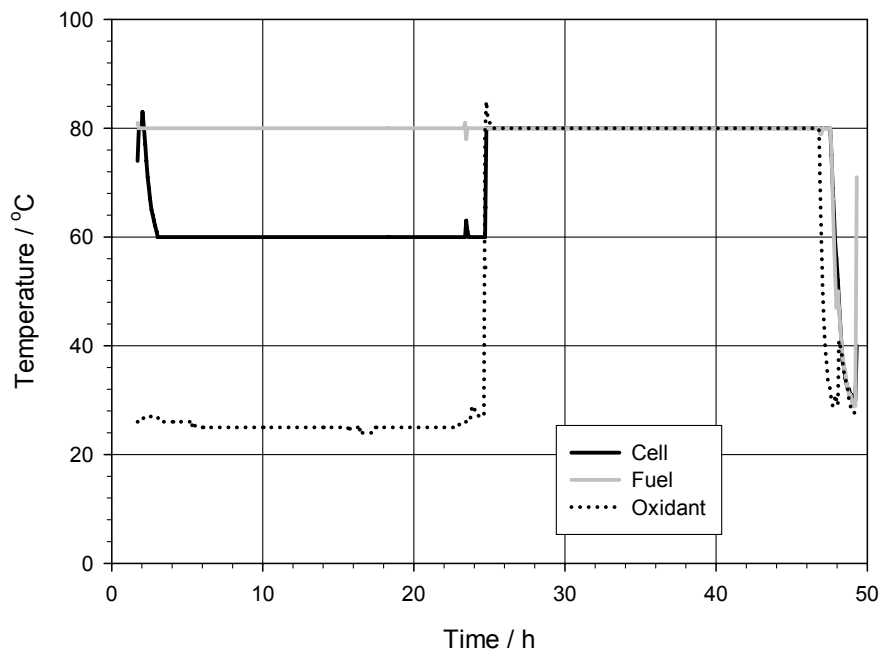


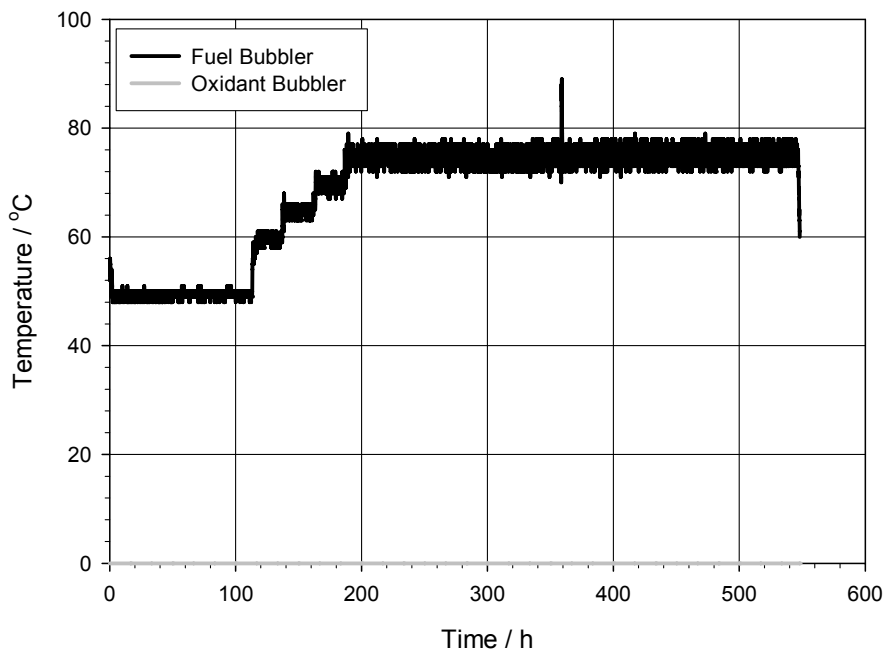**Fig. 46: Temperature history of styrene based membrane M1.**
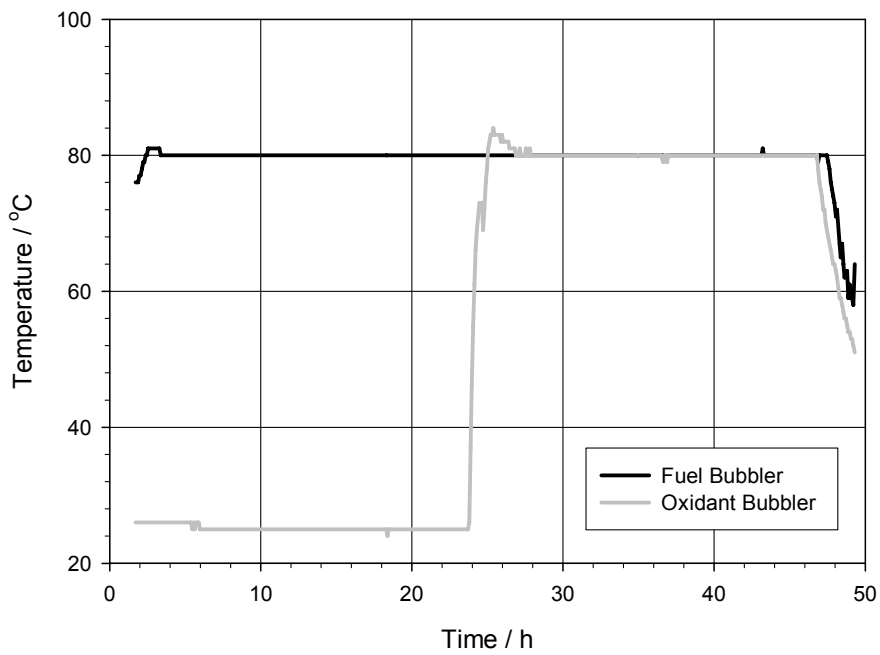
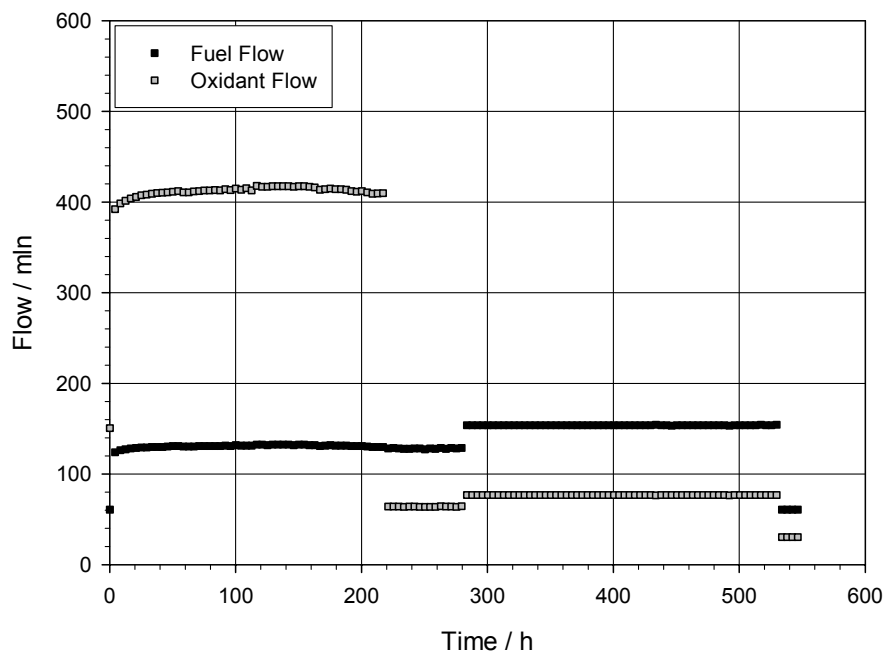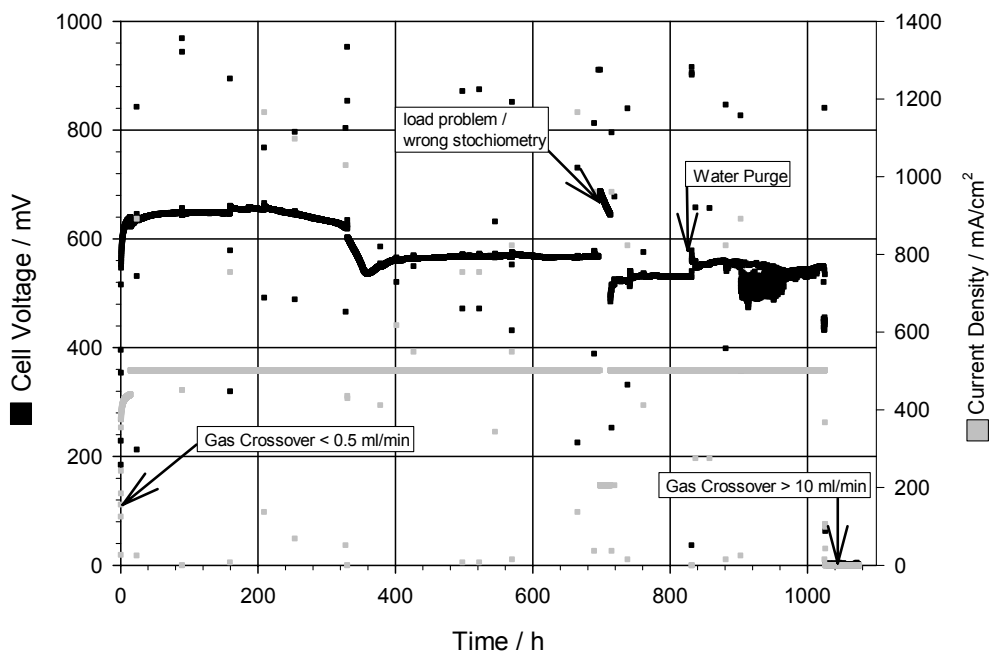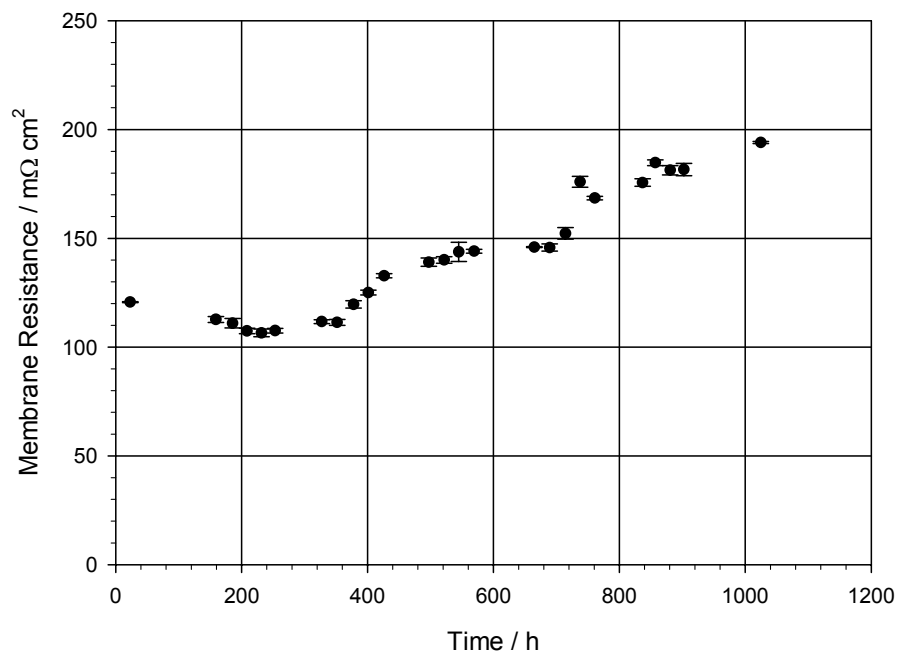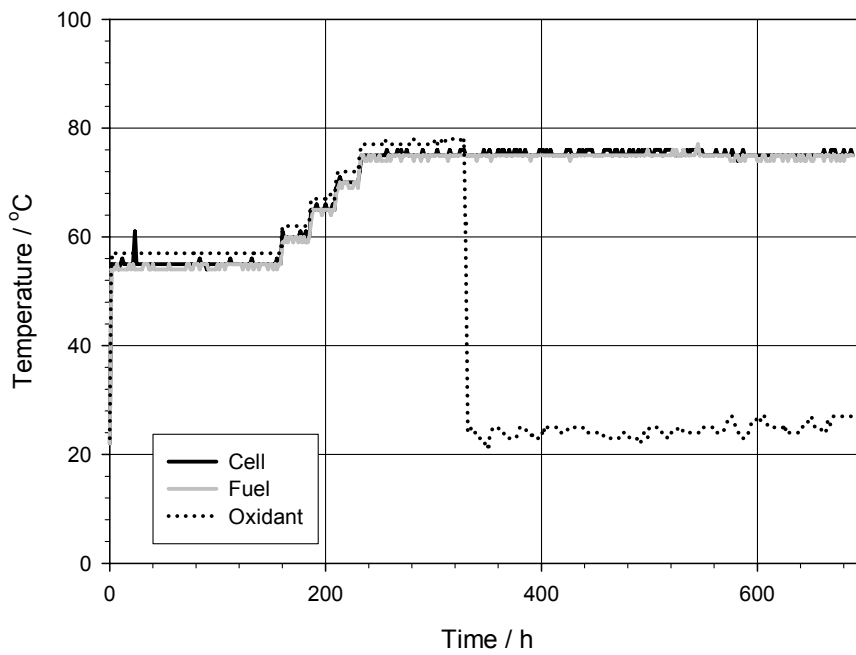**Fig. 47: Temperature of bubblers in the experiment with membrane M1.**
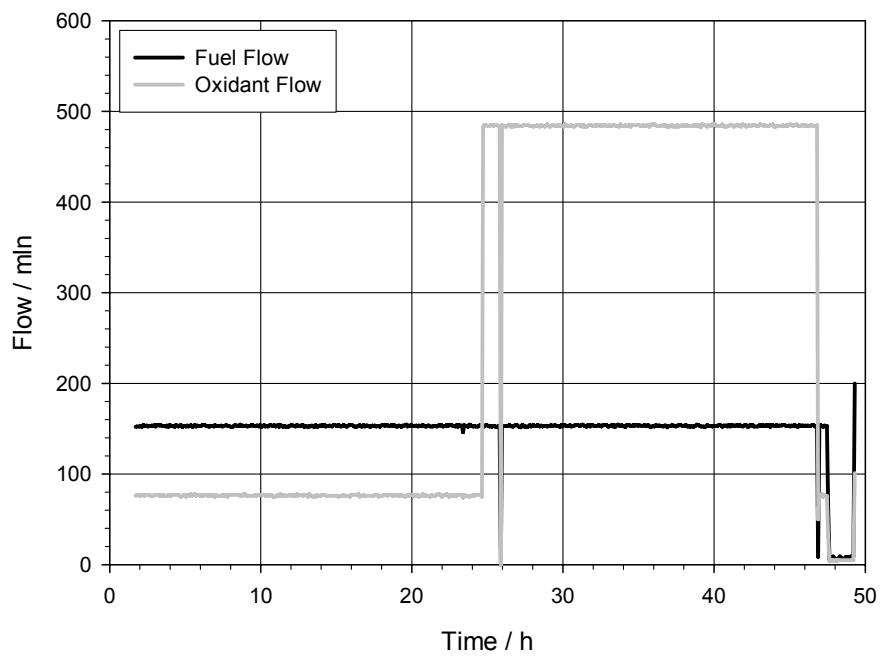


**Fig. 48: Flow  plot of the experiment with styrene based membrane M1.**
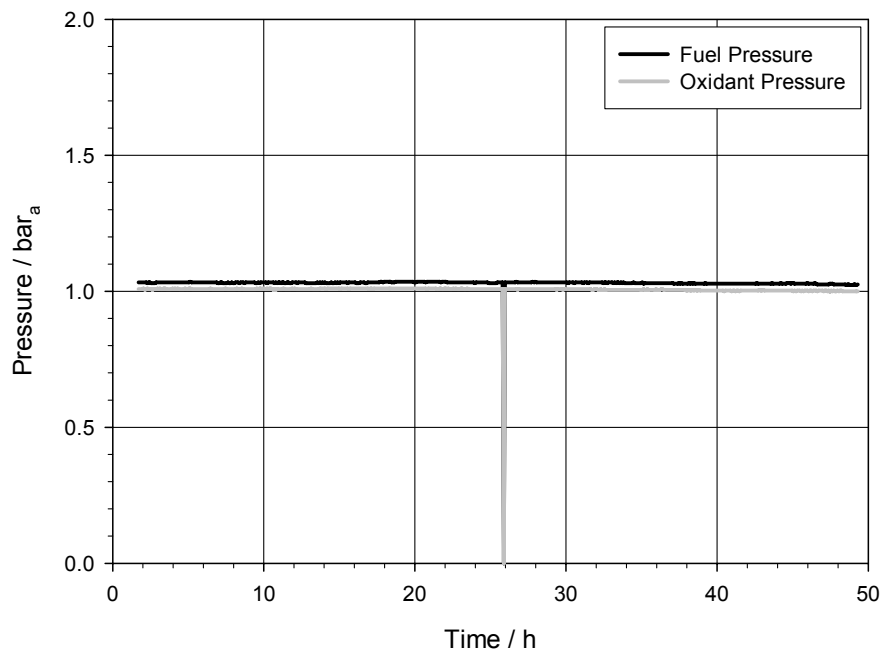
**Fig. 49: Pressure plot of the experiment with the styrene based membrane M1.**
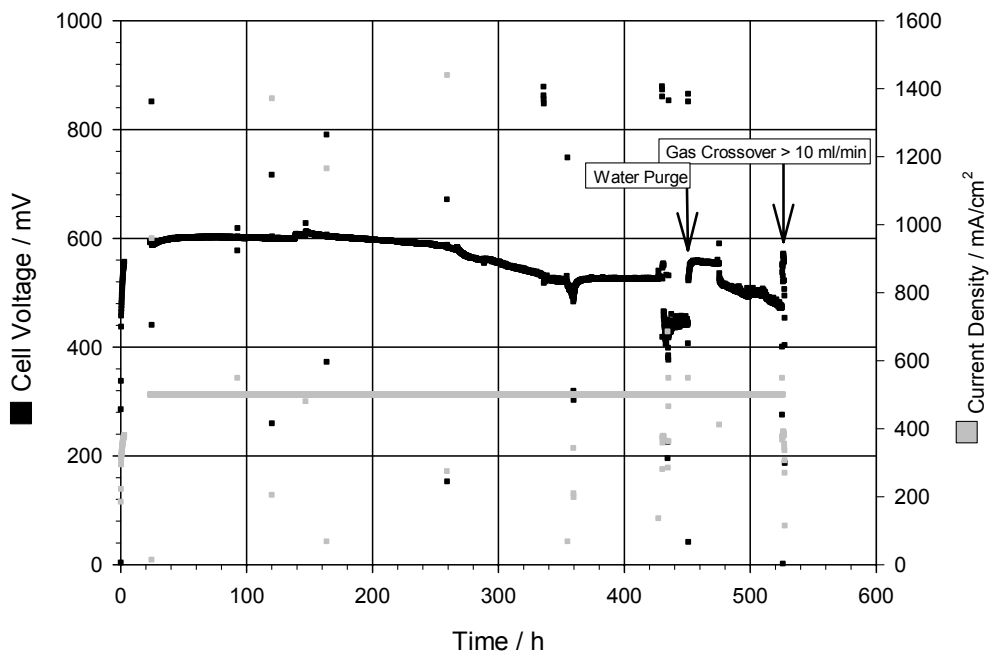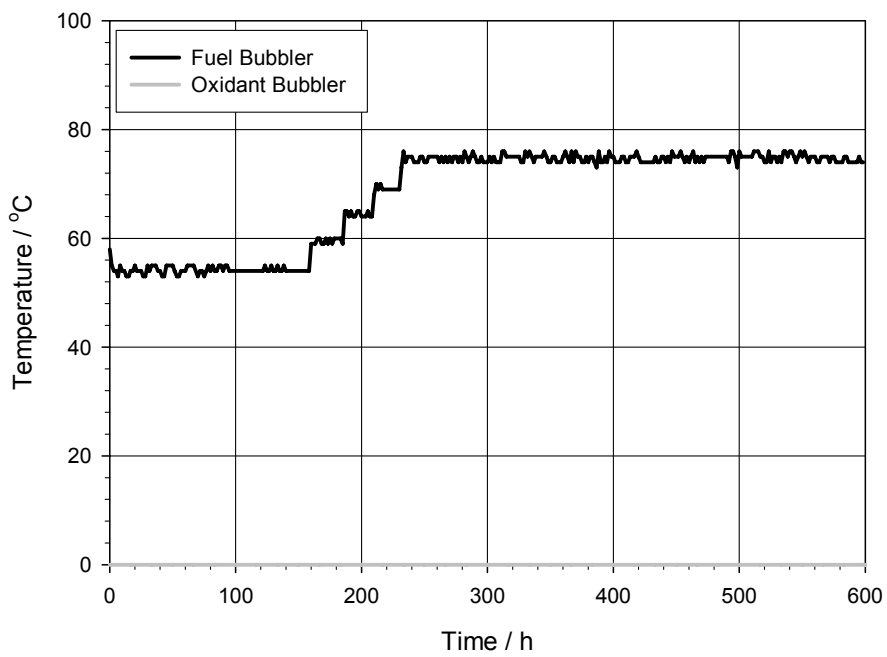


**Fig. 50: Performance of AMS/MAN membrane M2.**

89
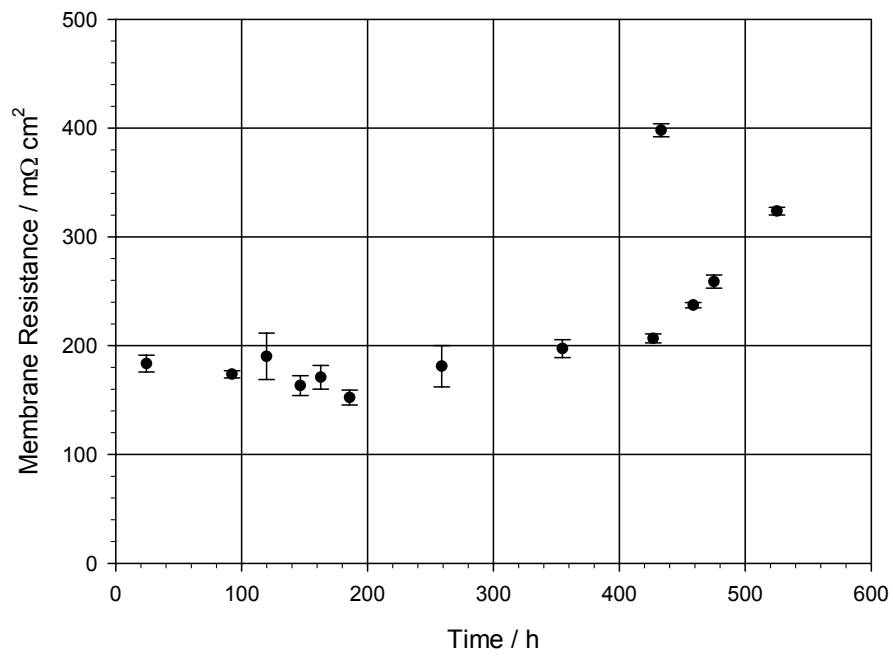
**Fig. 51: Resistance of the membrane M2.**
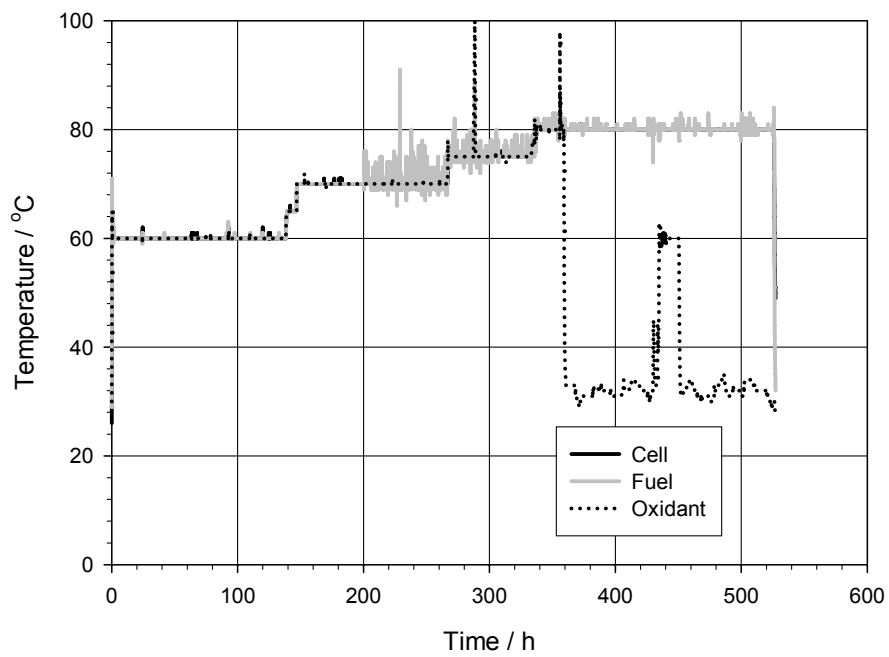


**Fig. 52: Temperature history of AMS/MAN membrane M2.**
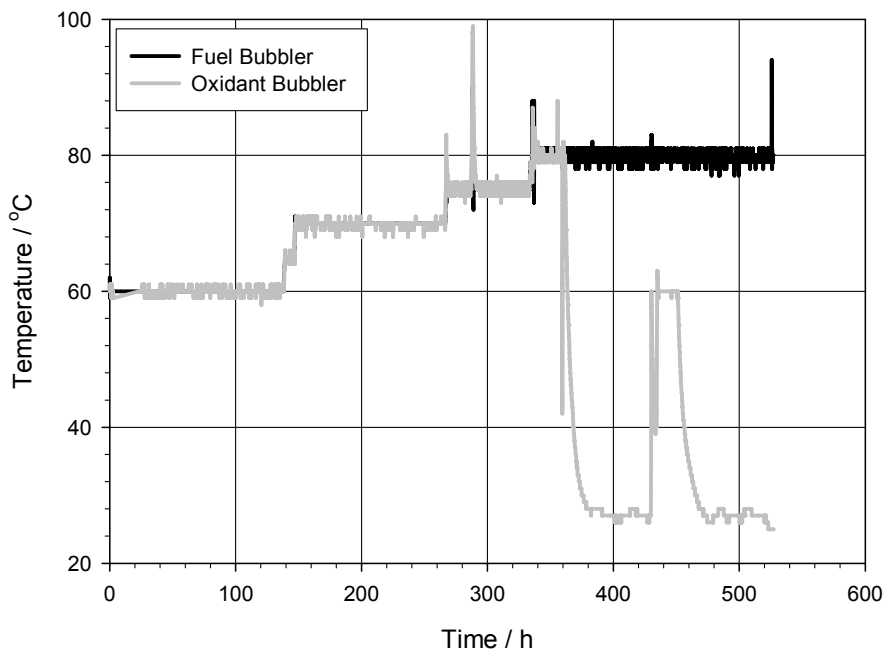
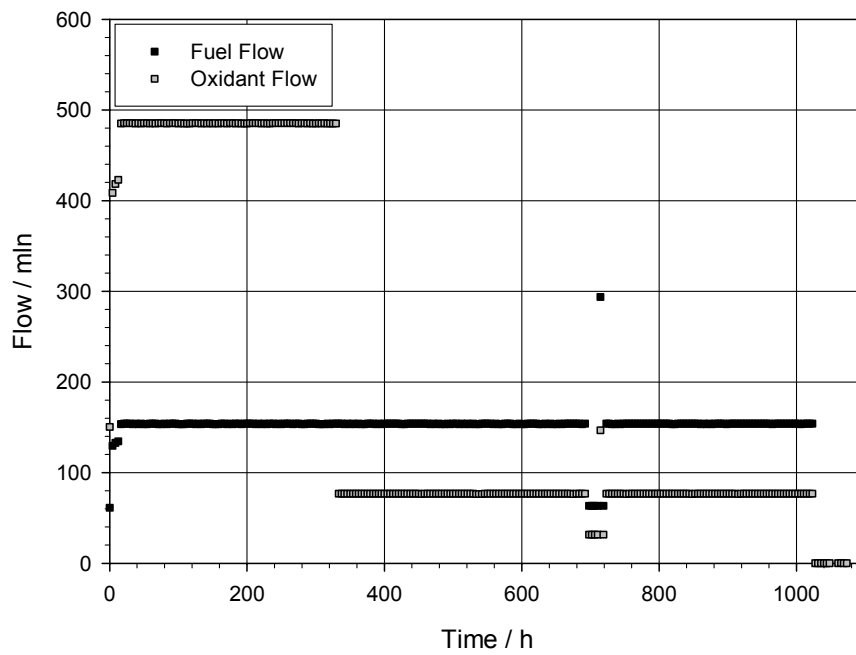**Fig. 53: Temperature of bubblers in the experiment with the membrane M2.**
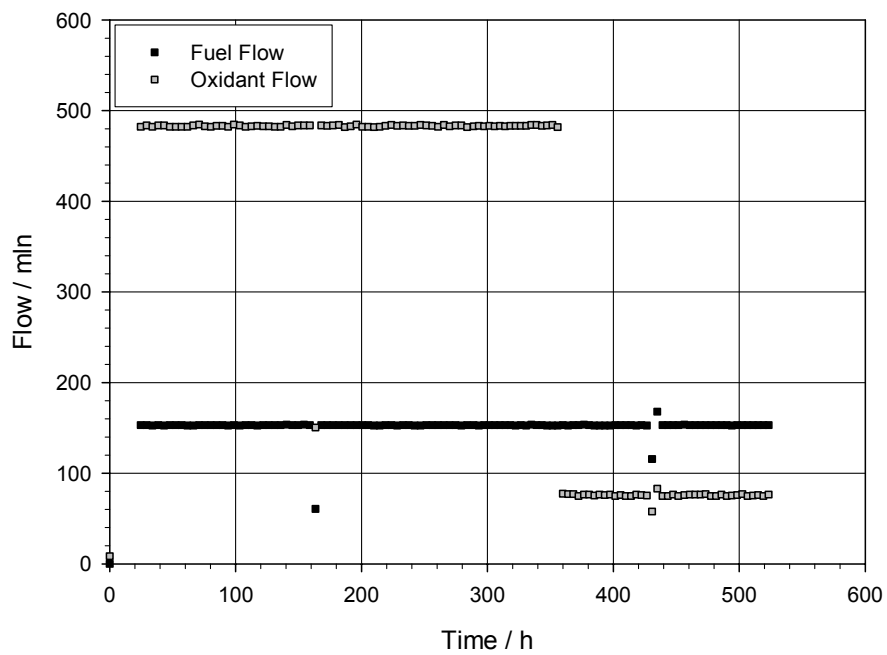


**Fig. 54: Flow plot of the experiment with AMS/MAN membrane M2.**
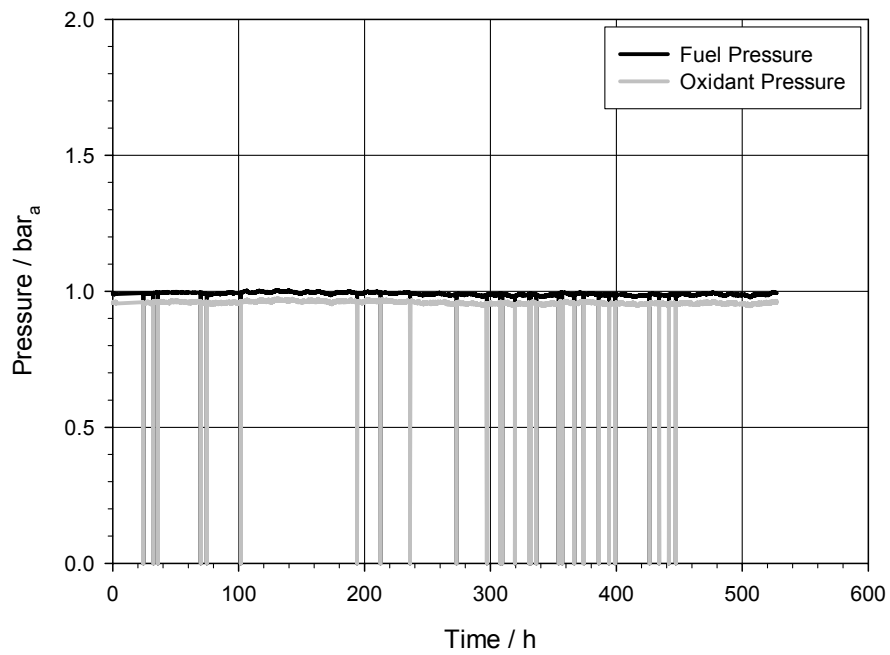
**Fig. 55: Pressure plot of the experiment with AMS/MAN membrane M2.**
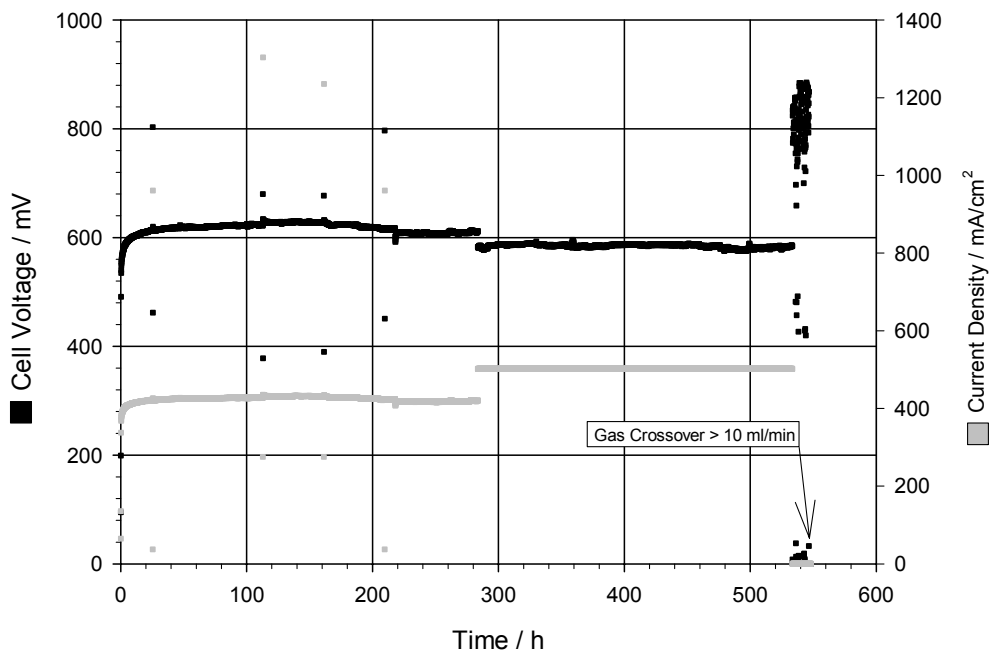


**Fig. 56: Performance of AMS/MAN membrane M3.**
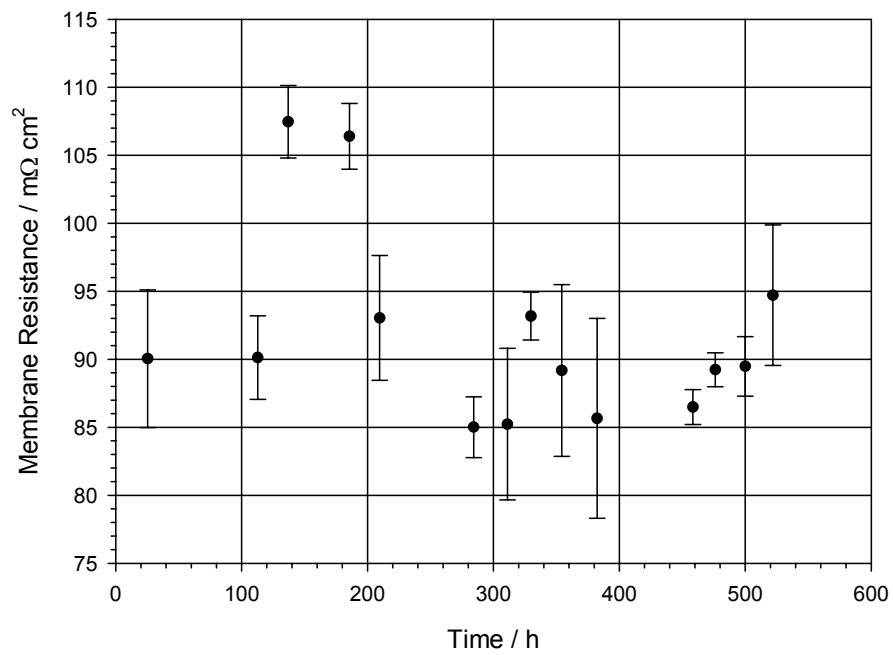
**Fig. 57: Resistance of the membrane M3.**
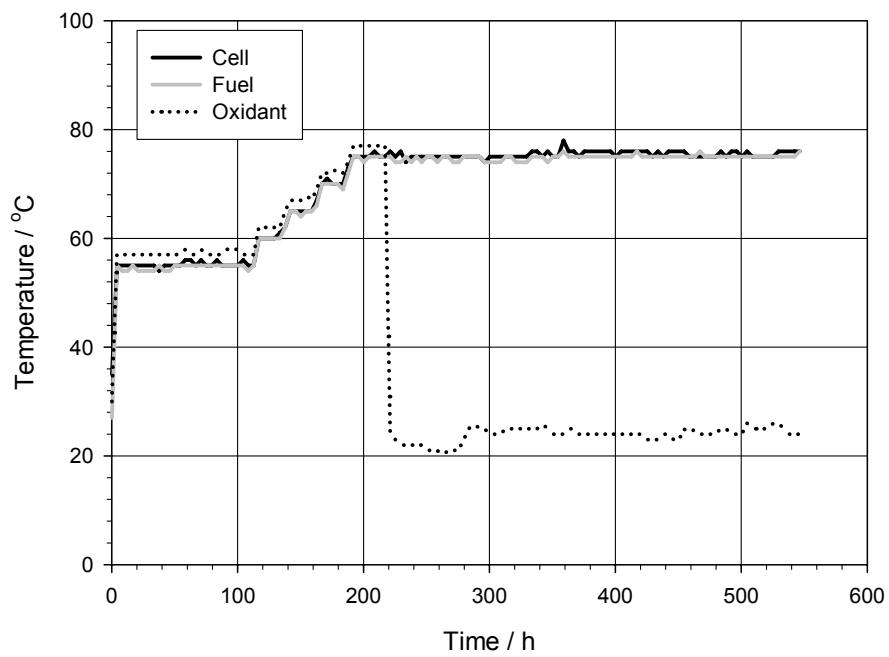


**Fig. 58: Temperature history of AMS/MAN membrane M3.**

**Fig. 59: Temperature of bubblers in the experiment with membrane M3.**



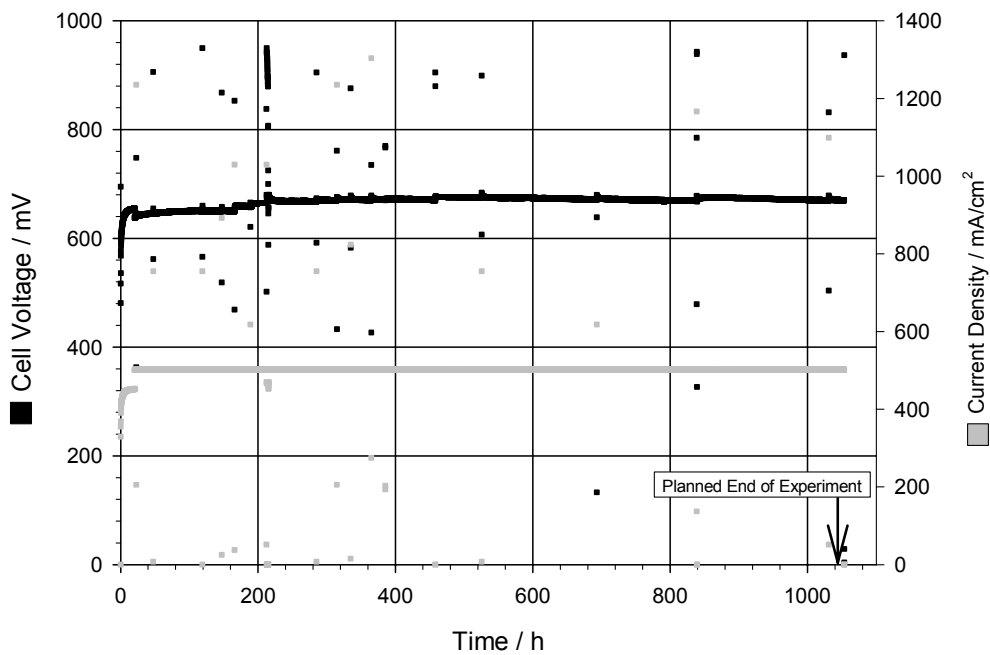**Fig. 60: Flow plot of the experiment with AMS/MAN membrane M3.**

94

**Fig. 61: Performance of AMS/MAN/DVB (crosslinked) membrane M4.**



**Fig. 62: Resistance of the membrane M4.**

**Fig. 63: Temperature history of AMS/MAN/DVB membrane M4.**



**Fig. 64: Temperature of bubblers in the experiment with membrane M4.**

**Fig. 65: Flow plot of the experiment with AMS/MAN membrane M4.**



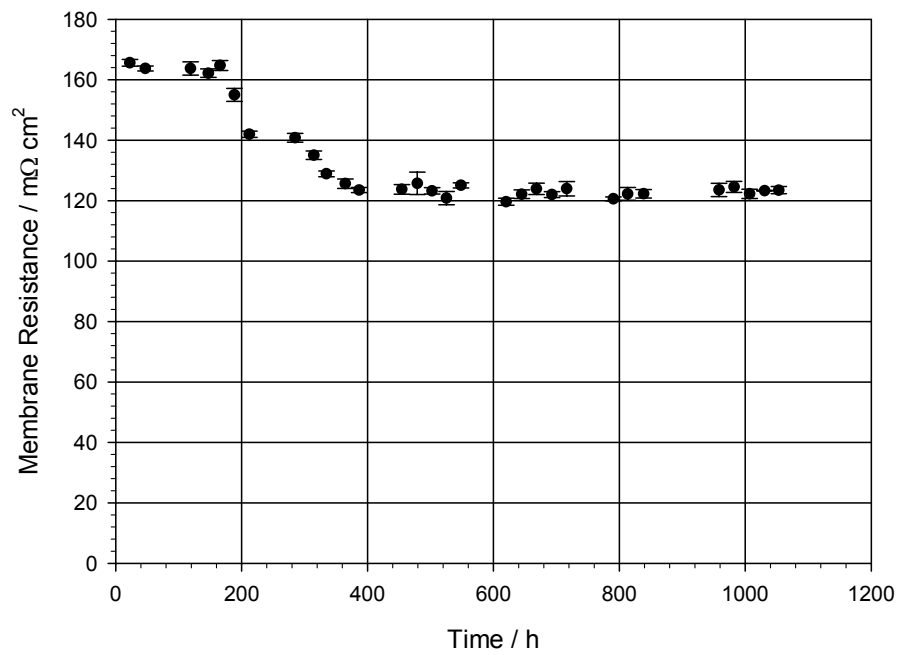**Fig. 66: Performance of AMS/MAN/DVB membrane M5.**
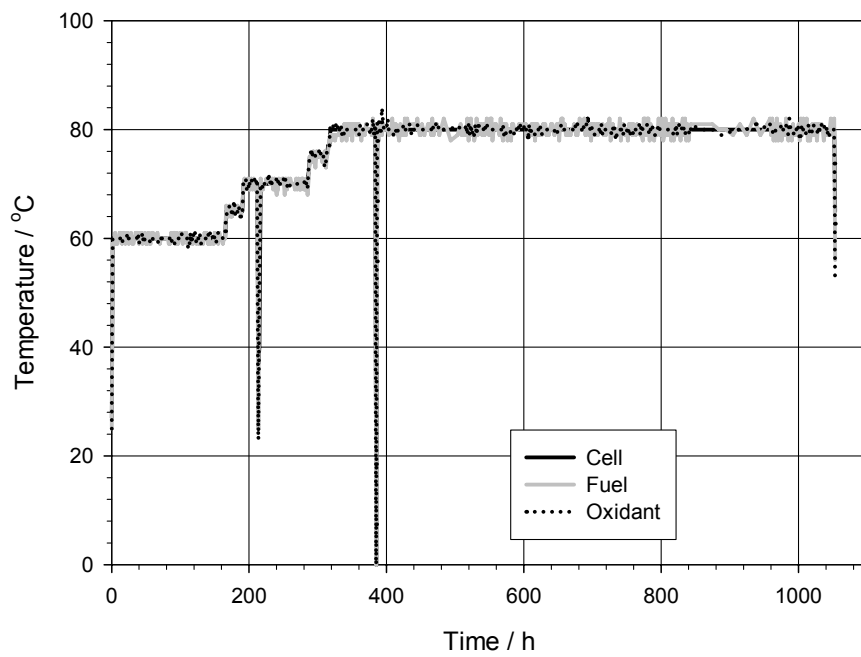
**Fig. 67: Resistance of the membrane M5.**



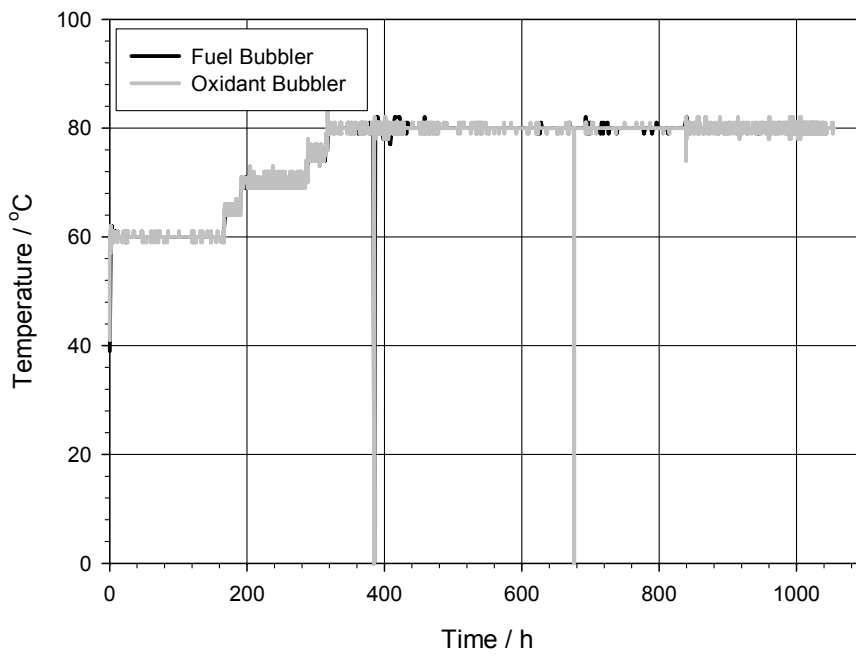**Fig. 68: Temperature history of AMS/MAN/DVB membrane M5.**

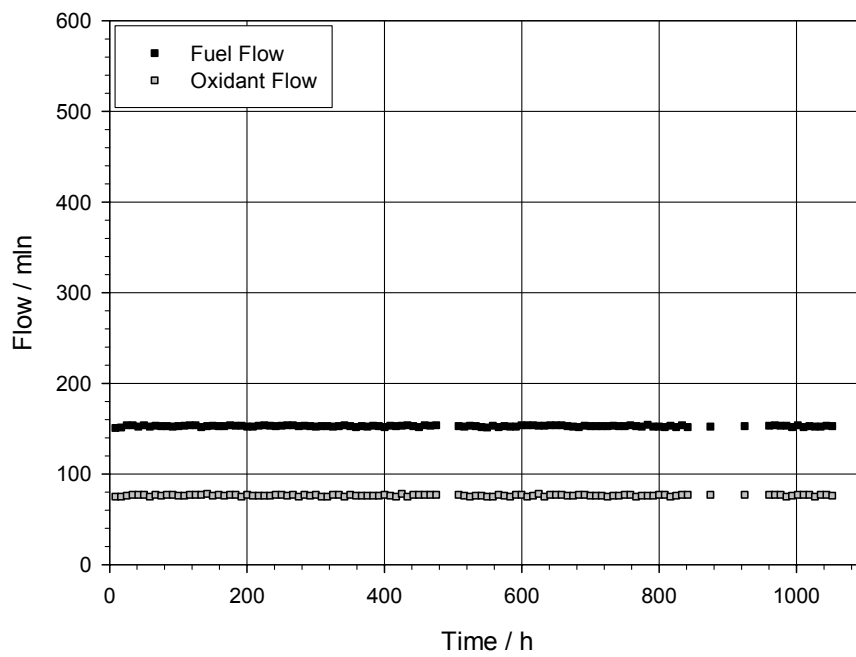**Fig. 69: Temperature of bubblers in the experiment with membrane M5.**



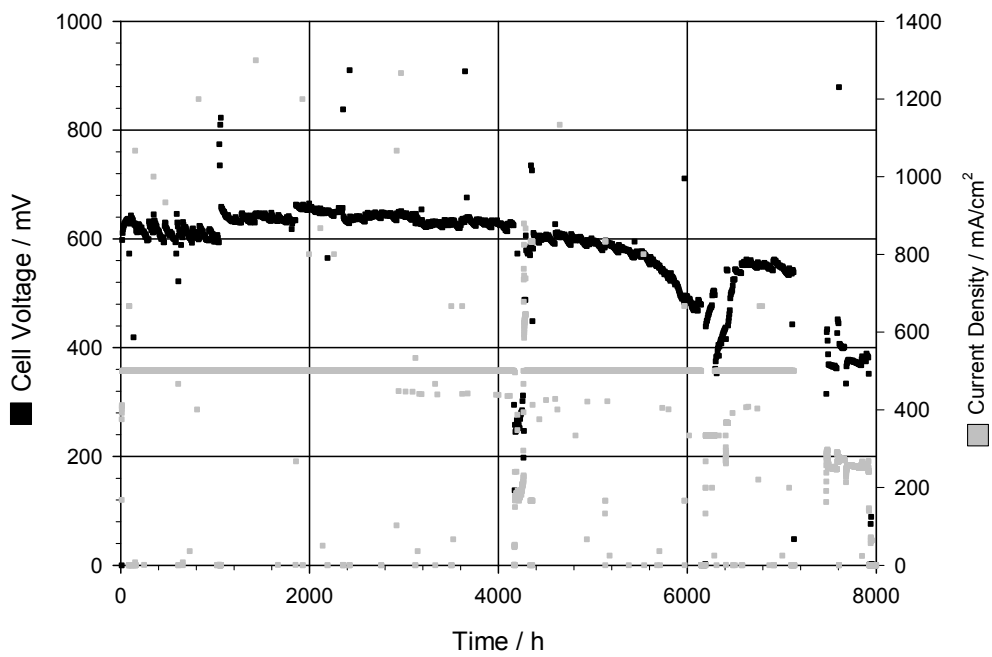**Fig. 70: Flow plot of the experiment with AMS/MAN/DVB membrane M5.**

**Fig. 71: Performance of styrene/DVB membrane M6. Pressure 1 bar$_a$, stoichiometry λ=1.5.**
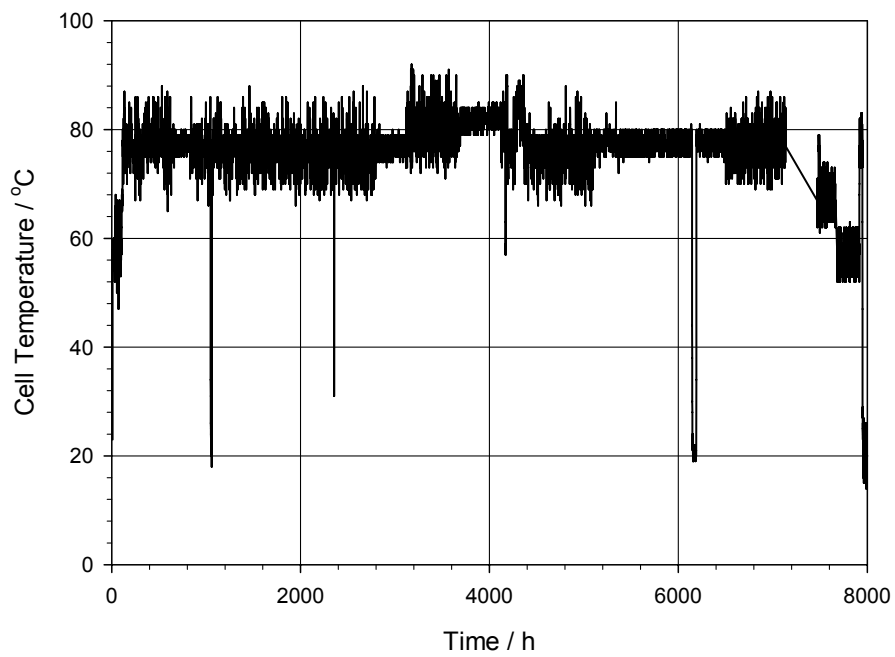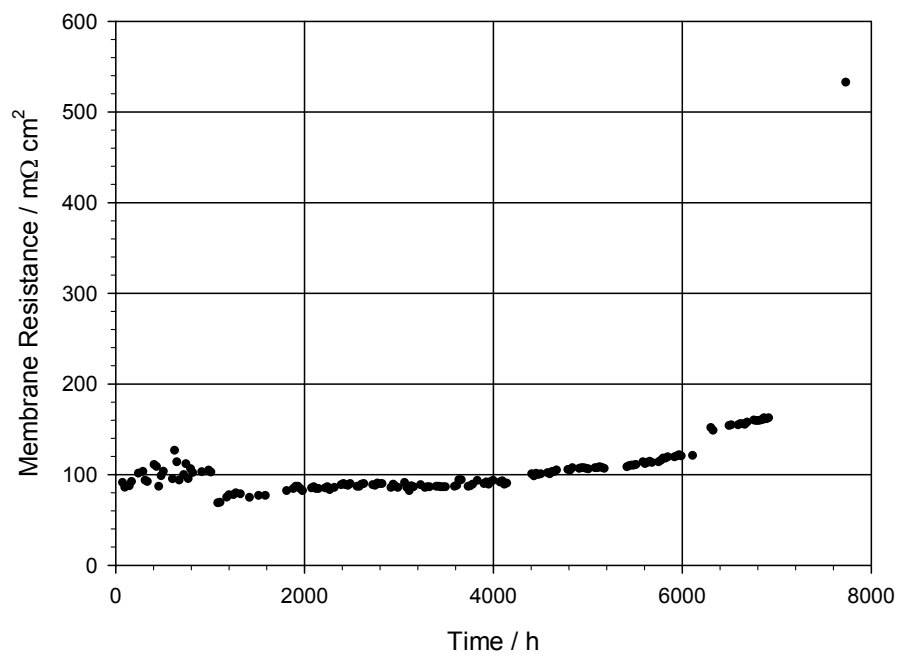


**Fig. 72: Cell temperature in the experiment with styrene/DVB membrane M6.**

100

**Fig. 73: Resistance of the membrane M6.**

# 13. Curriculum Vitae

Name:         Michał Wiesław

Surname:    ŚLASKI

Date of Birth: 29.09.1973

Place of Birth: Warsaw, Poland

Nationality: Polish

**Professional Experience:**

11/2002 -10/2006    Paul Scherrer Institut (Villigen, Switzerland), PhD student in the field: Synthesis of proton conducting membranes for polymer electrolyte fuel cells.

10/2001 - 9/2002    Novartis Pharma AG (Basel, Switzerland) – Stagiaire (trainee) position in Novartis Compound Archive (Lead Discovery Center). Evaluation and selection of chemical compounds for a global screening library.

3/2001 – 9/2001    Institute of Industrial Organic Synthesis (Warsaw, Poland), Research Associate. Synthesis of aldehydes.

**Education Register:**

11/2002-12/2006    Swiss Federal Institute of Technology Zurich (ETHZ), Department of Chemistry and Applied Biosciences, PhD study on proton conducting membranes for polymer electrolyte fuel cells.

4/2000 – 9/2000    Army Training Center for Telecommunication and Informatics.

10/1994 – 3/2000    Warsaw University of Technology (Warsaw, Poland), Faculty of Chemistry, Degree: Master of Science, Engineer, Specialization: polymer technology. Title of thesis: "Synthesis and Properties of Tricyclic Calix[4]arene Chromoionophores".

9/1990-6/1994    Technical College of Chemistry No. 3 (Warsaw, Poland), Degree of Technician of Chemical Processes.

**Patents:**

M. Slaski, L. Gubler, G. G. Scherer, "A method for preparing a radiation grafted fuel cell membrane with enhanced chemical stability and a membrane electrode assembly" European Patent Application WO 2006/084591 A1.

H.-P. Brack, C. Padeste, M. Slaski and H. Solak, "Method for grafting a chemical element or compound to a support substrate", European Patent Application WO 2005/014702 A1.

**Publications:**

L. Gubler, M. Slaski, A. Wokaun, G. G. Scherer, „Advanced monomer combinations for radiation grafted fuel cell membranes", Electrochemistry Communications, 8 (2006) 1215–1219.

H.-P. Brack, M. Slaski, L. Gubler, G.G. Scherer, S. Alkan, A. Wokaun, "Characterization of Fuel Cell Membranes as a Function of Drying by Means of Contact Angle Measurements", Fuel Cells, 4: (3) 2004 1-6.

C. Padeste, H.H. Solak, H-P. Brack, M. Slaski, S. Alkan Gürsel, G. G. Scherer, "Patterned Grafting of Polymer Brushes onto Flexible Polymer Substrates", Journal of Vacuum Science and Technology A, 22 (6) 2004 3191-3195.

H-P. Brack, C. Padeste, M. Slaski, S. Alkan, and H. H. Solak, "Preparation of Micro- and Nanopatterns of Polymer Chains Grafted onto Flexible Polymer Substrates", Journal of American Chemical Society 126. (4), 1004 -1005, 2004.

H.-P. Brack, D. Ruegg, H. Bueher, M. Slaski, S. Alkan, G.G. Scherer, "Differential Scanning Calorimetry and Thermogravimetric Analysis Investigation of the Thermal Properties and Degradation of Some Radiation-Grafted Films and Membranes", Journal of Polymer Science: Part B: Polymer Physics, 42: 2612–2624, 2004.

H.-P. Brack, D. Fischer, G. Peter, M. Slaski, G. G. Scherer, "Infrared and Raman spectroscopic Investigation of Crosslinked Polystyrenes and Radiation-Grafted Films", Journal of Polymer Science Part A: Polymer Chemistry 42: (1), 59 – 75 2003.

**Conferences:**
Polymer Group of Switzerland 2005 Fall Meeting – Neuchatel, Poster Presentation.
3rd European PEFC Forum, Lucerne/Switzerland 2005, Poster Presentation.
2nd European PEFC Forum, Lucerne/Switzerland 2003, Poster presentation.

# 14. References

[1] RyanO'Hayre, Suk-Won Cha, Whitney Corella, Fritz B. Prinz, "Fuel Cell Fundamentals", Wiley & Sons New York, ISBN 13 978-0-471-74148-0.

[2] W. T. Grubb US Patent 2,913,511 (1959).

[3] D. James et. al. US Patent 3,282,875 (1966).

[4] F. G. Bordwell Acc. Chem. Res. 1988, 21, 456.

[5] Handbook of Chemistry and Physics 86th Edition, ISBN: 0849304865.

[6] A. G. Ryder, S. Power, T. J. Glynn, Appl. Spectrosc. 2003, 57(1), 73-79.

[7] J. T. Wang, R. F. Savinell, J. Wainright, M. Littb, H. Yu, Electrochim. Acta, 1996, 41(2), 193-197.

[8] M. Rikukawa, K. Sanui, Prog. Polym. Sci. 2000, 25, 1463-1502.

[9] L. Gubler, S. A. Gürsel, G.G. Scherer, Fuel Cells 2005, 5(3), 317-335.

[10] A. Chapiró, "Radiation Chemistry of Polymeric Systems", Wiley-Interscience, New York (1962), ISBN: 0470392851.

[11] M. V. Rouilly, E. R. Kötz, O. Haas, G. G. Scherer, A. Chapiró, J. Membr. Sci., 1993, 81, (1-2), 89-95.

[12] F. N. Büchi, B. Gupta, O. Haas, G. G. Scherer Electrochim. Acta 1995, 40(3), 345-353.

[13] M. Taniguchi, J. Pieracci, W. A. Samsonoff, G. Belfort, Chem. Mater., 2003, 15(20), 3805-3812.

[14] A. Bhattacharya, B. N. Misra, Prog. Polym. Sci. 2004, 29, 767–814.

[15] M. M. Nasef, E. A. Hegazy, Prog. Polym. Sci. 2004, 29, 499–561.

[16] T. R. Dargaville, G. A. George, D. J. T. Hill, A. K. Whittaker, Prog. Polym. Sci. 2003, 28, 1355–1376.

[17] V. Y. Kabanov, L. P. Sidorova, V. I. Spitsyn, Eur. Polym. J., 1974, 10(12), 1153-1158.

[18] T. Rager, Helv. Chim. Acta, 2003, 86(6), 1966-1981.

[19] F. Yuee, S. J. Tianyi, Membr. Sci., 1988, 39, 1-9.

[20] A. Elmidaoui, S. Belcadi, Y. Houdus, T. Cohen, C. Gavach, J. Polym. Sci., Part A: Polym. Chem., 1992, 30, 1407-1412.

[21] J. Bohdziewicz, M. Bodzek, E. Wasik, Desalination, 1999, 121, 139-147.

22 R. Aliev, L. Strannikova, V. Teplyakov, G. Burillo, Radiat. Phys. Chem., 1998, 53, 533-538.

23 L. Gubler, N. Beck, S. A. Gürsel, F. Hajbolouri, D. Kramer, A. Reiner, B. Steiger, G. G. Scherer, A. Wokaun, B. Rajesh, K. R. Thampi, Chimia, 2004, 58, 826–836.

24 P. D. Beattie, F. P. Orfino, V. I. Basura, K. Zychowska, J. F. Ding, C. Chuy, J. Schmeisser, S. Holdcroft, J. Eelectroanal. Chem., 2001, 503(1-2), 45-56.

25 H-P. Brack, M. Slaski, L. Gubler, G. G. Scherer, S. Alkan, A. Wokaun, Fuel Cells 2004, 4 (3) 1-6.

26 J. Huslage, T. Rager, B. Schnyder, A.Tsukada, Electrochim. Acta, 2002, 48, 247-254.

27 H. Wang, G. A. Capuano, J. Electrochem. Soc., 1998, 145(3), 780-784.

28 U. A. Paulus, T. J. Schmidt, H. A. Gasteiger, R. J. Behm, J. Electroanal. Chem., 2001, 495, 134–145.

29 R. Adzic, "Recent Advances in the Kinetics of Oxygen Reduction in Electcatalysis", Chapter 5, Ed. J. Lipkowski, P. N. Ross, Wiley-VCH, New York 1998, 197-141.

30 W. Liu, D. Zuckerbrod, J. Electrochem. Soc., 2005, 152(6), A1165-A1170.

31 "Fuel Cell Handbook", 5th edition, ISBN: 0442319266.

32 A. Panchenko, H. Dilger, E. Möller, T. Sixt, E. Roduner, J. Power Sources, 2004, 127, 325–330.

33 A. Panchenko, H. Dilger, J. Kerres, M. Hein, A. Ullrich, T. Kazc, E. Roduner, PCCP, 2004 ,6 ,2891–2894.

34 G. Huebner, E. Roduner, J. Mater. Chem., 1999, 9, 409-418.

35 M. M Nasef, H. Saidi, H. M. Nor, O. M. Foo, J. Appl. Polym. Sci., 2000, 76(1), 1-11.

36 W. Becker, G. Schmidt-Naake, Chem. Eng. Technol., 2001, 24(11), 1128-1132.

37 J. Li, F. Muto, T. Miura, A. Oshima, M. Washio, S. Ikeda, M. Iida, Y. Tabata, C. Matsuura, Y. Katsumura, Eur. Polym. J., 2006, 42, 1222–1228.

38 A. B. LaColnti, M. Hamdan and R. C. McDonald, "Handbook of Fuel Cells – Fundamentals, Technology and Applications", Chapter 49, Vol. 3, Edited W. Vielstich, H.A. Gasteiger, A. Lamm, John Viley & Sons Ltd., ISBN: 0-471-49926-9.

39 F. N. Büchi, B. Gupta, O. Haas, G. G. Scherer, J. Electrochem. Soc., 1995, 142(9) 3044-3048.

40 L. Gubler , H. Kuhn, T. J. Schmidt, G.G. Scherer, H-P Brack, K. Simbeck, Fuel Cells, 2004, 4(3), 196 – 207.

[41] S. G. Cohen, H. T. Wolosinski, P. J. Scheuer, JACS, 1949, 71(10), 3439-3440.

[42] O. Savadogo J. New. Mat. Electrochem. Systems, 1998, 1, 47.

[43] P. D. Bartlett, G. M. Cohen, JACS, 1973, 95(23), 7923-7925.

[44] M. Prober, JACS, 1953, 75(4), 968-973.

[45] T. Momose, H. Yoshioka, I. Ishigaki, J. Okamoto, J. Appl. Polym. Sci., 1989, 37(10), 2817-2826.

[46] R. B. Hodgdon, J.Polym. Sci. Part A: Polym. Chem. 1968, 6, 171.

[47] C. Stone, A. E. Steck, B. Choudhury, United States Patent No. 6,723,758, Ballard Power Systems Inc., 2004.

[48] C. Stone A. E. Steck. Unisted States Patent No. 6,359,019, Ballard Power Systems Inc. 2002.

[49] A. E. Steck, O. Savadogo, P. R. Roberge, T. N. Verizoglu, "New Materials for Fuel Cell Systems I: Proceedings of the first international symposium of new materials for fuel cell systems", l'Ecole Polytechnique de Montreal, Montreal 1995 p 74.

[50] Rui-qi Pan, Xing-xin Liu, Min-zhi Deng, J. Fluorine Chem. 1999, 95, 167-170.

[51] T. Narita, Prog. Polym. Sci., 1999, 24, 1095-1148.

[52] T. Narita, Macromol. Rapid Commun., 2000, 21 (10): 613-627.

[53] L. Steuernagel, PhD Thesis: „Synthese von Vinylverbindungen zur Darstellung oxidationsstabiler Membranen für die Brennstoffzellenanwendung", ISBN 3-89720-779-6.

[54] S. A. Gürsel, Z. Yang B. Choudhury M. G. Roelofs, G. G. Scherer, J. Electrochem. Soc., 2006, 153(10), A1964-A1970.

[55] R. A. Assink, C. Arnold, R. P. Hollandsworth, J. Membr. Sci. 1991, 56(2), 143-151.

[56] Modern Styrenic Polymers Polystyrenes and Styrenic Copolymers, John Wiley & Sons Ltd., ISBN: 0-471-49752-5.

[57] D. B. Priddy, T. D. Traugott, R. H. Seiss, Polym. Prepr., 1989, 30(2), 195-196.

[58] Z. M. O. Rzaev, Prog. Polym. Sci., 2000, 25,163–217.

[59] J. M. G. Cowie, "Alternating Copolymers", New York: Plenum 1985, ISBN: 0306417790.

[60] C. S. Pilcher, W. T. Ford, J. Polym. Sci., Part A: Polym. Chem., 2001, 39, 525–529.

[61] J. Fleischhauer, G. Schmidt-Naake, D. Scheller, Angew. Makromol. Chem., 1996, 243, 11.

[62] "Polymer Handbook", 4th ed., J. Bandrup and E. H. Immergut, Eds., Wiley, New York, 1999, p.309, ISBN: 0471166286.

[63] W. Becker, M. Bothe, G. Schmidt-Naake, Angew. Makromol. Chem., 1999, 273, (1),57-62.

[64] H. K. Johnston, A. Rudin, Macromolecules, 1971,4(6), 661-667.

[65] J. F. Kenney, P. J. Patel, J. Polym. Sci., Part A: Polym. Chem., 1976, 14, 105-111.

[66] H. K. Johnston, A. Rudin, Macromolecules, 1971, 4(6), 661-667.

[67] J. F. Kenney, P. J. Patel, J. Polym. Sci., Part A: Polym. Chem., 1976, 14, 105-111.

[68] K. I. Suresh, J. Othegraven, K. V. S. N. Raju, E. Bartsch, Colloid. Polym. Sci., 2004, 283(1), 49-57.

[69] H. A. Colvin, J. Muse, CHEMTECH, 1986, 16(8), 500-504.

[70] J. G. Drobny, "Technology of Fluoropolymers", CRC Press, ISBN: 0-8493-0246-3.

[71] J. Li, K. Sato, S. Ichiduri, S. Asano, S. Ikeda, M. Iida, A. Oshima, Y. Tabata, M. Washio, Eur. Polym. J., 2004, 40, 775–783.

[72] N. Walsby, R. Sundholm, T. Kallio, G. Sundholm, J. Polym. Sci., 2001, 39, 3008-3017.

[73] J. Chen, M. Asano, Y. Maekawa, M. Yoshida, J. Membr. Sci., 2006, 277, 249–257.

[74] K. Matyjaszewski, T. P. Davis, "Handbook of Radical Polymerization", John Wiley & Sons Inc. ISBN 0-471-39274-X.

[75] T. J. Mason, J. P. Lorimer, "Applied Sonochemistry" Wiley-VCH Verlag GmbH & Co., ISBN 3-527-30205-0.

[76] F. R. Mayo, F.M. Lewis, JACS, 1944, 66, 1594.

[77] G. Odian, "Principles of Polymerization", John Wiley & Sons Inc.,4th Ed., ISBN:0-471-27400-3.

[78] S. M. S. Jamaludina, M. R. Nor Azlan, M.Y. Ahmad Fuad, Z.A. Mohd Ishak, U. S. Ishiaku, Polym. Test., 2000, 19, 635–642.

[79] H-P. Brack, C. Padeste, M. Slaski, S. Alkan, H.H. Solak, JACS, 2004, 126(4), 1004 -1005.

[80] C. Padeste, H. H. Solak, H-P. Brack, M. Slaski, S. A. Gürsel, G. G. Scherer, J. Vac. Sci. Technol. A., 2004, 22 (6), 3191-3195.

[81] D. W. Marquardt J. Soc. Ind. Appl. Math., 1968, 11, 431-441.

[82] B. Elsner, H. Boehni, Cross. Sci., 1983, 23, 341.

[83] B. Andreaus, A. J. McEvoy, G. G. Scherer, Electrochim. Acta, 2002, 47, 2222-2229.

[84] M. V. Rouilly, R. Koetz, O. Haas, G. G. Scherer, A. Chapiro, J. Membr. Sci., 1993, 81, 89.

[85] H-P. Brack F. N. Buechi, J. Huslage, G. G Scherer, Proceedings Paper 194th ECS Meeting 1-6.11.98, Boston, MA, USA.

[86] Jack L. Koenig, "Spectroscopy of Polymers", 2nd edition, Elsevier, ISBN: 0-444-10031-8.

[87] C. Pretsch, S. Seible, "Tabellen zur Strukturaufklärung organischer Verbindungen mit spektroskopischen Methoden", Dritte Auflage, Springer-Verlag, ISBN 3-540-15895-2.

[88] H. K. Johnston, A. Rudin, Macromolecules, 1971, 4(6), 661-667.

[89] M. M. Nasef, H. Saidi, Polym. Degrad. Stab., 2000, 70(3), 497-504.

[90] H.-P. Brack, D. Fischer, G. Peter, M. Slaski, G. G. Scherer, J. Polym. Sci., Part A., 2003, 42(1), 59-75.